0031-6997/06/5803-621–681$20.00
PHARMACOLOGICAL REVIEWS
Vol. 58, No. 3
60308/3141065
Printed in U.S.A

Pharmacol Rev 58:621–681, 2006

Theoretical Basis, Experimental Design, and Computerized Simulation of Synergism and Antagonism in Drug Combination Studies[S]

TING-CHAO CHOU

Preclinical Pharmacology Core Laboratory, Molecular Pharmacology and Chemistry Program, Memorial Sloan-Kettering Cancer Center, New York, New York

Address correspondence to: Dr. Ting-Chao Chou, Memorial Sloan-Kettering Cancer Center, 1275 York Ave., New York, NY 10021. E-mail: chout@mskcc.org

The author is a principal in and holds the copyright to CompuSyn, the software used for the analyses performed in this article. His son, who contributed to the software's development, is in a position to receive royalties for its publication.

Article, publication date, and citation information can be found at http://pharmrev.aspetjournals.org.
doi:10.1124/pr.58.3.10.

[S] The online version of this article (available at http://pharmrev.aspetjournals.org) contains supplemental material.

***Abstract*——The median-effect equation derived from the mass-action law principle at equilibrium-steady state via mathematical induction and deduction for different reaction sequences and mechanisms and different types of inhibition has been shown to be the unified theory for the Michaelis-Menten equation, Hill equation, Henderson-Hasselbalch equation, and Scatchard equation. It is shown that dose and effect are interchangeable via defined parameters. This general equation for the single drug effect has been extended to the multiple drug effect equation for *n* drugs. These equations provide the theoretical basis for the combination index (CI)-isobologram equation that allows quantitative determination of drug interactions, where CI < 1, = 1, and > 1 indicate synergism, additive effect, and antagonism, respectively. Based on these algorithms, computer software has been developed to allow automated simulation of synergism and antagonism at all dose or effect levels. It displays the dose-effect curve, median-effect plot, combination index plot, isobologram, dose-reduction index plot, and polygonogram for in vitro or in vivo studies. This theoretical development, experimental design, and computerized data analysis have facilitated dose-effect analysis for single drug evaluation or carcinogen and radiation risk assessment, as well as for drug or other entity combinations in a vast field of disciplines of biomedical sciences. In this review, selected examples of applications are given, and step-by-step examples of experimental designs and real data analysis are also illustrated. The merging of the mass-action law principle with mathematical induction-deduction has been proven to be a unique and effective scientific method for general theory development. The median-effect principle and its mass-action law based computer software are gaining increased applications in biomedical sciences, from how to effectively evaluate a single compound or entity to how to beneficially use multiple drugs or modalities in combination therapies.**

I. Introduction

Ever since the earliest days of recorded history, drug combinations have been used for treating diseases and reducing suffering. The traditional Chinese medicines, especially herbal medicines, are vivid examples. As the science of isolation technology and chemical synthetic capability advance, drug combinations have been more defined and sophisticated and their scope continues to broaden. Attempts have been made during the past century to quantitatively measure the dose-effect relationships of each drug alone and its combinations and to determine whether or not a given drug combination would gain a synergistic effect. Because biological systems as well as dose-effect models are exceedingly complex, there have been numerous models, approaches, hypotheses, and theories as well as controversies on drug combination analysis during the past century, as elaborated in many review articles, such as those by Fraser (1872), Loewe (1928, 1957), Le Pelley and Sullivan (1936), Plackett and Hewlett (1948), Finney (1952, 1971), Elion et al. (1954), Veldstra (1956), Goldin and Mantel (1957), Lacey (1958), Ariens and Simonis (1961), Venditti and Goldin (1964), Goldin et al. (1968), Skipper (1974), Schabel (1975), Grindey et al. (1975), Chou and Talalay (1977, 1981, 1983, 1984), Steel and Peckham (1979), Ashford (1981), Berenbaum (1981, 1989), Copenhaver et al. (1987), Carter et al. (1988), Greco et al.

(1990), Poch et al. (1990), Prichard and Shipman (1990), Suhnel (1990), Chou (1991), Schinazi (1991), Jackson (1991), Lam (1991), Tallarida (1992), and Greco et al. (1995). Among them, a recent review by Berenbaum (1989) has listed >560 references and another review by Greco et al. (1995) has categorized 13 different approaches and methods for the determination of synergism and antagonism. The main difference of the present review from the earlier reviews is that the rather fruitless and confusing debates of the past will not be repeated. Instead, in this review article the focus will be on the drug combination analyses that have physical-chemical bearings and have mathematically verifiable equations and theories. After continued and persistent devotion on this single subject for >35 years, I propose a seemingly simple way to hopefully end all the controversies on how to determine synergism or antagonism and introduce an explicit mass-action law-based method that allows automated computerized simulation of synergism and antagonism. Here, the general theory of dose and effect will be presented, the experimental design will be illustrated, the algorithms for computer simulation will be given, and examples of applications in various fields of biomedical sciences and on real data sample sets will be demonstrated.

A. Why Drug Combination?

The use of multiple drugs may target multiple targets, multiple subpopulations, or multiple diseases simultaneously. The use of multiple drugs with different mechanisms or modes of action may also direct the effect against single target or a disease and treat it more effectively. The possible favorable outcomes for synergism include 1) increasing the efficacy of the therapeutic effect, 2) decreasing the dosage but increasing or maintaining the same efficacy to avoid toxicity, 3) minimizing or slowing down the development of drug resistance, and 4) providing selective synergism against target (or efficacy synergism) versus host (or toxicity antagonism). For these therapeutic benefits, drug combinations have been widely used and became the leading choice for treating the most dreadful diseases, such as cancer and infectious diseases, including AIDS.

B. Pitfalls in Drug Combination Studies

1. Synergism versus Enhancement or Potentiation. Let us consider the simplest situation in which two drugs, A and B, are combined. If drug A has an effect and drug B has no effect and if in combination they have an effect that is greater than that of drug A, then it is enhancement or potentiation. We can describe the effect simply as percent enhancement or -fold of potentiation. If A and B alone each has an effect, then in combination they may produce a synergistic, an additive, or an antagonistic effect. By definition, synergism is an effect that is more than additive, whereas the definition for antagonism is an effect that is less than additive. Clearly, defining what is an "additive effect" is the most crucial criterion for defining synergism and antagonism. I spent more than 10 years (1972–1983) in attempting to define the additive effect by deriving and publishing several hundred specific equations and several general equations.

2. The Most Common Errors. In most cases, medical researchers or clinical practitioners perform drug combinations for perusing synergism. However, there are many common errors associated with these claims:

1. $A + B > A$ or $A + B > B$ says nothing about synergism. This is a simple arithmetic fact that needs neither proof nor requires an elaborated statistical task, such as determining p values.
2. Additive effect is not a simple arithmetic sum of two (or more) drugs. If A and B each inhibits 30%, then the additive effect is not 60% because if A and B each inhibits 60%, the combined additive effect cannot be 120%.
3. If A and B each inhibits 60%, then it is oversimplification to say that the additive effect is 84% inhibition. Based on the reasoning by Webb (1963), this type of problem can be solved by $(1 - 0.6)(1 - 0.6) = 0.16$, $1 - 0.16 = 0.84$. Chou and Talalay (1984) called it the fractional product method. This method will never lead to a combination effect exceeding 100% inhibition. Chou and Talalay (1984), however, have also proved that this method has limited validity because it takes into account the potency (e.g., fractional inhibition) but ignores the shape of the dose-effect curve (e.g., hyperbolic or sigmoidal). The importance of the "shape" in a dose-effect analysis is shown in Fig. 1. Chou and Talalay (1984) indicated that Webb's method is valid only when both drugs have hyperbolic curves (i.e., in simple Michaelis-Menten kinetics when dose-effect curves are hyperbolic, i.e., $m = 1$ in the median-effect plot) and is not valid when $m \neq 1$, such as sigmoidal ($m > 1$) or flat sigmoidal ($m < 1$) curves. Furthermore, Webb's method is valid when the effects of two drugs are mutually nonexclusive (e.g., totally independent) and is not valid for mutually exclusive (e.g., similar mechanisms or modes of actions, as assumed for the classic isobologram, see below).

C. Truth or Fallacy and Its Consequences

On an Internet Web search, the term "drug combination" had 43,722 hits and 6,350,000 hits by PubMed and Google, respectively, and the term "synergistic effect" has been cited 14,296, 7186, and 963,000 times by PubMed, ISI, and Google, respectively. However, it is to be noted that in one review article by Goldin and Mantel (1957) alone, seven different definitions for synergism were given, and none of them supported the others. In a more recent review by Greco et al. (1995), 13 different methods for determining synergism were listed. Again, none of them supported the others. Thus, it is hard to

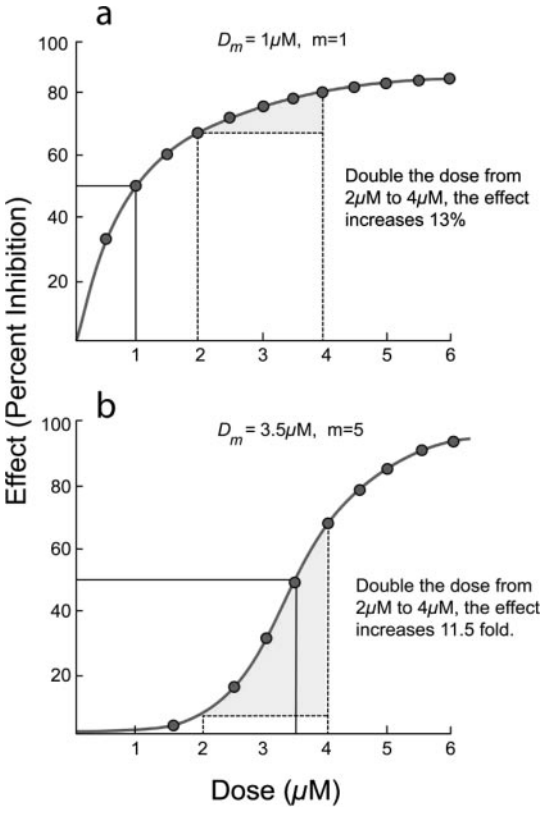

FIG. 1. Examples of dose-effect curves simulated by the median-effect equation (see eq. 9) for two drugs using CompuSyn software (Chou and Martin, 2005). The graphs are drawn manually for highlights. Shape (m) and potency (D_m) parameters of dose-effect curves for drug a: hyperbolic curve ($m = 1$) with IC_{50} (D_m) of 1 μM; for drug b: sigmoidal curve with $m = 5$ and $D_m = 3.5$ μM. Note that doubling the dose from 2 to 4 μM increases the effect by 13%. However, doubling the dose in b from 2 to 4 μM increases the effect by 11.5-fold. These drastic differences underscore the difficulty to predict by inspection what would be the "additive effect" when two drugs are combined at a given ratio. The hyperbolic curve usually occurs in a simple system, such as an enzyme or receptor. The sigmoidal curve ($m > 1$) usually occurs in a complex system, e.g., cellular, multicellular, or in vivo systems. High m values are most common in radiation effects, thermo effects, and animal lethality studies.

find any other field in biomedical science that has more controversy and more confusion than drug combinations. The meaning of synergism has become an individual's preference, agenda, or wishes. The seriousness of faulty or unsubstantiated or erroneous claims of synergy is clearly obvious, since it is frequently referred to as therapy for treating patients.

It is not likely that the different definitions of synergism are all correct or the different methods for determining synergism are all valid. In the presence of so much ambiguity, doubt, bias, and confusion, science has been under siege and challenged. The longing for fact and truth in this field of discipline of research is ever strengthening.

D. An Approach for Extinguishing Controversies

For each hypothesis, approach, and theory of drug combination, we need to demand theoretical thoroughness and rigorous derivations. A mathematical formula does not really constitute a proven method, if it is empirical without actual derivation (Chou, 1977b). Often, a formula with obscure origin and lack of sound theoretical basis emerges and dominates the drug combination field for decades until a new one replaces it (Table 1). The complexity in biology and pharmacology apparently underlies this imperfectness. Therefore, the issues that have been raised are 1) How was the formula obtained? 2) Are all the parameters or constants defined and do they have any chemicophysical bearings? and 3) Are the formulae for a single drug expandable to multidrug systems? During the past seven decades, evidence indicated that dose-effect analysis per se was a physicochemical problem rather than a statistical problem. In other words, it was deterministic rather than probabilistic. At this time, I recommend a set of criteria for the credibility of a theory or a method, whether it existed or it will be newly proposed. These criteria include 1) Are there any derived equations to be based upon? If so, how, when, and where were they derived? 2) Are there any algorithms? If not, how can the procedure be executed or how can a computer program be established? and 3) Are the conclusions or claims quantitatively indicated or merely descriptive? We demand a quantitative conclusion. It is proposed that the right or wrong of a method for drug combination data analysis can be illustrated by the following fictional narrative, which can serve as a simple litmus test:

TABLE 1
Dose-effect relationship laws used by different schools

Modified from "Quantitation of Synergism and Antagonism of Two or More Drugs by Computerized Analysis," Chou TC, in *Synergism and Antagonism in Chemotherapy* (Chou TC and Rideout DC eds) pp 223–244. Copyright 1991 with permission from Elsevier.

POWER LAW (Nordling, 1953; Armitage and Doll, 1954)	$f_a = bD^k$; $\log(f_a) = k \log(D) + \log b$
PROBIT (Bliss, 1939; Finney, 1947, 1952, 1971)	$f_a = \frac{1}{\sigma\sqrt{2\pi}} \int_{-\infty}^{\log D} e^{-\frac{1}{2\sigma^2}(\log D - \log Dm)^2} d(\log D)$ where $Y = (\log D - \log D_m)/\sigma$
LOGIT (Berkson, 1946; Thompson, 1947)	$f_a = 1/[1 + e^{-(\alpha + \beta \log D)}]$
The median-effect equation of the MASS-ACTION LAW (Chou, 1974, 1976)	$f_a/f_u = (D/D_m)^m$; $\log[(f_a)^{-1} - 1]^{-1} = m \log(D) - m \log(D_m)$

D, dose; D_m, median-effect dose; m, kinetic order; f_a, fraction affected; f_u, fraction unaffected; σ^2, variance; Y (PROBIT − 5) or normal equivalent deviate; a, k, α, and β, undefined constants.

Once upon a time, there was a Master who held two bottles of antitumor ingredients. The red bottle contained drug A, and the blue bottle contained drug B. He then gave the two bottles to his disciples, John and Paul. The Master asked them to conduct drug combination studies in different proportions and to determine whether they were synergistic or antagonistic by using any of their best choice of assay method and by using the best choice of theory for their dose-effect data analysis. Weeks later, John said they were synergistic, whereas Paul said they were antagonistic. However, the Master, without hesitation, said "No!" to both of them. Why? It was because drug A and drug B were the same, and therefore, it could only be an "additive effect"! The ingredient in the bottles was panaxytriol isolated from red ginseng that yielded highly sigmoidal dose-effect curves in a variety of assays. In fact, the additive effect conclusion should always be valid no matter what assay method was used, and it was not relevant whether or not the shape of a dose-effect curve was hyperbolic or sigmoidal and whether the drug interaction was determined at ED_{30}, ED_{50}, ED_{70}, ED_{95}, or ED_{99} levels. It should yield an additive effect under all circumstances. Using this approach, one should be able to determine whether any hypothetical method for determining synergism or antagonism is valid or faulty. The sigmoidicity of a dose-effect curve (e.g., for panaxytriol) greatly magnifies the differences among the different methods or theories. Thus, the main controversies in drug combination analysis in the past century can be readily resolved.

II. Theoretical Basis for Dose-Effect Analysis

A *general equation of dose and effect* and its theorem of combination index have been developed by using the approach of merging the physicochemical principle of the mass-action law with the mathematical principle of induction and deduction. After deriving hundreds of equations and three and one-half decades of progression, Chou presented an overview of this systematic approach to complex biosystems that leads to the genesis of some of the fundamental rules in nature. Remarkably, the derived general theory of dose and effect has been proven to be the *unified theory* of the four basic equations in biomedical sciences pioneered by Henderson-Hasselbalch, Michaelis-Menten, Hill, and Scatchard. Furthermore, the present theory not only leads to the derivation of the combination index theorem but also leads to the derivation of the isobologram equation, the dose-reduction index equation, and the generation of polygonograms. Their informatics has been explored on theoretical grounds. Their algorithms have allowed for the creation of computer software to facilitate their applications into a broad discipline in biomedical sciences, especially in the field of parameter determination, and have allowed for the simulation of synergism or antagonism in drug combinations at all dose and effect levels. Based on an ISI Web of Science search (Institute for Scientific Information 1976–2006; http://portal.isiknowledge.com/portal.cgi?DestApp=WOS&Func=Frame), one article alone on the median-effect principle (Chou and Talalay, 1984) has been cited in >1294 scientific papers in hundreds of biomedical journals.

A. An Approach of Merging the Mass-Action Law with Mathematical Induction and Deduction

1. The Power of Mathematical Induction and Deduction. Whether the proposition 1 + 2 + 3 + 4 + 5 +. . . + 6789 = 23,048,655 is right or wrong can be determined in several ways. One may actually count and add, step by step to prove it, whereas another may create an iterative program using a computer for a virtually error-free calculation. But for an individual, familiar with mathematical induction and deduction, it can be proven in less than 30 s with the aid of a pocket calculator or even by hand, given approximately 3 minutes, by using a pencil and a piece of paper.

Therefore, there is a seemingly magical power in mathematical induction and deduction. Since the 1970s and early 1980s, Chou has attempted to use this approach for biological systems by using the basic rules of physics and chemistry. Three and one-half decades later, we now have the second-degree Pascal's triangle (Chou, 1970, 1972), the median-effect equation (Chou, 1974, 1976, 1977; Chou and Talalay, 1977), the combination index equation (Chou and Talalay, 1981, 1983, 1984; Chou, 1991; Chou et al., 1994), the dose-reduction index equation (Chou and Talalay, 1984; Chou, 1987; Chou, 1991, 1994), the general equation for the isobologram (Chou and Talalay, 1984, 1987; Chou, 1991; Chou et al., 1991), and the creation of the polygonogram (Chou et al., 1991; Chou and Martin, 2005), along with their computer software (Chou JH et al., 1983; Chou JH and Chou, 1985; Chou and Hayball, 1997; Chou and Martin, 2005). Remarkably, the median-effect equation, which has been independently derived mathematically, is, in fact, the "unified theory" for the Michaelis-Menten equation of enzyme kinetics, the Hill equation for higher-order ligand binding saturation, the Henderson-Hasselbalch equation for pH ionization, and the Scatchard equation for receptor binding (Chou, 1977, 1991).

2. Nature's Law. In the physical world of nature, there is the mass-action law (C. M. Guldberg and P. Waage, 1864), the equilibrium law (A. F. Horstmann, J. W. Gibbs, and J. H. Van't Hoff, 1873–1886), and the absolute reaction rate theory (M. Polanyi and H. Eyring, 1935) [For references, see Bothamley (2002).] Using the equilibrium and steady-state approach at a constant temperature and pressure, enzyme kinetics and receptor theory have flourished. These developments have provided a golden opportunity to merge these physicochemical approaches with mathematical induction and deduction for biological systems. A general theory and their theorems with broad applicability for diversified biolog-

ical applications have thus been created. Consequently, the algorithms for computerized simulation and analysis on these theorems have also been developed.

3. Dealing with Diversified Biological and Pharmacological Systems. Using the well-developed field of enzyme kinetics as a model, Chou in the 1960s, as a pharmacology Ph.D. graduate student at Yale University, learned how to derive the Michaelis-Menten equation, which described a single substrate-single product reaction at a steady-equilibrium state (Chou 1970, 1974). Intrigued by the intricacy of this process, Chou gradually and systematically extended the derivation to various multiple substrate-multiple product reactions. This extension and pattern analysis used various notations introduced by Cleland (1963), such as the sequential ordered mechanism, the ping-pong mechanism, and the random mechanism, with different numbers of complexes, enzyme species, and stable enzyme forms. A systematic approach, similar to mathematical induction, with substrate and product for $n = 1, 2, 3, \ldots$ allows the derivation of many specific equations (Chou, 1972, 1974). Through the combination and permutation of different numbers of substrate and product reactants in conjunction with the above mechanisms, hundreds of specific equations have been derived (Chou, 1974, 1976, 1977; Chou and Talalay, 1977, 1981, 1983, 1984).

Most drugs, as described in pharmacology, are inhibitors that suppress enzymes, receptors, or pathways. The enzymatic mechanisms, indicated above, can be considered the mini-pathways. Introduction of a competitive, noncompetitive, or uncompetitive inhibitor to the above enzyme kinetic derivations (e.g., I, competitive with substrate A, noncompetitive with substrate B, uncompetitive with substrate C, etc.) again, allows for hundreds of specific equations to be derived (Chou, 1974). The mathematical deduction of these specific equations is greatly facilitated by taking the ratio of reaction rate equations in the presence (v_i) and absence (v_0) of an inhibitor. This ratio (v_i/v_0) is the fraction that is unaffected or uninhibited (f_u). Taking the ratio of f_i/f_u or $(1 - f_u)/f_u$ is equal to $[(f_u)^{-1} - 1]$ or $[(1 - f_u)^{-1} - 1]^{-1}$, where $1 - f_u = f_a$ (the fraction that is affected or inhibited). By the system and pattern analysis and by mathematical induction and deduction, it is shown that the ratio of $(1 - f_u)/f_u$, in turn, is always equal to the ratio of $(I/IC_{50})^m$,[1] where m is the kinetic order. More importantly, it is shown that $K_i/I_{50} = E_x/E_t$, where E_t is the total amount of enzyme and E_x is the fractional availability of the enzyme species with which the inhibitor may combine to (Chou, 1974; Chou and Talalay, 1981). This relationship holds irrespective of the number of substrates or products or their reaction mechanisms and it is also irrespective of the mechanism type of inhibition of the inhibitor. Therefore, this approach allows kinetic constants such as K_m and K_i as well as V_{max}, to be canceled out, leaving only the dose-effect relationship of the inhibitor.

Pattern analysis on numerous specific equations by using an approach similar to the mathematical deduction created the median-effect equation in 1976 (Chou, 1976, 1977), which is called *the general theory of dose and effect*. It is shown that the dose-generated effects are not random variables. There is a fundamental rule, i.e., the mass-action law, that underlies and governs them. They are not governed by empirical curves. Most importantly, it is shown that "dose" and "effect" are interchangeable.

Similarly, the introduction of multiple inhibitors, such as I_1 competitive with substrate A and noncompetitive with substrate B, and I_2 competitive with substrate B and noncompetitive with substrate C, etc., again, allows for the derivation of hundreds of specific equations (Chou and Talalay, 1981). Using pattern analysis and the ratio of equations for mathematical deduction, *the multiple drug-effect equation* was derived and introduced by Chou and Talalay (1977, 1981), presented as *the combination index equation* (Chou and Talalay, 1983, 1984), and is also called *the combination index theorem* (Chou and Martin, 2005).

The logical steps for the derivation of the above theory and theorems are given in Fig. 2a and the flow chart of the method of derivation using the median-effect as the common link is given in Fig. 2b, along with the relevant references. More details of derivations are given in Appendix I. The fundamental equation of dose and effect, as well as the general theorems indicated above, should hold regardless of the number of reactants (substrates, products, and inhibitors), of the reaction mechanism (ordered sequential, ping-pong, or random), or the type of inhibition (competitive, noncompetitive, or uncompetitive) and, therefore, can be generally applied to diverse fields of biology, including biochemistry, pharmacology, and medicine.

[1] Abbreviations: IC_{50} (or D_m), concentration (or dose) required to inhibit (or to affect) a system by 50%; CI, combination index; DRI, dose-reduction index; HIV, human immunodeficiency virus; MDR, multidrug resistance; MTD, maximal tolerated dose; MEP, median-effect principle; VP-16, etoposide; SDA, serial deletion analysis; MSKCC, Memorial Sloan-Kettering Cancer Center; HSV, herpes simplex virus; MGH, Massachusetts General Hospital; MAb, monoclonal antibody; AZT, 3′-azido-3′-desoxythymidine; CPT-11, irinotecan; 5-FU, 5-fluorouracil; IFN, interferon; GCSF, granulocyte colony stimulating factor; CCNU, lomustine; EGFR, epidermal growth factor receptor; Ara-C, 1-β-D-arabinofuranosylcytosine; r, recombinant; AZT, zidovudine; DDC, 2′,3′-dideoxycytidine; DDI, 2′,3′-dideoxyinosine, didanosine; HIV-1 or HIV/AZT, zidovudine-sensitive or -resistant HIV-1; RO-131, a protein inhibitor from Roche Pharmaceuticals; BI-RG-587, *N*11-cyclopropyl-4-methyl-5,11-dihydro-6*H*-dipyrido[3,2-*b*:2′,3′-*e*]-[1,4]diazepine-6-one, nevirapine; C_SA, cyclosporine; Rapa, rapamycin (sirolimus); FK-506, tacrolimus; CisPt, cis-diammine-dichloroplatinum(II); TK, thymidine kinase; LY294002, 2-(4-morpholinyl)-8-phenyl-chromone; ADP-R, ADP-ribose; dUrd, deoxyuridine; MTX, methotrexate; D4T, 2′,3′-didehydro-2′,3′-didesoxythymidine; NEV, nevirapine; ABT-538 (A-84538), (2*S*,3*S*,5*S*)-5-[*N*-[*N*-[[*N*-methyl-*N*-[(2-isopropyl-4-thiazolyl)methyl]amino]carbonyl]valinyl]amino]-2-[*N*-[(5-thiazolyl)methoxycarbonyl]amino]-3-hydroxy-1,6-diphenylhexane (for more specific information on some of the abbreviations used in this article, please see Glossary on page 672).

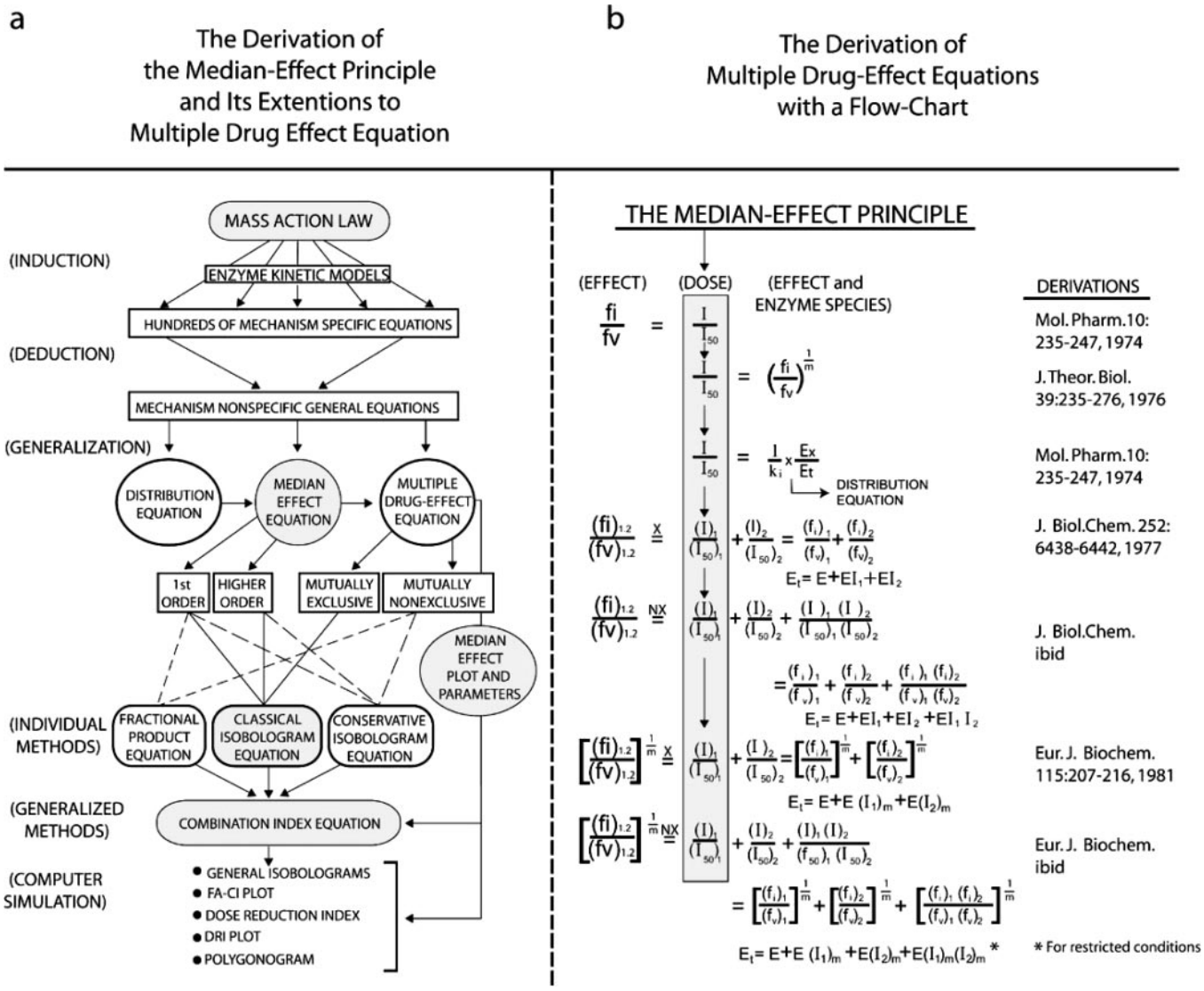

FIG. 2. Derivation of the median-effect equation as the general theory for the related theorems (updated from Chou, 1991). a, merging the mass-action law with mathematical induction-deduction to derive general equations to create individual methods, general methods, and computer software. b, flow chart showing the derivation of the multiple drug-effect equation from the single drug-effect equation and the derivation of the higher order equation from the first order equation using the median-effect principle as the common link. f_i, fractional inhibition; f_v, fractional velocity that is not inhibited; X, mutually exclusive among inhibitors; NX, mutually nonexclusive among inhibitors. More details of the derivation are given in Appendix I. Figure modified from "Quantitation of Synergism and Antagonism of Two or More Drugs by Computerized Analysis," Chou TC, in *Synergism and Antagonism in Chemotherapy* (Chou TC and Rideout DC eds) pp 223–244. Copyright 1991 with permission from Elsevier.

B. The Derivation of Equations and Theorems Based on the Mass-Action Law

1. The Median-Effect Equation. A systematic analysis, with the classic kinetic models of enzyme-substrate-inhibitor interactions with different number of substrates, different reaction mechanisms, and different types or mechanisms of inhibition has been carried out (Chou, 1974). It has been concluded that for all cases, fractional velocity (f_v) and fractional inhibition (f_i) in the presence of an inhibitor (I) can be expressed by

$$f_v = [1 + (I/K_i)(E_x/E_t)]^{-1} \quad (1)$$

and

$$f_i = [1 + (K_i/I)(E_t/E_x)]^{-1} \quad (2)$$

respectively, where K_i is the enzyme-inhibitor dissociation constant, E_t is the total amount of enzyme, and E_x is the amount of the enzyme species with which the inhibitor may combine. The ratio E_x/E_t can be quantitatively expressed by the distribution equation for each reaction mechanism of the enzyme and for each inhibition mechanism of the inhibitor (Cleland, 1963; Chou, 1974). By definition, $f_v = v_i/v$ and $f_i = (v - v_i)/v$, where v_i and v are the reaction velocities in the presence and absence of an inhibitor.

Another general relation was induced from the analysis (Chou, 1974) which gives

$$K_i/I_{50} = E_x/E_t \quad (3)$$

where I_{50} is the concentration of I required for 50% inhibition.

Therefore, K_i will never be greater than I_{50}, and the ratio of K_i and I_{50} expresses the fractional distribution of the enzyme species in an enzyme reaction under specified experimental conditions. Thus, the ratio provides a simple experimental basis for determining the availability of the enzyme species for inhibitor binding.

Substitution of eq. 3 into eqs. 1 and 2 gives

$$f_v = 1/[1 + (I/I_{50})] \quad (4)$$

and

$$f_i = 1/[1 + (I_{50}/I)] \quad (5)$$

Therefore, if I_{50} is known, the degree of inhibition at any other concentrations of the inhibitor can be calculated.

Dividing eq. 5 by eq. 4 gives another form of describing the median-effect principle:

$$f_i/f_v = I/I_{50} \quad (6)$$

Further analysis with the pharmacological receptor system, yielded a similar conclusion, which led to a general median-effect equation. The *median-effect equation* (Chou, 1976, 1977) describes dose-effect relationships in the simplest possible term, which is given by

$$f_a/f_u = (D/D_m)^m \quad (7)$$

where D is the dose (or concentration) of a drug, f_a is the fraction affected by D (i.e., percentage inhibition/100), and f_u is the fraction unaffected (i.e., $f_u = 1 - f_a$). D_m is the median-effect dose (e.g., IC_{50}, ED_{50}, or LD_{50}) that inhibits the system under study by 50%, and m is the coefficient signifying the shape of the dose-effect relationship, where $m = 1$, > 1, and < 1 indicate hyperbolic, sigmoidal, and flat sigmoidal dose-effect curves, respectively (Chou, 1976, 1977). Equation 7 is believed to be the simplest possible form for relating the dose (right side) and the effect (left side). Rearranging it yields

$$D = D_m [f_a/(1 - f_a)]^{1/m} \quad (8)$$

and

$$f_a = 1/[1 + (D_m/D)^m] \quad (9)$$

Therefore, *the dose and the effect are interchangeable* since the dose (D) for any given degree of effect (f_a) in eq. 8 can be determined if the values for D_m and m are known. Likewise, in eq. 9, the effect (f_a) for any given dose (D) can be determined if the values for D_m and m are known (Chou, 1975).

Plotting $x = \log(D)$ versus $y = \log(f_a/f_u)$ based on the logarithm form of eq. 7, as defined by Chou, is called *the median-effect plot* (Chou, 1976), where

$$\log(f_a/f_u) = m \log(D) - m \log(D_m) \quad (10)$$

linealizes all the hyperbolic and sigmoidal dose-effect curves. Note that eq. 10 has the form of a classic straight line equation:

$$y = mx + b \quad (11)$$

In the median-effect plot, m is the slope and (D_m) is the antilog of the x-intercept, which can be easily determined. As indicated above, $m = 1$, > 1, and < 1 signify hyperbolic, sigmoidal, and flat sigmoidal dose-effect curves, respectively. On the basis of eqs. 10 and 11, the D_m value can be calculated easily by the following:

$$D_m = 10^{-(y-\text{intercept})/m} \quad (12)$$

An example for transforming the dose-effect curves into a linear form by the median-effect plot is illustrated in Fig. 3.

The conformity of the data to the median-effect plot of the mass-action law can be readily manifested by the linear correlation coefficient (r) of the median-effect plot in which $r = 1$ indicates perfect conformity. The use of the median-effect principle for a dose-effect analysis is a distinct departure from the conventional statistical approach in which an *empirical curve* is drawn to fit the scattering data points. However, in Chou's approach, the scattering data points are used to fit *the median-effect principle of the mass-action law*. Using a statistical approach, it is not possible to draw a "curve" for the accurately determined "two data points," whereas this can be accomplished with ease using the median-effect principle (see analysis for Tables 7–9). Many empirical formulae in biomedical sciences, such as the power law (Nordling, 1953; Armitage and Doll, 1954), the logit law (Reed and Berkson, 1929), or the probit law (Finney, 1952) can linealize dose-effect curves reasonably well. However, their coefficients or parameters and their slopes and intercepts in the plots have no physical or chemical bearings. These empirical approaches or statistical approaches render enormous difficulties when dealing with more complicated situations, such as drug combinations.

2. The Unified Theory. It should be noted that the parameters of the median-effect equation (eq. 7) have physical bearings related to the mass-action law. Thus, D_m signifies potency, m signifies the shape of the dose-effect curve ($m = 1$, hyperbolic; $m > 1$, sigmoidal; or $m < 1$, flat sigmoidal), and r signifies the conformity of the data to the mass-action law (Chou, 1976). Computer software has been developed to facilitate the simulation and the automated calculation of these parameters from the dose-effect data (Chou and Chou, 1985; Chou and Hayball, 1997; Chou and Martin, 2005). It should also be noted that both sides of the generalized median-effect equation (eq. 7) are ratios and, thus, are dimensionless quantities in equality.

As shown in Fig. 4, rearrangement of the median-effect equation and/or taking its logarithmic form gives

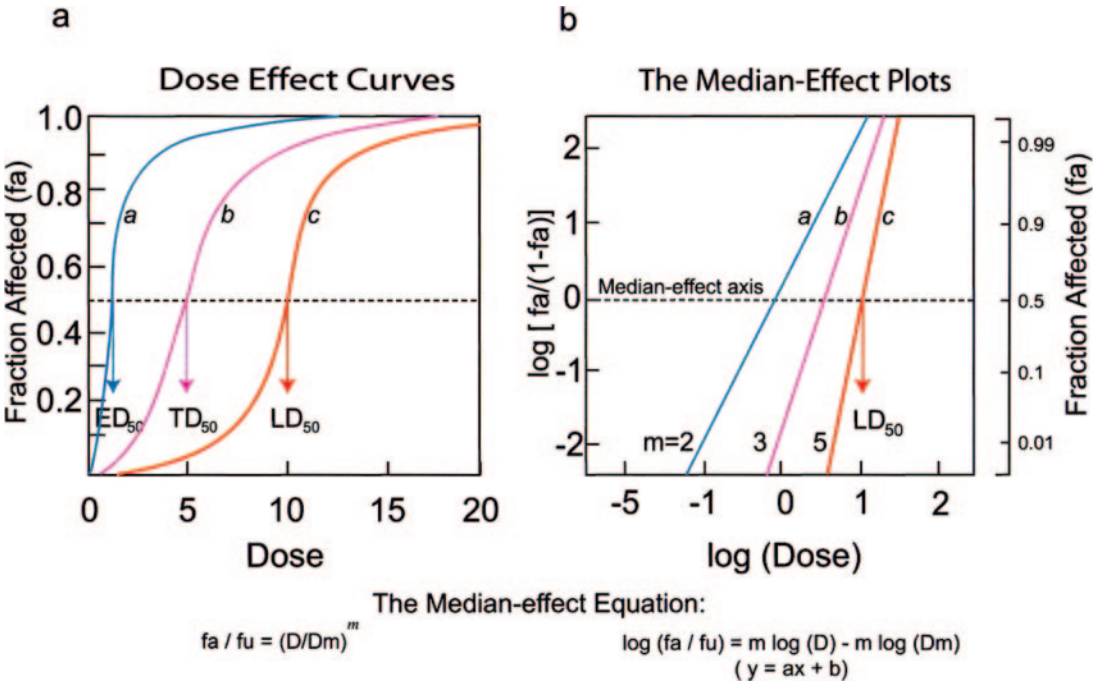

FIG. 3. Transformation of various sigmoidal dose effect curves (a) into the corresponding linear forms (b) by the median-effect plot, where $y = \log(f_a/f_u)$ versus $x = \log(D)$. The slopes (in this case, equal to 2, 3, and 5 for curves *a, b,* and *c*) signify the degree of sigmoidicity, and the antilogs of the x-intercepts on the axis, where $f_a/f_u = 1$ [or $\log(f_a/f_u) = 0$], give the D_m values, which signify the potency of each drugs, such as ID_{50}, ED_{50}, or LD_{50}.

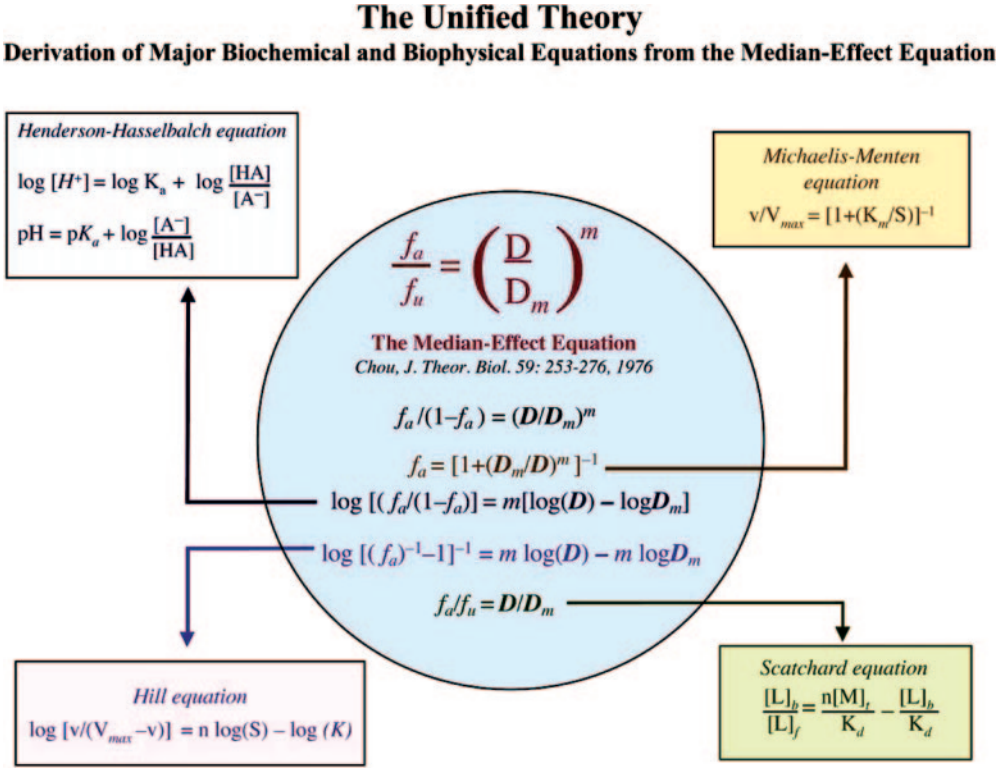

FIG. 4. The median-effect equation as the unified general theory for the Michaelis-Menten, Hill, Henderson-Hasselbalch, and Scatchard equations. See Chou (1977, 1991). Reproduced from "Quantitation of Synergism and Antagonism of Two or More Drugs by Computerized Analysis," Chou TC, in *Synergism and Antagonism in Chemotherapy* (Chou TC and Rideout DC eds) pp 223–244. Copyright 1991 with permission from Elsevier.

rise to the four major equations in biomedical sciences, i.e., the Michaelis-Menten equation (Michaelis and Menten, 1913) for first-order enzyme kinetics ($m = 1$); the Hill (1910, 1913) equation for primary ligand occupancy at high order of biological receptors, such as oxygen-hemoglobin interaction ($m = n$); the Scatchard (1949) equation for ligand-receptor binding and dissociation; and the Henderson-Hasselbalch equation for pH ioniza-

tion (Clark, 1928; Goldstein et al., 1968). Thus, equations that share the same mathematical form may have different physicochemical meanings. A comparison of distinctions between the median-effect equation (Chou, 1976) and the Hill (1913) equation are given in Table 2. When the endpoint of the measurement of the *fraction affected* (f_a) (e.g., the fractional inhibition, f_i, or percent inhibition/100) in the median-effect equation is changed to fractional saturation, fractional occupancy, fractional binding, and fractional ionization, respectively, the correspondence among the above-mentioned equations becomes clear. Retrospectively, it is not surprising that half-affected (D_m) is corresponding to half-saturated (K_m), half-occupied (K), half-bound and half-free (K_D), and half-ionization, the antilog of (pK_a), where pH = $-\log [H^+]$ (Chou, 1977, 1991; Chou and Chou, 1990b).

Thus, the four major equations pioneered by Michaelis-Menten, Hill, Henderson-Hasselbalch, and Scatchard with obviously different appearances for different purposes in biomedical sciences can all be derived from the median-effect equation of the mass-action law principle. Thus, the median-effect equation is called the general theory of dose and effect. The normalization of the dose-effect curves based on eq. 4 is illustrated in Fig. 5. As indicated in the this subsection, the general equation of median and effect even allows *drawing a dose-effect curve for only two data points*.

C. Extension of Mass-Action Law to Multiple Drug-Effect Systems

1. The Multiple Drug-Effect Equation. The median-effect equation for a single drug can be extended to multiple drugs. Thus, for a two-drug combination, in a first-order system (when $m = 1$), we get (Chou and Talalay, 1981, 1984; Chou et al., 1983)

$$\frac{(f_a)_{1,2}}{(f_u)_{1,2}} = \frac{(f_a)_1}{(f_u)_1} + \frac{(f_a)_2}{(f_u)_2} = \frac{(D)_1}{(D_m)_1} + \frac{(D)_2}{(D_m)_2} \tag{13}$$

and when $m \neq 1$, then

$$\left[\frac{(f_a)_{1,2}}{(f_u)_{1,2}}\right]^{1/m} = \left[\frac{(f_a)_1}{(f_u)_1}\right]^{1/m} + \left[\frac{(f_a)_2}{(f_u)_2}\right]^{1/m} = \frac{(D)_1}{(D_m)_1} + \frac{(D)_2}{(D_m)_2} \tag{14}$$

More detailed derivations for the multiple drug-effect equation are given in Fig. 2; see also Appendix I.

Equations 13 and 14 are based on the generalized assumption that two drugs share similar modes of action (i.e., effects are mutually exclusive), which is in complete agreement with the assumption of the classic isobologram. If one assumes that two drugs have totally different modes of actions (i.e., effects are purely mutually nonexclusive), then the resulting equation should, in theory, have a third term, which is the product of the first two terms (Chou and Talalay, 1984), thus,

$$\left[\frac{(f_a)_{1,2}}{(f_u)_{1,2}}\right]^{1/m} = \frac{(D)_1}{(D_m)_1} + \frac{(D)_2}{(D_m)_2} + \frac{(D)_1(D)_2}{(D_m)_1(D_m)_2} \tag{15}$$

Because partially exclusive or partially nonexclusive (i.e., nonpure) cases may exist and eq. 15 may underestimate synergistic drug interactions, it is concluded that eq. 14 should be used as the "base equation" and that any mutually nonexclusive condition, if it exists, should be considered as a contributing factor for the intrinsic synergistic effect under the assumption of eq. 14 (Chou, 1991; Chou JH, 1991).

When two drugs are combined and subjected to serial dilutions, the combined mixture of the two drugs behaves as the third drug for the dose-effect relationship. Thus, $y = \log [(f_a)_{1,2}/(f_u)_{1,2}]$ versus $x = \log [(D)_1 + (D)_2]$ will give $m_{1,2}$, $(D_m)_{1,2}$, and $r_{1,2}$ values (Chou, 1991).

2. The Combination Index Theorem and Plot. Based on eqs. 13 and 14, Chou and Talalay in 1983 introduced the term *combination index* (CI) for quantification of synergism or antagonism for two drugs (Chou and Talalay, 1983, 1984; Chou, 1991):

$$CI = \frac{(D)_1}{(D_x)_1} + \frac{(D)_2}{(D_x)_2} = \frac{(D)_1}{(D_m)_1[f_a/(1-f_a)]^{1/m_1}} + \frac{(D)_2}{(D_m)_2[f_a/(1-f_a)]^{1/m_2}} \tag{16}$$

where CI $<$ 1, $=$ 1, and $>$ 1 indicate synergism, additive effect, and antagonism, respectively. In the denominator, (D_x) is for D_1"alone" that inhibits a system x%, and $(D_x)_2$ is for D_2"alone" that inhibits a system x%. The $(D_x)_1$ and $(D_x)_2$ values can be calculated from eq. 8. In the numerators, $(D)_1 + (D)_2$"in combination" also inhibit x%. If the sum of these two fractional terms in eq. 16 is equal to 1, additive is indicated. If the CI value is smaller than 1, synergism is indicated, and if the CI value is greater than 1, antagonism is indicated.

A plot of CI on the y-axis as a function of effect levels (f_a) on the x-axis is called F_a-CI plot or in brief, CI plot

TABLE 2
Comparison of the median-effect equation and the Hill equation

Median-Effect Equation[a]	Hill Equation and Michaelis-Menten Equation[b]
$\frac{fa}{fu} = \left(\frac{D}{Dm}\right)^m$	$\frac{v}{Vmax} = \frac{S^n}{S^n + K}$
$\log[(f_a)^{-1} - 1]^{-1} = m \log D - m \log D_m$ when $m = 1$: $f_a = 1/[1 + (D_m/D)]$	$\log[v/(V_{max} - v)] = n \log S - \log K$ when $n = 1$: $v/V_{max} = 1/[1 + (K_m/S)]$

[a] Features: 1) inhibitor-oriented; 2) for ligand effect; 3) easily expandable to two or more inhibitors; 4) derived by mathematical induction and deduction.
[b] Features: 1) substrate-oriented; 2) for substrate saturation; 3) difficult to expand to two or more substrates; 4) derived by phenomenal observation and reasoning.

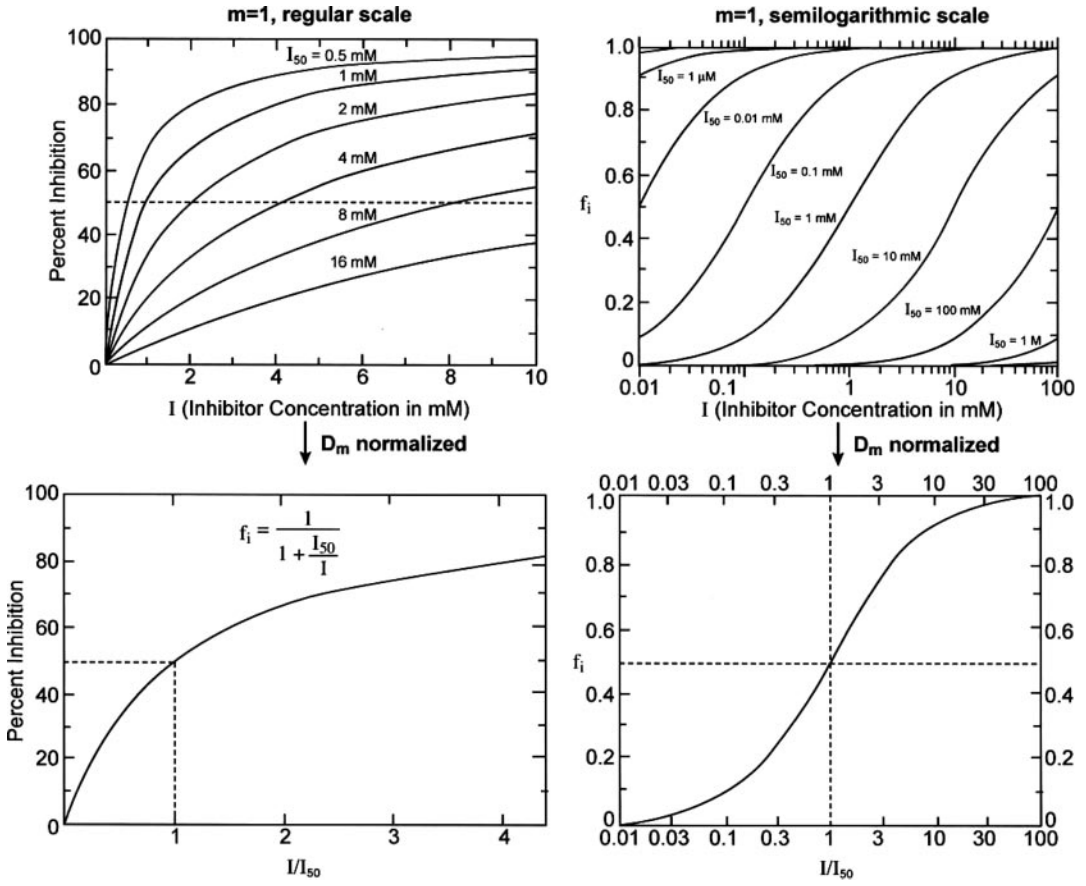

FIG. 5. Normalization of dose-effect curves by the D_m (IC_{50}) values. Left, plots based on eq. 4 in which IC_{50} values range from 0.5to 16 mM and [I] concentrations range from 0 to 10 mM. Right, [I] varies from 0.01 to 100 mM and IC_{50} values range from 0.1 μM to 10 M. Reprinted from "Derivation and Properties of Michaelis-Menten Type and Hill Type Equations for Reference Ligands," *Journal of Theoretical Biology*, volume 59, pp 253–276. Copyright 1976 with permission from Elsevier.

(Chou and Talalay, 1981, 1984). It should be noted that the extreme end of the CI values for synergism is 0 to 1 and for antagonism is 1 to infinity. F_a-log(CI) plot, not only reduces the out-of-scale points in the F_a-CI plot, but also makes the presentation symmetrical with the *additive effect axis* (CI = 1) locating at zero [i.e., log(CI) = log(1) = 0]. Therefore, in the F_a-log(CI) plot, synergism is indicated by a negative value [i.e., log(CI) <0], and antagonism is indicated by a positive value [i.e., log(CI) > 0]. Therefore, at a special case of eq. 16 when CI = 1, the classic ED_{50} isobologram for two drugs at ED_{50} is described as (Chou and Talalay, 1981, 1984)

$$\frac{(D)_1}{(D_m)_1} + \frac{(D)_2}{(D_m)_2} = 1 \qquad (17)$$

and the ED_x isobologram for two drugs for x% inhibition is described as

$$\frac{(D)_1}{(D_x)_1} + \frac{(D)_2}{(D_x)_2} = 1 \qquad (18)$$

Figure 6a illustrates the conventional "classic isobologram" and Fig. 6b illustrates the dose-normalized isobologram. The typical isobolograms and their interpretations are also illustrated in Fig. 8b and 8c.

3. The General Equation for Combination of n Drugs. The detailed description for the derivation of the multiple drug-effect equation based on the median-effect principle (Chou, 1976) has been given in Chou and Talalay (1977, 1981, 1984). This process, including the flow chart, has been outlined in Fig. 2 of this article. The early steps of derivations are summarized in Appendix I, which lead to the combination index equation.

Similar to eq. 16, the general equation of a five-drug combination at x% inhibition is

$$\begin{aligned} {}^5(CI)_x = {} & \frac{(D_x)_{1\text{–}5}[P/(P+Q+R+S+T)]}{(D_m)_1\{(f_{a_x})_1/[1-(f_{a_x})_1]\}^{1/m_1}} \\ & + \frac{(D_x)_{1\text{–}5}[Q/(P+Q+R+S+T)]}{(D_m)_2\{(f_{a_x})_2/[1-(f_{a_x})_2]\}^{1/m_2}} \\ & + \frac{(D_x)_{1\text{–}5}[R/(P+Q+R+S+T)]}{(D_m)_3\{(f_{a_x})_3/[1-(f_{a_x})_3]\}^{1/m_3}} \\ & + \frac{(D_x)_{1\text{–}5}[S/(P+Q+R+S+T)]}{(D_m)_4\{(f_{a_x})_4/[1-(f_{a_x})_4]\}^{1/m_4}} \\ & + \frac{(D_x)_{1\text{–}5}[T/(P+Q+R+S+T)]}{(D_m)_5\{(f_{a_x})_5/[1-(f_{a_x})_5]\}^{1/m_5}} \end{aligned} \qquad (19)$$

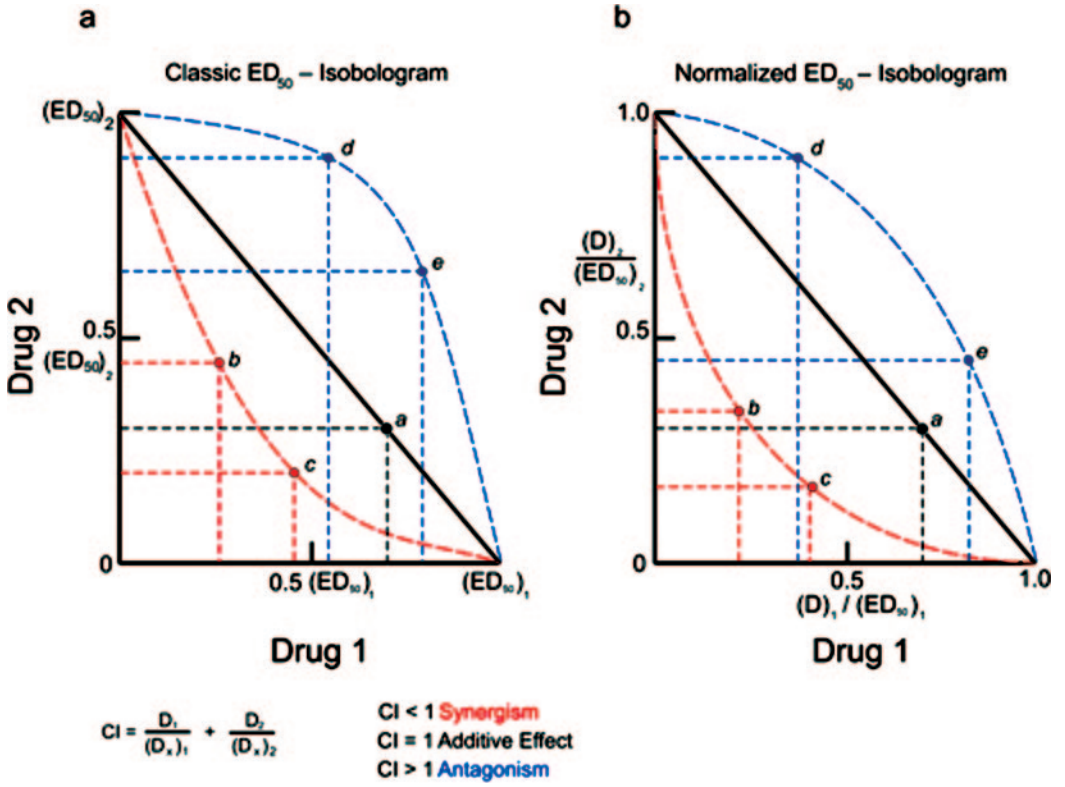

FIG. 6. The ED_{50} isobologram. a, classic isobologram for two drugs with actual doses on the *x*- and *y*-axis. b, dose-normalized isobologram for two drugs with normalization of dose with ED_{50} to unity on both *x*- and *y*-axis. In both cases, ED_{50} can be extended to ED_x for the *x*% inhibition. The isobols hold irrespective of the combination ratio or shapes of dose-effect curves and irrespective of the mechanisms of the drugs or the units of the drugs. If the combination data points fall on the hypothenuse (e.g., point *a*), an additive effect is indicated. If the combination data points fall on the lower left (e.g., points *b* and *c*) or on the upper right (e.g., points *d* and *e*), synergism or antagonism is indicated, respectively. If the combinations are in a constant ratio, the classic isobologram (a) can be constructed with a stroke of the key using computer software (Chou JH and Chou, 1985; Chou and Hayball, 1997; Chou and Martin, 2005). If the combinations are in nonconstant ratios (e.g., varying the doses of drug 1 while keeping the dose of drug 2 constant), the normalized isobologram (b) can be constructed automatically (see Fig. 8, b and c). The constant-ratio combination design [e.g., at $(ED_{50})/(ED_{50})_2$ ratio] is recommended. Multiple dose-effect data points for each drug *alone* is a prerequisite for drug combination studies so that m_1, $(D_m)_1$, m_2, and $(D_m)_2$ values can be determined, whereas the number of the combination data points can be one or more.

The general equation for *n*-drug combination at *x*% inhibition becomes

$$^{n}(\mathrm{CI})_x = \sum_{j=1}^{n} \frac{(\mathrm{D})_j}{(\mathrm{D}_x)_j}$$

$$= \sum_{j=1}^{n} \frac{(\mathrm{D}_x)_{1-n}\{[\mathrm{D}]_j/\sum_{1}^{n}[\mathrm{D}]\}}{(\mathrm{D}_m)_j\{(f_{a_x})_j/[1-(f_{a_x})_j]\}^{1/m_j}} \qquad (20)$$

where $^{n}(\mathrm{CI})_x$ is the combination index for *n* drugs at *x*% inhibition, $(D_x)_{1-n}$ is the sum of the dose of *n* drugs that exerts *x*% inhibition in combination, $([D]_j/\Sigma_1^n[D])$ is the proportionality of the dose of each of *n* drugs that exerts *x*% inhibition in combination, and $(D_m)_j\{(f_{a_x})_j/[1-(f_{a_x})_j]\}^{1/m_j}$ is the dose of each drug alone that exerts *x*% inhibition, where D_m is the median-effect dose (antilog of the *x*-intercept of the median-effect plot), f_{a_x} is the fractional inhibition at *x*% inhibition, and *m* is the slope of the median-effect plot, which depicts the shape of the dose-effect curve (where $m = 1$, > 1, and < 1 indicate hyperbolic, sigmoidal, and flat sigmoidal curve, respectively).

4. Algorithms for Determining Synergism and Antagonism. The combination index equation as shown in eqs. 16 and 20, in conjunction with eqs. 8 and 9, can be used as algorithms for computerized simulation for the combination index values at different effect levels (i.e., at different f_a values). This multiple-step calculation for simulation is shown in Fig. 7. The computer program for fully automated simulation has been developed (Chou and Chou, 1988). Chou and Talalay (1984) and Chou and Chou (1985) have named this graphic *the F_a-CI plot* and later *the combination index plot* or *the CI plot*. A typical F_a-CI plot and its interpretation is shown in Fig. 8a, where CI < 1, $= 1$, and > 1 indicate synergism, additive effect, and antagonism, respectively.

5. Main Features of the General Equation. The most unique and important feature for both the general theory of dose and effect (eq. 1) and the combination index theorem (eq. 20, including eqs. 13–18) is that *each term of the equation is a ratio*. So, for each drug entity, the

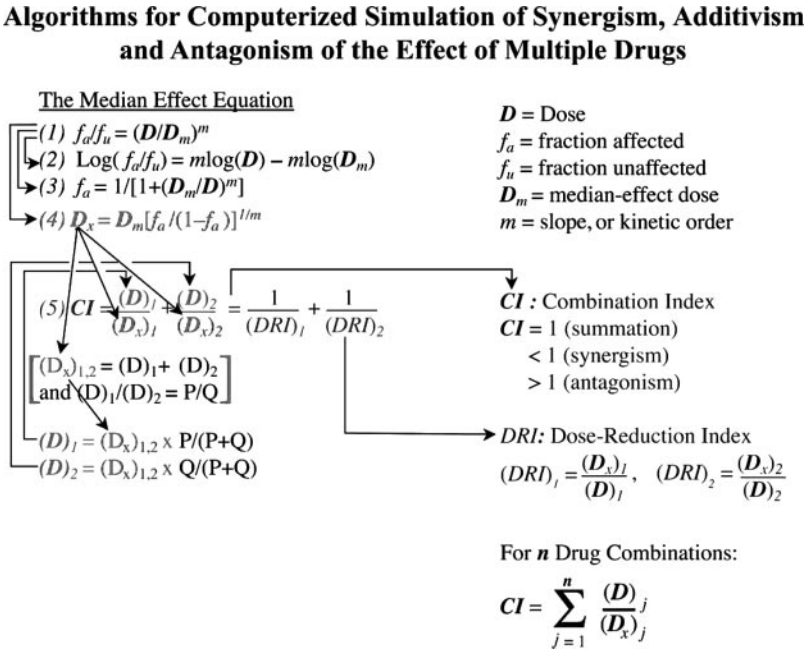

FIG. 7. Algorithms for computerized simulation of CI plot and DRI plot at different effect levels (f_a values). The combination ratio for $(D)_1$ and $(D)_2$ is designated as P/Q. Both plots are valid irrespective of the number of drugs combined, the combination ratios, the mechanisms of drugs, and the units of the drugs and irrespective of the nature of the targets. These algorithms are the bases for the computer software.

unit is canceled out and thus becomes a dimensionless quantity. This feature is essential for their general broad applicability. It is important to note here that based on the Web search of ISI citation records, one article alone (Chou and Talalay, 1984) has been cited in >1294 scientific papers in biomedical journals. Furthermore, due to the dimensionless feature of the combination index equation, D_1 can be in micromolar concentrations, D_2 in micrograms per milliliter, D_3 in international units, and D_4 in multiples of infection and their interactions in terms of synergism, additive effect, or antagonism can still be determined, as long as there is a conformity to the mass-action law principle (e.g., $r >$ 0.95). In addition, the drugs can be unknown entities without knowing their chemical structures, molecular weights, or mechanism of action. One may also combine one mixture with another mixture and determine their interactions (e.g., for Chinese herbal medicines). The applications have been extended to the combination of a drug with radiation or a drug combination at different oxygen tensions for cytotoxicity studies (Chou and Talalay, 1984; Chou, 1991; Chou JH, 1991). The application to hyperthermia and pH remains to be explored. However, these latter applications require very accurate measurements, since very steep dose-effect relationships (i.e., high m values in the median-effect plot) are expected.

As indicated above (see section II.B.2.), the median-effect equation allows the demonstration of how to draw a dose-effect "curve" with a minimum of only "two data points" if the data are accurately determined (see also Fig. 11 and Supplemental Data Appendices II and III; http://pharmrev.aspetjournals.org/cgi/content/full/pr.58.3.10/DC1). Furthermore, based on the combination index theorem, synergism or antagonism can be quantitatively determined for a minimum of only a "single combination data point" if the parameters (m and D_m) for each drug are determined by the median-effect plot (for examples, see the illustrations given in Supplemental Data Appendices II and III). Thus, these feature the simplest bare-bones situations for *any* dose-effect analysis. The applications of this theory and/or theorems not only provide sound rational basis for biomedical research but also allow for smaller experiments than in the past and, therefore, lead to saving time, effort, and research cost, as well as conserving the use of laboratory animals and, thus, minimizing the pain and suffering of laboratory animals in a general way (see section VI.D.).

6. The F_a-Combination Index Plot and Isobologram Are Two Sides of the Same Coin. An isobologram is a graph with equipotency sum of doses. The isobol concept was conceived about a century ago (Loewe, 1928, 1957; Berenbaum, 1989). However, it was not very well received then and generated some confusion and controversies. It lacked theoretical tools for rigorous treatment in the early studies. Several decades ago, researchers used graph paper for drawing isoeffective points from extrapolation or interpolation of dose-effect curves, which would take ½ h to complete. Now with the isobol equation, the median-effect principle, and the computer program that is widely available, multiple effect level isobolograms (e.g., ED_{50}, ED_{75}, and ED_{95} isobolograms)

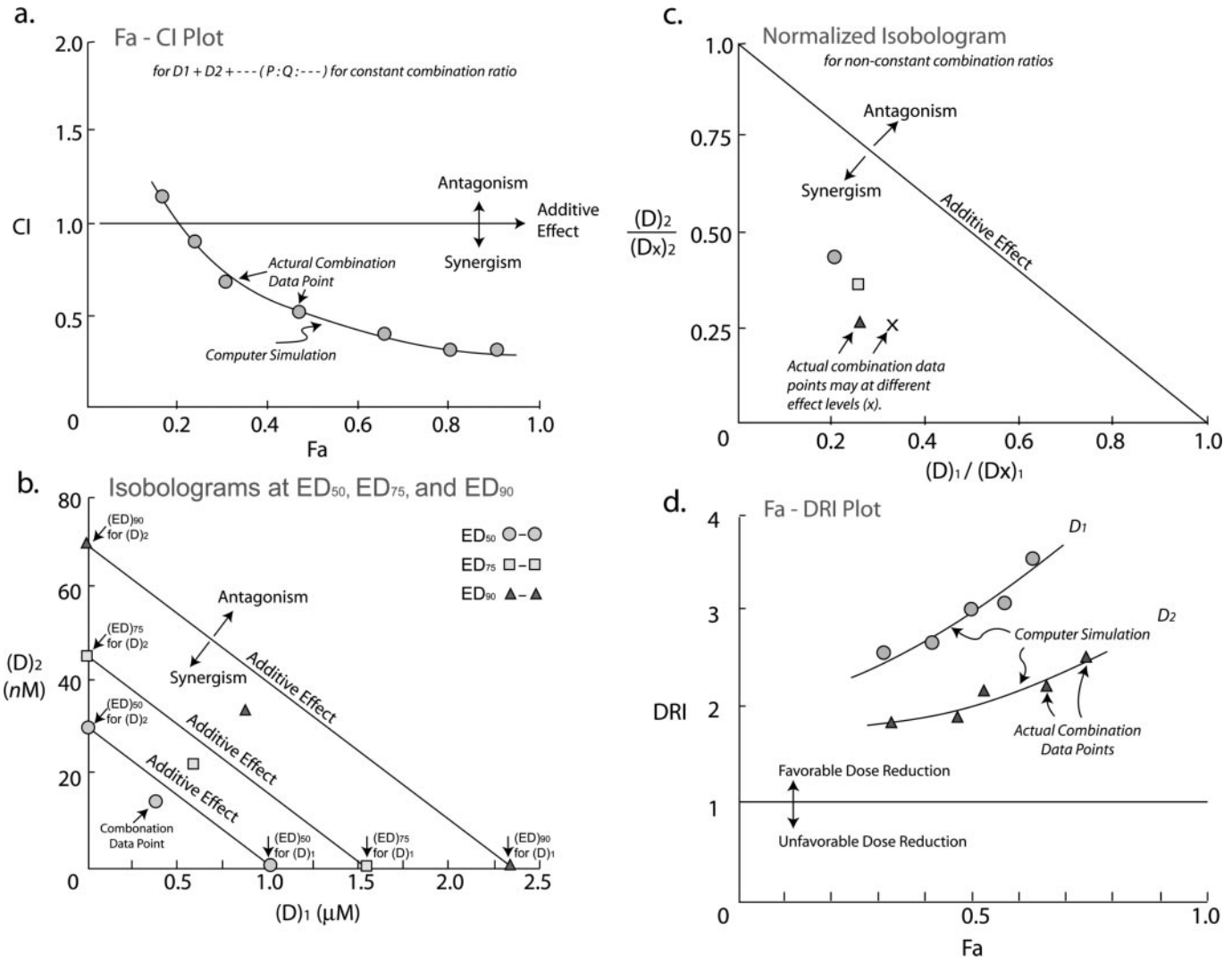

FIG. 8. Typical examples of drug combination plots and their interpretations based on the Chou and Talalay combination index theorem. a, F_a-CI plot. b, classic isobologram at ED_{50}, ED_{75}, and ED_{90}. c, normalized isobologram for combination at different combination ratios, and d, the F_a-DRI plot. All of these plots can be generated automatically by using CompuSyn (Chou and Martin, 2005).

for a pair of drugs can be constructed in a split second. For an example of an ED_{50} isobologram, see Fig. 6.

Webb's fractional product method for the inhibition of single substrate-single product Michaelis-Menten system with two inhibitors (Webb, 1963) had been expanded to the multiple-substrate and multiple-product Michaelis-Menten system ($m = 1$) with n inhibitors by Chou and Talalay (1977, 1981). A comparison of Webb's method and Loewe's method and the CI method for multidrug inhibition is given in Table 3.

In theory, both the isobologram and the F_a-CI plot of Chou and Talalay should yield exactly identical conclusions in drug combination studies, since both graphics are based on the same combination index equation. They are like two sides of the same coin: the isobologram is a *dose-oriented* graphic and the CI plot is an *effect-oriented* graphic, but both are based on the combination index theorem of Chou and Talalay.

However, the isobologram has some practical limitations. First, an isobologram has two dimensions, which is convenient for two-drug combinations. For three-drug combinations, it is not convenient to construct a three-dimensional isobologram, and even if it were constructed, it would not be easy to read (Chou and Chou, 1992). Alternatively, one can split n-drug combination into two parts and assign them to two axes (Chou, 1991). For example,

$$\sum_{j=1}^{n} = \sum_{j=1}^{m} + \sum_{j=m+1}^{n}$$

where $1 \leq m \leq n - 1$ and n and m are integers. Second, if two-drug isobolograms are shown at three or fewer effect levels (e.g., at ED_{50}, ED_{70}, and ED_{90}), usually the graph will be readable by inspection. But if an isobologram were to be constructed for four or more effect levels, it would usually be too messy to read because of data scattering or data point congestion or overlapping. By contrast, the CI plot of Chou and Talalay can be

TABLE 3
Comparison of applicability of different methods for drug combination studies
Modified from "Quantitation of Synergism and Antagonism of Two or More Drugs by Computerized Analysis," in *Synergism and Antagonism in Chemotherapy* (Chou TC and Rideout DC eds) pp 223–244. Copyright 1991 with permission from Elsevier.

	Nature of Dose-Effect Curves and Drug Interactions			
	Mutually exclusive (similar mode of action)[a]		Mutually nonexclusive (independent mode of action)[b]	
	First order[c]	Higher order[d]	First order[c]	Higher order[d]
Webb's fractional product method[e]	No	No	Yes	No
Loewe's isobologram method[f]	Yes	Yes	No	No
Multiple drug effect equation[g]	Yes	Yes	Yes	Yes

[a] Mutually exclusive drugs in mixture give a parallel median-effect plot with respect to each drug alone.
[b] Mutually nonexclusive drugs in mixture give a upwardly concave dose-effect curve with respect to each drug alone.
[c] Hyperbolic dose-effect curve.
[d] Sigmoidal dose-effect curve.
[e] $i_{1,2} = 1 - [(1 - i_1)(1 - i_2)]$ or $(f_u)_{1,2} = (f_u)_1 (f_u)_2$ (see Webb, 1963).
[f] See Loewe (1957).
[g] see Eq. 16, which is the classic isobologram for mutually exclusive drugs. The conservative isobologram is for mutually nonexclusive drugs (Chou and Talalay, 1984). Since the early 1990s Chou has proposed using the mutually exclusive assumption as the universal standard for synergism and antagonism analysis, and, therefore, integrated the nonexclusive condition as an intrinsic contribution to the synergistic effect in the overall synergism and antagonism analysis. Thus, the isobologram and the F_a-CI plot become two sides of the same coin (see section II.C.6 or Chou, 1991, 1994, 1998): the F_a-CI plot is 'effect-oriented', whereas the isobologram is 'dose-oriented'.

shown at all f_a levels simultaneously with any number of drugs that are combined.

7. How Much Synergism Is Synergy? We frequently hear that "drug A and Drug B in combination are synergistic." However, when this claim is made, there are a string of conditions that are attached to it. Obviously, the claim is valid for the experimental conditions and experimental designs that are used (e.g., temperature, oxygen tension, cell lines, species, gender, age, race, sequence of drug addition, ratio of drug combination, schedule of drug administration, and so on), although some variations in conditions may make little or no difference in the conclusions. After all, the synergism or antagonism determinations are based on the mass-action law principle.

At the extremes, synergism is CI = 0 to 1, and antagonism is CI = 1 to infinity. Therefore, log(CI) will provide symmetric presentation of the CI graphics [i.e., in the F_a-log(CI) plot for additive effect, log(CI) = 0; for synergism CI = 0.1 and 0.01 will give log(CI) = −1 and −2; for antagonism CI = 10 and 100 will give log(CI) = 1 and 2, etc.]. It is important to note that synergism and antagonism can be different at different dose levels or different effect levels. Therefore, in many publications, the CI and dose-reduction index (DRI) values are presented in the summary table for the ED_{50}, ED_{75}, ED_{90}, and ED_{95} levels (e.g., Chou et al., 1994, 2005). For some chronic or physiological conditions or diseases, synergism or antagonism at low dose or low effect levels is important. But for infectious diseases or cancer therapies, synergism at high effect levels (e.g., at ED_{90}, ED_{95}, or ED_{99}) is much more therapeutically relevant than at low effect levels (e.g., ED_{30} or ED_{50}). Therefore, synergism or antagonism at different effect levels may have different significance for different diseases. In addition, selective synergism against the target and antagonism toward the host is also of practical importance. Furthermore, whether the concentrations for synergism are achievable in the body (e.g., blood or body fluid) is also an issue to be considered.

In the past, Chou and co-workers have proposed semi-quantitative methods for describing the degrees of synergism or antagonism (Chou and Talalay, 1984; Chou and Hayball, 1997). These methods are now refined and expanded as shown in Table 4. Using the log(CI) grading, synergism is subdivided into (near) additive (±), slight synergism (+), moderate synergism (++), synergism (+++), strong synergism (++++), and very strong synergism (+++++). Antagonism is divided in the same way, except using "−" sign(s); thus, the corresponding symbols are ±, −, − −, − − −, − − − −, and − − − − − (Table 4). In polygonograms (Fig. 9), for visual distinction, synergism is represented by a solid line and antagonism is represented by a dash line. The degree of synergism or antagonism is represented by the thickness of the line. Synergism or antagonism in polygonograms can be represented by colors. Usually, synergism is represented by red-tone colors and antagonism is represented by blue-tone colors. Colors in the polygonogram are used for enhancing the visual contrast.

D. The Dose-Reduction Index Equation and Plot

One of the major objectives of having synergistic drug combination is to reduce the dose of the drug used, thereby reducing the toxicity while maintaining efficacy. The concept of *the dose-reduction index* was formally introduced by Chou JH and Chou TC in 1988 and has since been used in many publications (Chou, 1991, 1994; Chou JH, 1991; Chou et al., 1991, 1994; Bertino and Chou, 1997). The DRI is a measure of how many -fold the dose of each drug in a synergistic combination may be reduced at a given effect level compared with the doses of each drug alone. Simply by inverting each term of eqs. 16 and 20, the DRI value for each corresponding drug is given. Thus, for two-drug combinations

$$CI = \frac{(D)_1}{(D_x)_1} + \frac{(D)_2}{(D_x)_2} = \frac{1}{(DRI)_1} + \frac{1}{(DRI)_2} \qquad (21)$$

TABLE 4

Description and symbols of synergism or antagonism in drug combination studies analyzed with the combination index method

The combination index method is based on those described by Chou and Talahay (1984) and the computer software of Chou and Martin (2005). The ranges of CI and the symbols are refined from those described earlier by Chou (1991). CI < 1, = 1, and > 1 indicate synergism, additive effect, and antagonism, respectively [modified from Chou and Martin (2005)].

Range of Combination Index	Description	Graded Symbols	Graphic Symbols
<0.1	Very strong synergism	+++++	
0.1–0.3	Strong synergism	++++	
0.3–0.7	Synergism	+++	
0.7–0.85	Moderate synergism	++	
0.85–0.90	Slight synergism	+	
0.90–1.10	Nearly additive	±	
1.10–1.20	Slight antagonism	−	
1.20–1.45	Moderate antagonism	− −	
1.45–3.3	Antagonism	− − −	
3.3–10	Strong antagonism	− − − −	
>10	Very strong antagonism	− − − − −	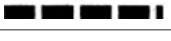

and for n-drug combinations

$$\mathrm{CI} = \sum_{j=1}^{n} \frac{(\mathrm{D})_j}{(\mathrm{D_x})_j} = \sum_{j=1}^{n} \frac{1}{(\mathrm{DRI})_j} \tag{22}$$

Therefore,

$$(\mathrm{DRI})_1 = \frac{(\mathrm{D_x})_1}{(\mathrm{D})_1}, (\mathrm{DRI})_2 = \frac{(\mathrm{D_x})_2}{(\mathrm{D})_2} \ldots, \text{etc}$$

or

$$(\mathrm{DRI})_1 = \frac{(D_\mathrm{m})_1[f_\mathrm{a}/(1-f_\mathrm{a})]^{1/m_1}}{(\mathrm{D})_1}, (\mathrm{DRI})_2 = \frac{(\mathrm{D_m})_2[f_\mathrm{a}/(1-f_\mathrm{a})]^{1/m_2}}{(\mathrm{D})_2} \tag{23}$$

The DRI is important in clinical situations, in which dose reduction leads to reduced toxicity toward the host while the therapeutic efficacy is retained. Although DRI > 1 is beneficial, it does not necessarily indicate synergism because, from the above equation, an additive effect or even slight antagonism may also lead to DRI > 1. If drug A and drug B each inhibit 50%, and if (0.5A + 0.5B) also inhibits 50% and if both drugs have no overlapping toxicity toward the host, then indeed DRI ≥1 may still be beneficial. The greater DRI value indicates a greater dose reduction for a given therapeutic effect, but does not necessarily always indicate synergism, as shown by the mathematical relationship of CI and DRI given in eq. 21.

Facilitating the use of the above, the computer program for automated simulation of DRI values at different f_a values for each drug in the combination (i.e., the DRI table or the DRI plot) has been developed (Chou and Martin, 2005). Selected examples for the F_a-DRI plots and the F_a-log(DRI) plots are illustrated in section VI. and Supplemental Data Appendices II through V (http://pharmrev.aspetjournals.org/cgi/content/full/pr.58.3.10/DC1). A typical F_a-DRI plot and its interpretation are illustrated in Fig. 8d.

E. The Polygonogram

The concept of the polygonogram comes not from mathematical derivations but rather from practical utility (Chou et al., 1994; Chou and Martin, 2005). For example, 7 drugs may have 120 possible combinations (i.e., $\Sigma\, C_\mathrm{r}^7 = 120$). It would be difficult to memorize and to contemplate these ramifications. As shown in Fig. 9a and discussed in section VI.C.3., a heptagonal graph for 7 anti-HIV agents allows a simplified visual presentation of the overall results (for the full report, see the CompuSyn printout in Supplemental Data online at http://pharmrev.aspetjournals.org/cgi/content/full/pr.58.3.10/DC1). Supplemental Data Appendix IV gives the experimental example of the polygonograms for the combination studies of five anticancer agents with different mechanism of actions. In Fig. 9b, pentagonal polygonograms based on two- and three-drug combinations are shown (Chou et al., 1994) with a red solid line representing synergism and a blue broken line representing antagonism, and the thickness of the line representing strong and weak, respectively. The combination results from two to n drugs (in this case, n being five or seven drugs) can now be shown in one page graphically for easy inspection. The polygonogram in solid synergistic patterns may be used to pick out the potentially interesting combinations for further exploration. To some extent, the polygonogram also allows the projection (or

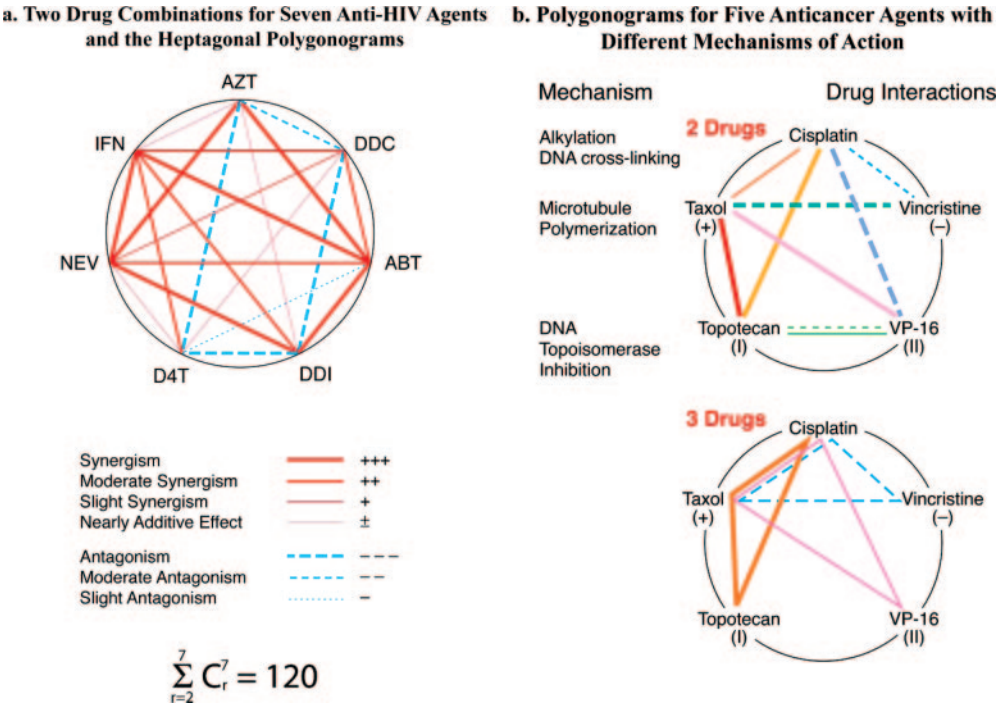

FIG. 9. Sample illustration of polygonograms. a, heptagonal polygonogram for seven anti-HIV agents using two-drug combinations in vitro (AZT, D4T, DDC, and DDI—all nucleoside reverse transcriptase inhibitors; NEV, a non-nucleoside reverse transcriptase inhibitor; INF, interferon-α-2a; and ABT-538, a protease inhibitor). Details of experimental results leading to this polygonogram are given in section VI.C.3. There are 120 possible combinations for seven drugs. More details are given in section VI.C.3., Fig. 12, and Tables 20 through 23. The CompuSyn printout (90 pages) for two- to five-drug combinations is given in Supplemental Data (http://pharmrev.aspetjournals.org/cgi/content/full/pr.58.3.10/DC1). Synergism is represented by the solid red-tone line, and antagonism is represented by the broken blue-tone line. The thickness of the line represents the strength of synergism or antagonism. A recommended semiquantitative description of the degrees of synergism and antagonism is shown. b, polygonograms for five antitumor agents with different mechanisms of action. Crude experimental data and the summary of analytical results are given in Tables 10 and 11 (Data from Chou et al., 1994). Further analysis for the complete CompuSyn report for printout is given in Supplemental Data Appendix IV.

prediction) of the combination outcomes in cases for which the experiments have not yet been carried out. For example, from the results of *many* two-drug combinations as shown in Fig. 9, one may semiqualitatively and semiquantitatively predict what would happen with three- or four-drug combinations (see also sections VI.A.3. and VI.C.3.).

III. Experimental Design for Drug Combinations

A. The Prerequisite and Theoretical Minimum Requirements for Drug Combination Studies

The prerequisite for synergism or antagonism determination is to know both the "potency" and the "shape" of the dose-effect curve for each drug. Therefore, it is necessary to know the dose-effect parameters of each drug alone [e.g., m_1, $(D_m)_1$, r_1, m_2, $(D_m)_2$, and r_2 for two-drug combinations] and thereby determine the CI value, which can be calculated based on eq. 16 for two-drug combinations or eq. 20 for n-drug combinations. Thus, the experiment for the dose-effect curves for each drug alone needs to be carried out. The above parameters can be easily determined from the median-effect plot (see Fig. 3) by using graph paper, but the available computer software can automatically calculate them with ease. It is highly recommended that the parameters for the combination [e.g., for two drugs, $m_{1,2}$, $(D_m)_{1,2}$, and $r_{1,2}$] be acquired, but they are not absolutely necessary, because for even a single data point (from a single combination dose) of a drug combination mixture, the CI value can still be calculated by eq. 16 or eq. 20. Thus, the theoretical minimum of data points for a two-drug combination is five [i.e., two points for each drug alone and one point for the combination, with effects (f_a) being calculated relative to the control]. However, for the in vitro drug combination studies, in which experiments are easily carried out, each drug and its combinations usually consist of five to eight data points. By contrast, for the in vivo studies, usually the numbers of data points are somewhat reduced (e.g., three to five data points each) because of the practicality of the sample size, experimental manipulability, and costs. In drug combination studies, the experiments for a single drug and its combinations should be carried out simultaneously to ensure the same experimental conditions, such as avoiding drug decomposition due to instability, variability due to assay conditions, personnel changes, and cells or animal inconsistency.

For determining synergism or antagonism, the knowledge of "mechanisms" for each drug alone is not required. The dose-effect relationship per se does not tell the mechanism. It only tells the mass-action law parameters. Furthermore, if eq. 16 or eq. 20 were mechanism-

dependent, it would be quite useless because of the imposed restrictions. Mechanism independence is the reason that eq. 7 is a general theory and eq. 16 or eq. 20 is a theorem.

Although it is good to know the mechanism before conducting drug combination studies, such as combining the MDR-substrate drugs with MDR-reversing agents, e.g., vinblastine + ardeemin (Chou et al., 1998a) or paclitaxel (Taxol) + ningalin (Chou et al., 2005b) and doxorubicin + M_4N (Chang et al., 2006), there is no way to predict synergism or antagonism when one combines cisplatin (a DNA cross-linking agent) and/or paclitaxel (a microtubule stabilization agent) and/or vincristine (a microtubule depolymerization agent) and/or topotecan (a DNA topoisomerase I inhibitor) and/or VP-16 (a DNA topoisomerase II inhibitor) until one has actually performed the experiment and analyzed the data as shown by Chou et al. (1994). These examples will be illustrated in detail in section VI.A.3., including the illustrations with polygonograms; in addition, the detailed computer printout is given in Supplemental Data Appendix IV for Taxol, cisplatin, and topotecan.

When presenting a synergistic effect, a question frequently asked is "What is the mechanism of the synergism?" This is a hard question to answer. In fact, we know the mechanisms of very few drugs. We even do not know the detailed mechanisms for old drugs, such as aspirin or ether. The argument here depends on what you mean by "mechanism." Are you talking about it at a pharmacological, biochemical, cellular, molecular, chemical, or quantum mechanics level? Even for a highly purified or crystalized enzyme such as horse alcohol dehydrogenase, when it is inhibited by a simple competitive inhibitor (ADP) in combination with a simple noncompetitive inhibitor (*o*-phenanthrolene), Chou and Talalay (1981) demonstrated that it was difficult to predict the result quantitatively, in terms of synergism, antagonism, or additive effect, without analyzing the experimental data first (see Supplemental Data Appendices II and III).

When we combine two cytotoxic agents (or other agents) to kill a cancer cell, we really do not know how many events there are from a living cell to a dead cell. It can be several steps or it can be a hundreds of steps. Furthermore, when we talk about synergism or antagonism of two or more drugs, they are considered to be "mutual." Although we know the dose or effect contributions in the combination, we so not know quantitatively the proportions of the mechanistic contributions of each drug that lead to the observed synergism or antagonism. Therefore, we need to be cautious when we state the causes and consequences in drug combinations, especially if one drug may have multiple mechanisms. When one of the two drugs by itself has no effect, then the enhancement (or augmentation or potentiation) or inhibition (or suppression) is easily described, simply by percent or by -fold. It is not possible to determine CI because it is not possible to determine the m, D_m, and r values when a drug by itself has no effect.

For a simple set of drug combination studies in vitro, it will take approximately 1 to 2 weeks for the quantitative determination of synergism or antagonism. But if one wants to know *how* and *why* synergism or antagonism occurs, it may take months or years and yet the conclusions may only be tentative, suggestive, or implied. Thus, *the determination of synergism or antagonism and the elucidation of how or why it occurs are separate issues*.

With the current state of the art, even if we elucidate the primary, secondary, and tertiary structure of an enzyme or a receptor, it is still hard to design an inhibitor for the drug development process. To "predict" synergism or antagonism for enzymes, receptors, or biological systems is expected to be even more difficult.

B. Constant Ratio Drug Combinations, Dose Range, Dose Density, and Experimental Scheme

The diagonal constant ratio combination design proposed by Chou and Talalay (1984) and Chou (1991) can greatly reduce the number of animals needed for experiments (i.e., greatly reduce the number of data points required) and yet one can still receive the maximal amount of useful information on combinations, thus increasing the cost-effectiveness of experimentation (see also section VI.D. for conservation of laboratory animals). The diagonal scheme proposed (Table 5), unlike the checkerboard or Latin-square scheme, is an easy experiment to conduct simply by serial dilution of a mixture with a small number of data points and yet it allows the construction of F_a-CI and F_a-DRI plots with

TABLE 5

A proposed experimental design showing the outlay of dose range and dose density of two drugs for drug combination analysis

Modified from "Quantitation of Synergism and Antagonism of Two or More Drugs by Computerized Analysis," Chou TC, in *Synergism and Antagonism in Chemotherapy* (Chou TC and Rideout DC eds) pp 223–244. Copyright 1991 with permission from Elsevier.

			Drug 1				
	0	0 Control $(f_a)_0$	0.25 × $(ED_{50})_1$ $(f_a)_1$	0.5 × $(ED_{50})_1$ $(f_a)_1$	$(ED_{50})_1$ $(f_a)_1$	2 × $(ED_{50})_1$ $(f_a)_1$	4 × $(ED_{50})_1$ $(f_a)_1$
Drug 2	0.25 × $(ED_{50})_2$ $(f_a)_2$		$(f_a)_{1,2}$				
	0.5 × $(ED_{50})_2$ $(f_a)_2$			$(f_a)_{1,2}$			
	$(ED_{50})_2$ $(f_a)_2$				$(f_a)_{1,2}$		
	2 × $(ED_{50})_2$ $(f_a)_2$					$(f_a)_{1,2}$	
	4× $(ED_{50})_2$ $(f_a)_2$						$(f_a)_{1,2}$

the actual combination data points. Furthermore, it also allows computer simulation of CI and DRI values at all effect levels (see sections IV and VI). It is further recommended that for an early-stage study, the constant combination ratio experiment should be carried out at an equipotency ratio [e.g., $(IC_{50})_1/(IC_{50})_2$ ratio] so that the contributions of effects of each drug to the combination would be roughly equal (Table 5) (see also Chou and Talalay, 1984; Chou JH, 1991).

C. The Nonconstant Ratios of Drug Combinations

Tests of the combination at other combination ratios can also be carried out to determine the optimal combination ratio for maximal synergy. In some special cases, experiments are carried out at nonconstant ratios [e.g., keep $(D)_1$ constant while varying the $(D)_2$ doses]. As long as the *m* and D_m values for each single drug are available, the CI values for each combination data point for the nonconstant ratio design can still be calculated. In these cases, the CI values for each data point on the F_a-CI plot will be shown, but the plot cannot be simulated (for examples, see section VI and Supplemental Data Appendices II and III). In addition, the normalized isobologram can be constructed for the nonconstant ratio combination design, but only the constant ratio combination design can yield the classic isobologram (see Fig. 8b and 8c).

D. The Optimal Combination Ratio for Maximal Synergy

Chou and Talalay (1983, 1984) recommend that the combination ratio be kept at an equipotency ratio (e.g., IC_{50} or ED_{50} ratio). This way, the contribution to the combination by each drug would be approximately equal. However, doing so is not absolutely required. A drug can be emphasized or deemphasized in many special situations, such as a severe type of toxicity (such as cardiotoxicity or renal toxicity), a narrow toxicity dose range for one drug but not another, or limited availability of a drug, such as source or price or poor solubility. Thus, in extended studies, one can set an arbitrarily particular desired ratio, carry out the experiment, and see what happens. One can also set the equipotent 1:1 dose ratio, add 1:3 and 3:1 dose ratios and find out which ratio yielded better synergy. While looking to synergy, one should also beware that the dose range is feasible in vivo and that the concentration or dose range is in a therapeutically effective range. The use of a computer software for determining the optimal combination ratios for maximal synergy has been proposed (Chou et al., 1986).

E. Combination Designs for Three or More Drugs

The equations for three or more drug combinations have been given in eq. 20, which shares the general form of the two-drug combinations (eq. 16). For a three-drug combination, D_1, D_2, and D_3, the recommendation is to use their IC_{50} ratios a:b:c. Therefore, $D_1 + D_2 + D_3$ is at (a:b:c). It is also recommended that two-drug combinations be carried out at the same time; thus, $D_1 + D_2$ (a:b), $D_2 + D_3$ (b:c), and $D_1 + D_3$ (a:c) (Fig. 10a). These, in fact, serve as a dissection of three-drug combination into two-drug combinations (Fig. 10b). In this way, not only are the corresponding CI values determined, but also determines the secondary CI (e.g., how the third drug affects the two drug combination can also be determined). In effect, three drugs are considered as if they were two drugs. Therefore, in this experimental design, we have the dose-effect curves for D_1, D_2, and D_3 alone, for two-drug combinations $D_1 + D_2$, $D_2 + D_3$, $D_1 + D_3$ and for three-drug combination $D_1 + D_2 + D_3$. In this case, the two-drug combinations are not absolutely required, although they dissect the three-drug combinations (e.g., $D_1 + D_2$ may be moderately synergistic, $D_2 + D_3$ may be antagonistic, $D_1 + D_3$ may be strongly synergistic, and $D_1 + D_2 + D_3$ may be synergistic). These dissections provide more insight into the pharmacological interactions of their components.

In theory, the CI values can be determined for *n*-drug combinations (see eqs. 19 and 20). To avoid experimental variability due to variables in assay conditions, it is recommended that dose-effect curves for each single drug and its combinations be carried out at the same

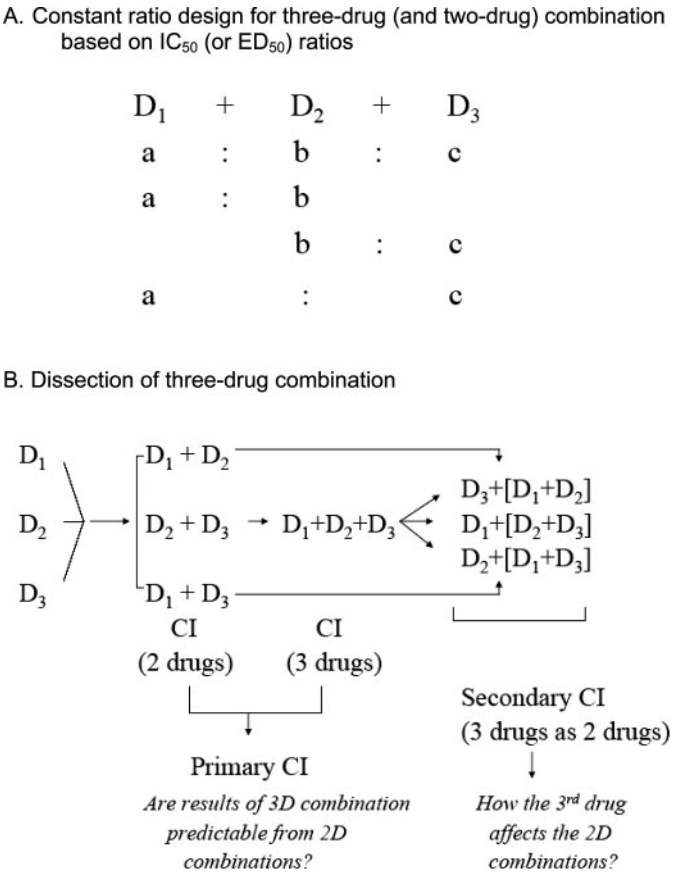

FIG. 10. Design for three-drug combination. 2D, two-drug; 3D, three-drug.

time, whenever possible. This practical consideration would limit the experimental size that is feasible to manage, although the availability of high-volume microwell high throughput assays in vitro would minimize part of the problem. Most drug combinations reported on so far with quantitative CI analysis have been two-drug combinations, although some three-drug combinations (Johnson et al., 1990; Kong et al., 1991; Pan et al., 1992; Kahan et al., 1993; Merrill et al., 1996; Tremblay et al., 1999; Hofmann-Lehmann et al., 2001a,b) and a few four-drug combinations have been reported on as well (Li et al., 1998; Baba et al., 2000; Kitabwalla et al., 2003). By using computer software, such as CompuSyn (Chou and Martin, 2005), the seven-drug combination (with some component combinations) has been carried out in the author's laboratory (Fig. 9a). Some of the above representations for multidrug combinations are illustrated in sections VI.A.3., VI.C.3., Supplemental Data, and Supplemental Data Appendix IV using the actual experimental designs and crude data, as examples for the computerized analysis.

The traditional Chinese herbal medicines pose a complex and challenging situation for drug combination studies. So far, no systematic analyses have been carried out or have been proposed. The median-effect principle and the combination index method may provide a scientific quantitative approach to these problems, since, in theory, the CI for *n*-drug combination can be determined. The main task is to separate, divide, and reduce by means of split elimination to deduce meaningful or useful conclusions.

F. Drug Combination in Vitro, in Vivo, and in Clinics

Experimental conditions for drug combination in vitro can be easily defined, fixed, or standarized, and the drug concentrations can be maintained at a relatively constant during the course of the experiment. Usually, it takes approximately 1 to 2 weeks to complete an in vitro drug combination study based on the CI-isobol method of Chou and Talalay (1984). It is quick, accurate, and economical, and, therefore, most drug combination studies in biomedical literature have been conducted in vitro, with dose-effect curves each consisting of five to eight data points for each drug alone and their combinations.

Compared with in vitro studies, determining synergism or antagonism in vivo using animals is obviously more time consuming and more costly and greater variability in measurements will be encountered. Therefore, in vivo drug combination studies are usually carried out only for selected drugs, after in vitro combination studies, and/or before clinical development.

For a two-drug combination therapeutic studies against human tumor xenografts in nude mice (Chou et al., 2005a), they usually consist of four groups: 1) the control group treated with solvent vehicle only, 2) the group treated with drug A at three to four doses, 3) the group treated with drug B at three to four doses, and 4) the group treated with a combination of drugs A and B, at a constant combination ratio (e.g., at the ED_{50} ratio) with several combination dose levels or at nonconstant combination ratios (e.g., keep drug A at constant dose and vary the dose of drug B at several levels). Each dose is used in four to five mice. Thus, approximately 60 nude mice would be needed for the experiment, if one already has preliminary information about the maximal tolerated dose (MTD), route of administration, and treatment schedule for each drug. The length of the study would be approximately 2 to 3 months, not including the follow-up studies, such as tumor remission or relapse. An example of a detailed in vivo drug combination study in nude mice based on the CI-isobol method is found in Chou et al. (2005a). Application of the combination index method in the design of clinical trials has been discussed by Mildvan et al. (1990), Chou et al. (1994), and Chou (1998). Combination therapy of HIV-1 infections has been widely implemented in clinical settings (Zhang et al., 1999).

Quantitative determination of the synergism or antagonism of two drugs in clinical trials is very difficult to carry out and, in most cases, practically impossible to perfect. This is apparently the reason why many drug combination clinical trials, such as the combination of anticancer natural product drug(s) + MDR-reversing agent(s), have failed or reached inconclusive results. These disappointing results point to the conclusion that the in vitro and animal drug combinations should not be overlooked (Chou, 1994, 1998; Chou et al., 1994, 1998a, 2005a; Chang et al., 2006). The complexities of clinical drug combination trials can be due to a variety of reasons: 1) the patient population varies in terms of sex, age, race, stage of disease, and the history of past treatments; 2) it is not ethical to treat patients with a placebo or suboptimal therapy of doses as required for the drug combination study design; and 3) death should not be allowed in clinical studies as a toxicity endpoint as in animal studies. Therefore, the success of a drug combination clinical trial would very much rely on the information provided by the in vitro and/or animal drug combination studies, which would include dose, schedule, route of administration, efficacy, toxicity, synergism/antagonism, and schedule dependence. There will be little or no flexibility in clinical trials. A comparison of drug combinations for a pair of antitumor agents in vitro, in animals and in clinics is shown in Table 6. This comparison is based on the combination index perspectives (e.g., dose range, dose density, D_m value, *m* value, *r* value, and quantitation by CI, DRI, and/or isobol) and based on the population size, population variability, as well as ethical considerations. This demonstrates that a clinical trial for drug combination is very difficult to carry out properly. One important issue raised from Table 6 is whether it is ethically acceptable or scientifically correct to conduct a drug combination study in humans without doing any drug combination studies in

TABLE 6
Comparison of drug combinations for a pair of antitumor agents in vitro, in vivo, and in clinics on the theoretical and practical perspectives

	In Vitro	In Vivo	
		In Animals	In Patients
Dose range	0, 1/8, ¼, ½, 1, 2, and 4 of IC_{50}	0, ¼, ½, 1, and 2 of ED_{50}	0, 0.25, 0.5, and 0.75 of MTD
Dose density	5–8	3–5	2–3
Population size	10^6	50–80	50–200
Population variability	Uniform	Inbred	Vary
r value required	>0.95	>0.90	Not certain (>0.80?)
Prevalent m value	0.8–1.5	0.8–3.0	Not known (0.8–3.0?)
Conclusions available	Quantitative synergism or antagonism	Quantitative synergism or antagonism	Net therapeutic benefit for better or for worse[a]
Method of assessment	Combination index, isobologram, dose-reduction index	Combination index, isobologram, dose-reduction index	Comparing with each drug alone at or near MTD; balance between efficacy and toxicity; synergism cannot be determined
Length of time required	1–2 weeks	2–3 months	1–2 years[a]
Flexibility of study	High	Low	Limited[a]
Death as endpoint for toxicity	Always	Frequently	Not allowed[a]
Ethical and liability considerations	None	Low	High[a]

[a] An open issue: Is it ethically acceptable or scientifically correct to conduct drug combination trials in humans without first doing drug combination studies in vitro or in animals?

vitro or in animals that will take only 1 to 2 weeks and 2 to 3 months to complete, respectively. Another issue is whether humans should be subjected to receipt of drug combination treatments under suboptimal conditions or subjected to trial-and-error testing or to the chance of for better or for worse results in clinical trials in the absence of any supporting evidence or established rationale for the specific combinations. These issues should be confronted by clinicians who conduct drug combination trials, as well as regulatory agencies, such as the U.S. Food and Drug Administration, which approves investigational new drug applications for drug combinations.

G. Schedule Dependence

For the combination of two drugs, A and B, they can be administered simultaneously, or one after another (e.g., A → B or B → A). The time gap between two drugs can be varied, depending on the need and the design. In sequential administrations, such as A → B, administration of A can be considered as preconditioning or pretreatment for sensitization, desensitization, or preventing toxicities, etc. If A or B by itself has no effect, then the potentiation (enhancement, augmentation) or suppression (inhibition) can be presented as percent inhibition or -fold potentiation. If both A and B have an effect, then synergism, antagonism, or an additive effect can be determined using the combination index or the isobol method. In this case, it is important that the assay conditions (such as the incubation time) for "each drug" alone in the sequential administration and for "its combinations" should be corresponding and identical, so that the dose-effect parameters (*m* and D_m values) can be used without any biases.

The schedule dependence studies for three or more drugs should follow the same rule, but it is expected to be more complex than the two-drug sequential combinations. However, sometimes we can lump together two or several drugs as a group and then conduct sequential drug combinations among the groups, such as (A + B) → (B + C), for determining the temporal significance on synergism or antagonism. The schedule dependence drug combination studies using the CI method have been carried out in various fields of research, such as those of Chang et al. (1987), Eron et al. (1992), Chou et al. (1996), Candinas et al. (1997), Longo et al. (1998), Rigas et al. (1999), Takahashi et al. (2002), and others.

H. Condition-Dependent Synergism or Antagonism and Combination of Drugs with Different Modalities, Different Units, and Mechanisms

The combination index theorem for two or more drugs (eqs. 16 and 20) as indicated above is valid for combinations of different entities of the drug with the same or different modes of actions. Because all terms in the equations are ratios, all the dose units in eqs. 13 to 20 are canceled out and become dimensionless quantities. Therefore, in drug combinations, drug A can be in micromolar concentrations, drug B can be in micrograms per milliliter, drug C can be in international unit, and so forth.

Although the most common combinations are drug-drug combinations (see section V.), the theorem for combination can be applicable to other conditions, such as drug + oxygen tension (Durand, 1990), drug + radiation (Leonard et al., 1996), drug + virus (Aghi et al., 1999; Bennett et al., 2004), drug + biomodulator (Hamashima et al., 1995; Finch et al., 2000), drug + antibodies (Wang et al., 1996; Li et al., 1997), or radiation + oxygen tension (Seo et al., 2006), and radiation + virus (Adusumilli et al., 2004), as long as the median-effect principle is followed by the dose-effect relationship (i.e., reasonably good *r* values in the median-effect plot). Whether it is applicable to drug + pH (Smith et al., 1989), drug + temperature (Lakhdar-Ghazal et al., 1986; Hegedus and

Khachatourians, 1996), and drug + magnetic field (Liang et al., 1997) remains to be further explored.

IV. Computerized Automation, Graphic Simulation, and Informatics

A. Computer Software

With the general equations of MEP and CI available, it becomes a logical consequence to develop a mass-action law based-computer software for automated data analysis. The first software of this kind was developed and demonstrated by a 13 year old, Joseph H. Chou, who presented it at the American Society of Pharmacology and Experimental Therapeutics annual meeting in Philadelphia (Chou et al., 1983). The first edition was for the Apple II computer (Chou and Chou, 1985) followed by the IBM-PC edition (Chou and Chou, 1987). Thereafter, the concept of DRI was introduced (Chou and Chou, 1988), and its applications were incorporated into a new version of software called CalcuSyn (Chou and Hayball, 1997), which was presented in Windows format. The most updated software, also for IBM-PC, is called CompuSyn (Chou and Martin, 2005). CompuSyn generates better quality graphics that are ready for publication (Chang et al., 2006), more options and flexibility and improved statistics and contains updated developments over the earlier versions (for more information, contact combosyn@gmail.com). Distinct from earlier versions of the software, CompuSyn is able to handle the data analysis of large-scale drug combination studies all at once. For example, 31 sets of data for 5 drugs have been analyzed simultaneously, and a 90-page report was generated, which includes 60 color graphics, many tables, and an overall summary (see Supplemental Data at http://pharmrev.aspetjournals.org/cgi/content/full/pr.58.3.10/DC1).

B. The Median-Effect Plot and the Simulation of Dose-Effect Curve

The general dose and effect theory as depicted by the median-effect equation (eqs. 7–9) has been estimated to have been tested in >20,000 sets of experimental data in >2600 scientific papers for single drugs and in combinations since its introduction in 1976. In the author's laboratory alone, >5000 sets of data have been used for analysis. The usefulness of the median-effect equation can be mathematically illustrated with the bold numbers given in Table 7, and its utility can be confirmed by the computer generated dose-effect curves and the median-effect plot in Fig. 11, color-matched with the numbers in Table 7.

The dose-effect relationship based on the median-effect equation (eq. 7) at $m = 1$, 3, and 5 and with D_m values at 0.5, 1, 2, 4, 6, 8, and 16 are given in Table 7. After entering the doses (D_x) and the corresponding f_a values on rows 4 to 6 into the computer, CompuSyn generates (Fig. 11) dose-effect curves (a) and the median-effect plot (b), which accurately manifest $D_m = 1$ μM (i.e., antilog 0 = 1), and the slopes of 1, 3, and 5. After entering the doses (D_x) and the f_a values on rows 1, 4, 7, 10, 13, 16, and 19 into the computer, CompuSyn again generates dose-effect curves (c) and the median-effect

TABLE 7

Dose-effect relationship based on the median-effect equation for the first- and higher-order systems, using the assigned m and D_m values to calculate the dose, D_x, for different effect, $(f_a)_x$

Equation 8: $(D)_x = D_m [(f_a)/(1 - f_a)]^{1/m}$, where x is the fractional inhibition as specified by $f_a = (f_a)_x$. The numbers in bold are used in Fig. 11, and the symbols correspond to the same symbols used in Fig. 11.

Assigned D_m Value for Potency	Assigned m value for Shape	Calculated Dose $(D)_x$ in μM at:						
		$(D)_{0.1}$ for f_a = 0.1	$(D)_{0.2}$ for f_a = 0.2	$(D)_{0.4}$ for f_a = 0.4	**$(D)_{0.5}$ for f_a = 0.5**	$(D)_{0.6}$ for f_a = 0.6	$(D)_{0.8}$ for f_a = 0.8	$(D)_{0.9}$ for f_a = 0.9
0.5 μM	***m* = 1**	**0.05555**	**0.125**	**0.3333**	**0.5** (○)	**0.75**	**2.0**	**4.5**
	m = 3	0.2404	0.315	0.4368	0.5	0.5724	0.7937	1.040
	m = 5	0.3222	0.3789	0.4611	0.5	0.5422	0.6598	0.7759
1 μM	***m* = 1** (○)	**0.11111** (○)	**0.25** (○)	**0.6666** (○)	**1.0** (□)	**1.5** (○)	**4.0** (○)	**9.0** (○)
	***m* = 3** (□)	**0.48075** (□)	**0.630** (□)	**0.8736** (□)	**1.0** (□)	**1.1447** (□)	**1.5874** (□)	**2.0801** (□)
	***m* = 5** (△)	**0.6444** (△)	**0.7579** (△)	**0.9221** (△)	**1.0** (△)	**1.0845** (△)	**1.3195** (△)	**1.5518** (△)
2 μM	***m* = 1**	**0.2222**	**0.5**	**1.3333**	**2.0** (△)	**3.0**	**8.0**	**18.0**
	m = 3	0.9615	1.260	1.747	2.0	2.2894	3.1748	4.1602
	m = 5	1.2888	1.5157	1.8442	2.0	2.1689	2.6390	3.1037
4 μM	***m* = 1**	**0.4444**	**1.0**	**2.666**	**4.0** (▽)	**6.0**	**16.0**	**36.0**
	m = 3	1.9230	2.520	3.494	4.0	4.5788	6.3496	8.320
	m = 5	2.5776	3.0314	3.688	4.0	4.3379	5.2780	6.2074
6 μM	***m* = 1**	**0.6666**	**1.5**	**4.0**	**6.0** (◇)	**9.0**	**24.0**	**54.0**
	m = 3	2.8845	3.780	5.241	6.0	6.8683	9.5244	12.480
	m = 5	3.8664	4.547	5.5326	6.0	6.5068	7.9170	9.3111
8 μM	***m* = 1**	**0.8888**	**2.0**	**5.333**	**8.0** (×)	12.0	**32.0**	**72.0**
	m = 3	3.6980	5.040	6.989	8.0	9.1577	12.699	16.641
	m = 5	5.1552	6.0629	7.377	8.0	8.6756	10.556	12.4148
16 μM	***m* = 1**	**1.7777**	**4.0**	**10.666**	**16.0** (+)	**24.0**	**64.0**	**144.0**
	m = 3	7.3960	10.080	13.977	16.0	18.315	25.398	33.281
	m = 5	10.310	12.126	14.754	16.0	17.352	21.112	24.8295

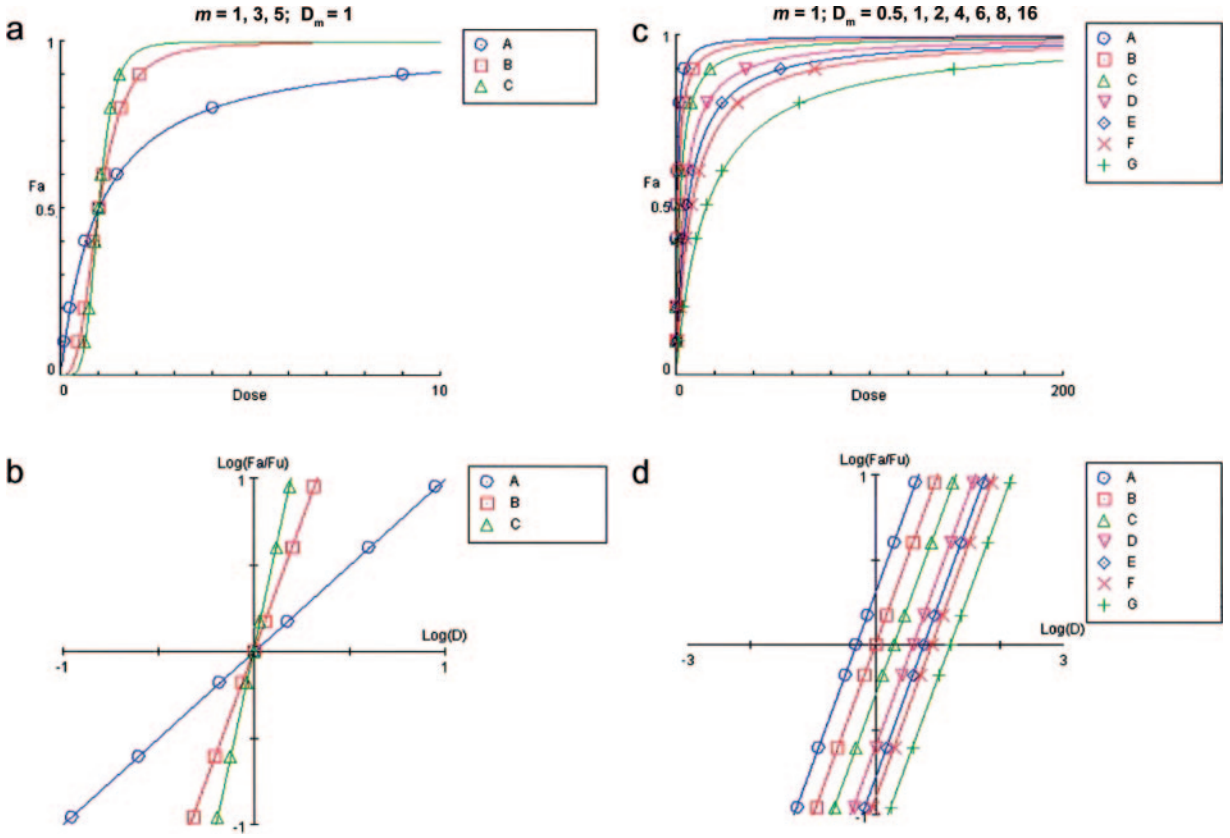

FIG. 11. CompuSyn-generated graphics based on numerical data given in Table 7. a, dose-effect curves when D_m = 1 μM, and when m = 1 (○), m = 3 (□), and m = 5 (△). b, median-effect plots of a. c, dose-effect curves when m = 1 and when D_m = 0.5 μM (○), 1 μM (□), 2 μM (△), 4 μM (▽), 6 μM (◇), 8 μM (×), and 16 μM (+). d, median-effect plots of c. Similar graphics can be generated by using other m and D_m values in Table 7. Note that in this figure, seven data points have been used for each dose-effect relationship. Remarkably, reducing the data points to only two, three, four, five, and six data points for each generates nearly identical corresponding dose-effect curves and median-effect plots by this mass-action law-based software CompuSyn. This indicates that very few data points can be used for dose-effect analysis if experimental data are accurately measured and the test system is uniform.

plot (d) with an accurately depicted slope of 1 with D_m values at 0.5, 1, 2, 4, 6, 8, and 16 μM, respectively.

It should be noted that even just entering iteratively "any two data points of each row" into the computer, CompuSyn will still generate a nearly identical full dose-effect curves faithfully. Thus, *it is possible to generate a dose-effect "curve" with only two data points, if the data are accurately measured*. This feature defies the commonly held belief that two data points can only draw a connecting straight line. Thus, the MEP of the mass-action law provides the rational basis for using a small (or a reduced) number of data points under the improved precision of measurement. This dose-number reduction can be translated into using a small number of animals and thus not only leads to cost-effective benefits, but also markedly reduces the unnecessary use of animals (Chou et al., 1984) (see also section VI.D.). Therefore, the median-effect principle of the mass-action law does a service to humanity.

C. Simulation of the F_a-Combination Index Plot

Incorporating the median-effect equation (eq. 8) into the combination index equation (eq. 16) can generate an algorithm used for simulating the calculated CI values at different effect (f_a) levels. For the combination of two drugs $(D)_1$ and $(D)_2$ at the combination ratio of $(D)_1$:$(D)_2$ = P:Q, in the combination, $(D)_{1,2} = (D)_1 + (D)_2$, we get $(D)_1 = (D)_{1,2} \times [P/(P + Q)]$ and $(D)_2 = (D)_{1,2} \times [Q/(P + Q)]$. The combination index equation

$$CI = \frac{(D)_1}{(D_x)_1} + \frac{(D)_2}{(D_x)_2}$$

indicates that for a given effect of $(f_a)_x$ for x% inhibition of the dose, D_x, the combined additive effect for the sum of the fractional doses of each drug, $(D)_1/(D_x)_1$ and $(D)_2/(D_x)_2$ should be equal to unity. This statement is simple, but the real merit is its actual derivation and its generality in that the relationship holds regardless of the mechanism of each drug and regardless of the types of the drug actions, as shown in the mathematical induction and reduction (Fig. 2). The denominators of eq. 16, $(D_x)_1$ and $(D_x)_2$ for each drug "alone" can be expressed by eq. 8: $D_x = D_m [(f_a)/(1 - f_a)]^{1/m}$, and the numerators of eq. 16 for the "combination" are the actual experimental doses $(D)_1$ and $(D)_2$ that in combination give rise to $(D)_{1,2}$. Because synergism is the effect that is more than additive (i.e., requires less dose for a given effect) and antagonism is an effect that is less than additive (i.e., requires more dose for a given effect), therefore, when

CI = 1, it indicates an additive effect, CI < 1, it indicates a synergistic effect, and CI > 1, it indicates an antagonistic effect.

Thus, by increasing the doses for the combinations, the effect levels can be increased to different effect (f_a) levels (Fig. 8a). The computer using the CompuSyn software will iteratively calculate the CI values at different $(f_a)_x$. In this way, the entire spectrum of CIs at different f_a values can be simulated. The simulation of the F_a-CI plot and its interpretation are shown in Fig. 8a. Note that both the F_a and the CI for the *x*- and *y*-axes are dimensionless quantities. This algorithm of multiple-step logic (Fig. 7) can be applied for *n*-drug combination, as shown by eq. 20.

D. Construction of the Classic and Normalized Isobologram

An isobologram is a graph of equipotency doses for two drug combinations. This concept has more than a century of history and has been subjected to decades-long intensive studies by Loewe (1928, 1953, 1957) and Berenbaum (1977, 1981, 1989). The construction of an isobol used to be carried out manually using graph paper for interpolations and extrapolations. The isobologram equation was formally derived and introduced by Chou and Talalay (1981, 1984) simply by setting the CI equation (eqs. 17 and 18) equal to 1. Thus, Chou and Talalay were able to construct an isobol at any effect levels with a keystroke after the dose-effect data entries. The algorithm for isobol construction is identical to the F_a-CI plot, except that the isobol is dose-oriented and the F_a-CI plot is effect-oriented graphs. Neither graph is dependent on the mechanisms and sites of drug actions, since they are derived from mathematical induction and deduction (see section II.). The practical advantages of the F_a-CI plot over the isobologram have been discussed in section II.C.3. The typical appearance and interpretations for both the classic and normalized isobolograms are illustrated in Fig. 8, b and c, respectively. The specific real data analyses are given in section VI. and Supplemental Data Appendices II to V.

For an experimental design using a constant ratio [e.g., the diagonal scheme with multiple doses in $(IC_{50})_1/(IC_{50})_2$ ratio], the m_1, $(D_m)_1$, r_1; m_2, $(D_m)_2$, r_2; and $m_{1,2}$, $(D_m)_{1,2}$, and $r_{1,2}$ can be determined and thereby allow the isobol to be constructed at any effect (f_a) levels. In these calculations, only the *m* and D_m values are used and the *r* value is only for statistical justification. However, when the nonconstant ratio combination design is used, $m_{1,2}$ and $(D_m)_{1,2}$ cannot be determined, so only the dose-normalized isobologram can be constructed (Fig. 8c). Theoretically, F_a-CI plot, classic isobol, and normalized isobol should yield exactly identical conclusions in terms of synergism or antagonism, since they are based on the same MEP general equation (Chou, 1976) and the same CI theorem (Chou and Talalay, 1983, 1984). This theoretical prediction was confirmed using the real experimental data of Yonetani and Theorell (1964) (see Tables 8 and 9 and their analysis) as illustrated by Chou and Talalay (1981), by using a pocket calculator before the term "combination index" was introduced (Chou and Talalay, 1983, 1984). Now, 26 years later, the same sets of experimental data are being analyzed with the fully automated computer software CompuSyn (Chou and Martin, 2005) as illustrated in detail in section VI.A.1. and by the CompuSyn analysis given in Supplemental Data Appendices II and III. Excellent agreements between data and theory and the conclusions from the earlier manual and the recent computerized analysis have been obtained.

For each single drug and its combinations, although serial dilution on drug concentrations is recommended, for convenience, the serial dilution can be carried out in different ways. For example, $(D)_1$ can be 2-fold serial dilution, $(D)_2$ can be 3-fold serial dilution, and $[(D)_1 + (D)_2]$ or $(D)_{1,2}$ can be 1.5-fold serial dilution if $(D)_1$ has a nearly hyperbolic dose-effect curve ($m \approx 1$), $(D)_2$ has a rather flat dose-effect curve ($m < 1$) and $[(D)_1 + (D)_2]$ has a steep or sigmoidal dose-effect curve ($m > 1$). In fact, random dilutions are also allowed for each drug as long as *m* and D_m (and *r*) values are determined. For the combination, even one data point can be used and the CI value can still be determined.

E. Simulation of the F_a-Drug-Reduction Index Plot

Using the MEP and CI principle/DRI equation and using the same logic of the algorithm for the F_a-CI plot, one can automatically construct a F_a-DRI plot by simulation; this will be illustrated in section VI. with several examples. In the case of strong synergism, the DRI value can be very large and out-of-scale. To condense the scale, the F_a-log(DRI) plot will also be simulated by default. The general appearance for F_a-DRI plots and their interpretations are given in Fig. 8d.

The applications of the DRI equation and the simulation of the F_a-DRI plot have toxicological imprints since reducing the dose (while maintaining the same effect) would lead to reduced toxicity. DRI > 1 indicates the reduced dose for a given drug combination compared with the dose of that drug alone. It should be noted that DRI is not an index for synergism or antagonism, whereas CI serves as an index. For example, when CI for two drugs indicates synergism (CI < 1), the DRI for drug 1, $(DRI)_1$ can be >1 whereas the DRI for drug 2, $(DRI)_2$, can be <1, depending on the properties of each drug, as well as the drug combination ratio that is being used.

In practical situations, because DRI is most relevant to toxicity in vivo, whether drug 1 and drug 2 have overlapping or nonoverlapping toxicity is of concern (e.g., such as gastrointestinal toxicity, cardiotoxicity, renal toxicity, and neurotoxicity) Furthermore, when determining synergism for "efficacy" in vivo, one should also consider whether there is synergism of "toxicity" toward the host in vivo. The best scenarios of two drug

TABLE 8

Inhibition of horse liver alcohol dehydrogenase reaction by two mutually exclusive inhibitors

The fractional inhibitions (f_i) of the horse liver alcohol dehydrogenase reaction were measured in the presence of I_1, ADP, and/or I_2, ADP-ribose. These f_i values are retrieved from the graph of experimental observations by Yonetani and Theorell (1964; Fig. 2D). These data were used as an example to check the median-effect principle and the multiple drug effect equation earlier (Chou and Talalay, 1981), before the computer software became available and before the term combination index was introduced. The computerized analyses of these data with CompuSyn are given in the table with full or partial data and in constant ratio and nonconstant ratio analysis. Some combinations (i.e., in diagonal [1]–[5]) are in constant ratio (1:190) and some (i.e., in two triangles) are in nonconstant ratios [for a CompuSyn printout, see Supplemental Data Appendix II (http://pharmrev.aspetjournals.org/cgi/content/full/pr.58.3.10/DC1)]. These full and partial analyses yield nearly indentical additive conclusions. Modified from "Studies on Liver Alcohol Hydrogenase Complexes. 3. Multiple Inhibition Kinetics in the Presence of Two Competitive Inhibitors," *Archives of Biochemistry and Biophysics*, volume 106, pp 243–251. Copyright 1964 with permission from Elsevier.

ADP	f_i at [ADP-ribose] of					
	0	95μM	190μM	285μM	380μM	475μM
μM						
0	0	0.389 (6)	0.535 (7)	0.639 (8)	0.707 (9)	0.748 (10)
0.5	0.224 (1)	0.472 [1]	0.585	0.670	0.735	0.763
1.0	0.371 (2)	0.554	0.637 [2]	0.697	0.746	0.784
1.5	0.468 (3)	0.587	0.681	0.734 [3]	0.762	0.799
2.0	0.555 (4)	0.627	0.712	0.748	0.781 [4]	0.802
2.5	0.605 (5)	0.676	0.727	0.767	0.796	0.817 [5]

combination are 1) both drugs have strong synergism in therapeutic efficacy (CI <); 2) both drugs have strong antagonism in toxicity toward the host (CI > 1); 3) the toxicities of both drugs in the host are not overlapping, and 4) both drugs (or at least one drug) allow significant dose reductions (DRI > 1) for a given effect. The same logic can be extended to three or more drug combinations.

F. Step-by-Step Use of CompuSyn Software for Single Drug and for Drug Combination Studies

Detailed procedures for using CompuSyn for automated dose-effect analysis for parameters of each drug and its combinations for quantitation/simulation of synergism or antagonism are given in the users guide for CompuSyn (Chou and Martin, 2005). In section V., examples of applications in various fields of biomedical sciences, using old and new software, are given. In section VI. and Supplemental Data Appendices II to V, real data samples of applications using CompuSyn are shown.

After data entry (for doses and effects), the CompuSyn software generates, for a single drug, the dose-effect table, the dose-effect curve, the dose-effect parameters (m, D_m, and r values), the median-effect plot, and the dose and effect interchange option. For multiple drugs (in addition as to the single drug) it generates the combination index table, the F_a-CI plot (with simulation curves if constant ratio combinations), the F_a-log(CI) plot, the dose-reduction index table, the F_a-DRI plot (with simulation curves if constant ratio combinations), the F_a-log(DRI) plot, the classic isobologram (for constant ratio combinations), the normalized isobologram (for nonconstant ratio combinations), and the polygonogram (for three or more drugs with constant ratio combinations for each pair of drugs). The CI table and DRI table at actual experimental combination data points are also automatically generated. The software also provides options for classic isobolograms and polygonograms at different effect levels, and options for F_a-CI plots with or without SDA. The software also provides a brief summary at the end of analysis indicating the project title, drug(s) name, abbreviation, file name, date, parameters, and, if applicable, combination ratio(s) and highlights of CI values at ED_{50}, ED_{75}, ED_{90}, and ED_{95}. In brief, the procedures for the analysis are summarized as follows:

1. Data Entry (takes 2–10 min depending on the size of the experiment).
   a. Enter a single drug dose effect (each dose for each effect) for Drug A alone and for Drug B alone (usually five to eight doses or concentrations for an in vitro experiment for each drug).
   b. Enter a combination dose-effect (each combination dose for each effect) for (Drug A + Drug B) mixtures, either at a constant combination ratio [usually the $(IC_{50})_1/(IC_{50})_2$ ratio is used with serial dilution for several doses] or at a nonconstant combination ratio

TABLE 9

Inhibition of horse liver alcohol dehydrogenase by a competitive (ADP) and a noncompetitive (o-phenanthrolene) inhibitors

The fractional inhibitions (f_i) of the horse liver alcohol dehydrogenase reaction were measured in the presence of I_1, ADP, and/or I_2, *o*-phenanthrolene. These f_i values were retrieved from the graph of experimental observations by Yonetani and Theorell (1964; Fig. 3E). These data were used as an example to check the median-effect principle and the multiple drug effect equation earlier (Chou and Talalay, 1981) before the computer software became available and before the term combination index was introduced. The computerized analyses of these data with CompuSyn are given in the table with full or partial data and with constant ratio and nonconstant ratio analysis. Some combinations (i.e., in diagonal [1]–[5]) are in constant ratio (1:17.4) and some (i.e., in two triangles) are in nonconstant ratios [for CompuSyn printout, see Supplemental Data Appendix III (http://pharmrev.aspetjournals.org/cgi/content/full/pr.58.3.10/DC1)]. These full and partial analyses yield nearly identical synergistic conclusions. Modified from "Studies on Liver Alcohol Hydrogenase Complexes. 3. Multiple Inhibition Kinetics in the Presence of Two Competitive Inhibitors," *Archives of Biochemistry and Biophysics*, volume 106, pp 243–251. Copyright 1964 with permission from Elsevier.

ADP	f_i at [*o*-Phenanthroline] of					
	0	8.7μM	17.4μM	26.1μM	34.8μM	43.5μM
μM						
0	0	0.132 (6)	0.267 (7)	0.411 (8)	0.476 (9)	0.548 (10)
0.5	0.175 (1)	0.507 [1]	0.633	0.738	0.777	0.816
1.0	0.358 (2)	0.676	0.769 [2]	0.829	0.858	0.882
1.5	0.492 (3)	0.742	0.823	0.872 [3]	0.895	0.915
2.0	0.542 (4)	0.783	0.865	0.900	0.919 [4]	0.932
2.5	0.598 (5)	0.817	0.883	0.914	0.934	0.944 [5]

(e.g., in combinations, keep Drug A at a constant dose while varying Drug B doses). It should be noted that the user should assign a proper unit for each drug (e.g., millimolar, micromolar, or nanomolar) so that the numerical dose entered will not be too small or too big, when using it for scaling the graphics. The computer recognizes (and calculates) only numbers. The user's assigned unit(s) will be used for report generation. It should also be noted that the computer takes into account each data point entered equally importantly, not just emphasizing the points close to IC_{50} or ED_{50}, which is usually done with eye inspections. Extremely low effect(s) or extremely high effect(s) that are beyond the accuracy of assay (or the determination method) should not be entered (e.g., $f_a < 0.01$ or $f_a > 0.999$). On the logarithmic scale, 0.01 and 0.001 or 0.999 and 0.9999 are 10-fold different and log 0 is negative infinity.

2. Report Generation (takes approximately 1–3 min depending on the speed of the computer): One will be asked to choose the items that will be included in the report (such as Single Drugs, Drug Combos at Constant Ratio, and Drug Combos at Nonconstant Ratios, . . .). Once the report has been created, it will automatically open in one's default Web browser (e.g., Internet Explorer or Mozilla). At this point, one is no longer in the CompuSyn application. When the generated report is saved, it is essential to delete the "*" or "*cse" and type a new file name. To make changes to the selected choices previously made in the generated report, CompuSyn must be opened first and one must click on "Recall Experiment."
3. Printing the Report (may consist of 7–90 pages depending on the size of the experiment): To print a report, simply choose Print from the Web browser's file menu. The exact dialog box and options vary from browser to browser. Depending on the experimental size, design, and print selections, the printout (in color) consists of the following items and in the following default order:
   a. Experiment title, date, file name, and description note.
   b. The dose and effect tables for each single drug and its combinations, an acknowledgment of the number of data points entered, and the calculated parameters: m, D_m, and r.
   c. The dose-effect curves for each drug and their combinations and corresponding median-effect plots.
   d. The F_a and CI tables for $f_a = 0.05$ to 0.97 for each combination (including total dose and combina-

tion ratio) as well as the CI values for each actual combination data point; F_a-CI plots for f_a = 0.05 to 0.97 for each combination with computer simulation as well as actual combination data points in the graph, if combinations are in constant ratio or with no computer simulation but with actual combination data points in the graph if combinations are in nonconstant ratios.

e. The F_a and DRI tables for f_a = 0.05 to 0.97, the dose required for each drug alone at a given effect (f_a) and the -fold dose reduction if combined for a given effect (f_a); DRI values for each of the actual combination data points; F_a-DRI plot for each drug and for each combination with computer simulation, as well as the actual combination data points located on the graphs; F_a-log (DRI) plot for each drug and for each combination with computer simulation as well as the actual combination data points on the graphs.

f. Isobolograms: The classic isobolograms will be automatically shown for each pair of drug combinations, if a constant ratio combination design is used (default at f_a = 0.5, 0.75, and 0.9; other options available). The normalized isobolograms will be automatically shown for each pair of drug combinations, if the nonconstant ratios combination design is used.

g. Polygonogram for more than three pairs of drug combinations, involving three or more drugs (default sets f_a = 0.9, other options available).

4. Summary Table: The summary table includes title, date, file name, description note; parameters (m, D_m, and r) for each drug and their combinations; the CI table for each combination at ED_{50}, ED_{75}, ED_{90}, and ED_{95} levels; and doses for each drug and their combinations required to produce ED_{50}, ED_{75}, ED_{90}, and ED_{95} (option for calculating ED_x is also available).

5. Options for Generating Report: The following selections are made from the menu in *Report Option,* the specified report will be generated by clicking *Generate Report* and by checking the items that one wants for tailoring the report. After checking OK, the full report will be generated and will appear on the screen. It may take a while to generate a report for a large-scale experiment. The generated report can be printed or saved. If one wants one, two, or more figures for making slides or for publication, then go back to *Generate Report*. Check off those items not needed, leave the items that are wanted, and click OK. The desired figures will appear on the screen almost instantly.

6. Some Features and Options.

a. Error entry of dose or effect for each drug and their combinations may be edited or deleted.

b. In constant ratio combinations, because the combination ratio has already been entered, enter the dose of any Drug or the Total Dose, and CompuSyn will automatically fill in all the other doses.

c. For nonconstant ratio combinations, one has to input the Dose and Effect of each drug individually.

d. It is recommended that one select not more than 10 Single Drugs and Drug Combos to be included in the report, as having too many items on each graph tends to make it overcrowded and unreadable.

e. All numbers are stored and calculated using 80 bit IEEE standard double floating point precision. This means that the largest gap between representable numbers is about 2×10^{-16}.

f. he numbers displayed in the report are rounded to seven decimal points.

g. "NaN" (Not a Number) appears in the place of a number, indicating that a mathematical error was made, such as dividing by 0 or $f_a > 1$.

h. Options for selecting "f_a for a value" to calculate the corresponding dose, to construct the corresponding isobologram, or to construct the corresponding polygonogram are available.

i. Options for automatically using colors for each dose-effect curve or for each line in a plot are available; in a polygonogram, synergism is shown as a green solid line and antagonism is shown as a red dashed line.

j. Split large graphs (on by default). When there are more than two Drugs and two Combos, the dose-effect plot and the median-effect plot will be automatically split into two graphs to avoid crowding.

k. For Scaling Window, everything is set to 0 by default, which tells CompuSyn to do the scaling automatically. If one wishes to use a custom scale on one of the graphs, he or she can manually override CompuSyn by entering something in the scale entry for a given graph. Note that for plots with multiple frames, such as Isobologram, the scale on all frames is affected.

G. Statistical Considerations

The derivation of the general median-effect equation as well as the CI equation is based on the physicochemical principle of the mass-action law and mathematical induction and deduction. These derivatives do not invoke any statistical principle, method, or assumptions. Therefore, the methods per se are deterministic not probabilistic. But for their applications, the variability in methods of assay measurements and the variability in biological systems cannot be avoided, and, therefore, they are subject to statistical considerations.

There are three levels of statistics available for conducting a drug combination analysis using the CompuSyn software:

1. The r value, i.e., the linear correlation coefficient of the median-effect plot (Chou, 1976) signifies the conformity or goodness of fit of the experimental

data with the median-effect principle. This first-line statistics is a default function of computer software such as CompuSyn.

2. The SDA, also known as serial deletion analysis, allows for an iterative analysis that deletes one data point (of a dose) at a time. These repeated reruns of calculations from crude data at the beginning to the CI results at the end allow the determination of variability of data, which generate results at different effect levels for the F_a-CI plot with vertical bars, indicating 95% confidence intervals. A typical example of a F_a-CI plot is given in Fig. 12.
3. An easy third-line statistics is to repeat the drug combination experiment several times and then run CompuSyn several times before calculating the regular statistics of mean ± S.D. or mean ± S.E. for parameters (m, D_m, and r), the CI values, and the DRI values.

V. Selected Examples of Cited Applications

Based on the PubMed or ISI Web search, >2600 scientific papers in the biomedical literature have used the median-effect equation or the combination index-isobologram equation in analysis of data for single drug or for drug combination studies.

In the following, selected examples of applications are categorized and the references are listed under References. Wherever appropriate, brief notations on the names of drugs, the number of drugs studied, and the type of the target of inhibitions are given immediately after the cited references. All examples of applications

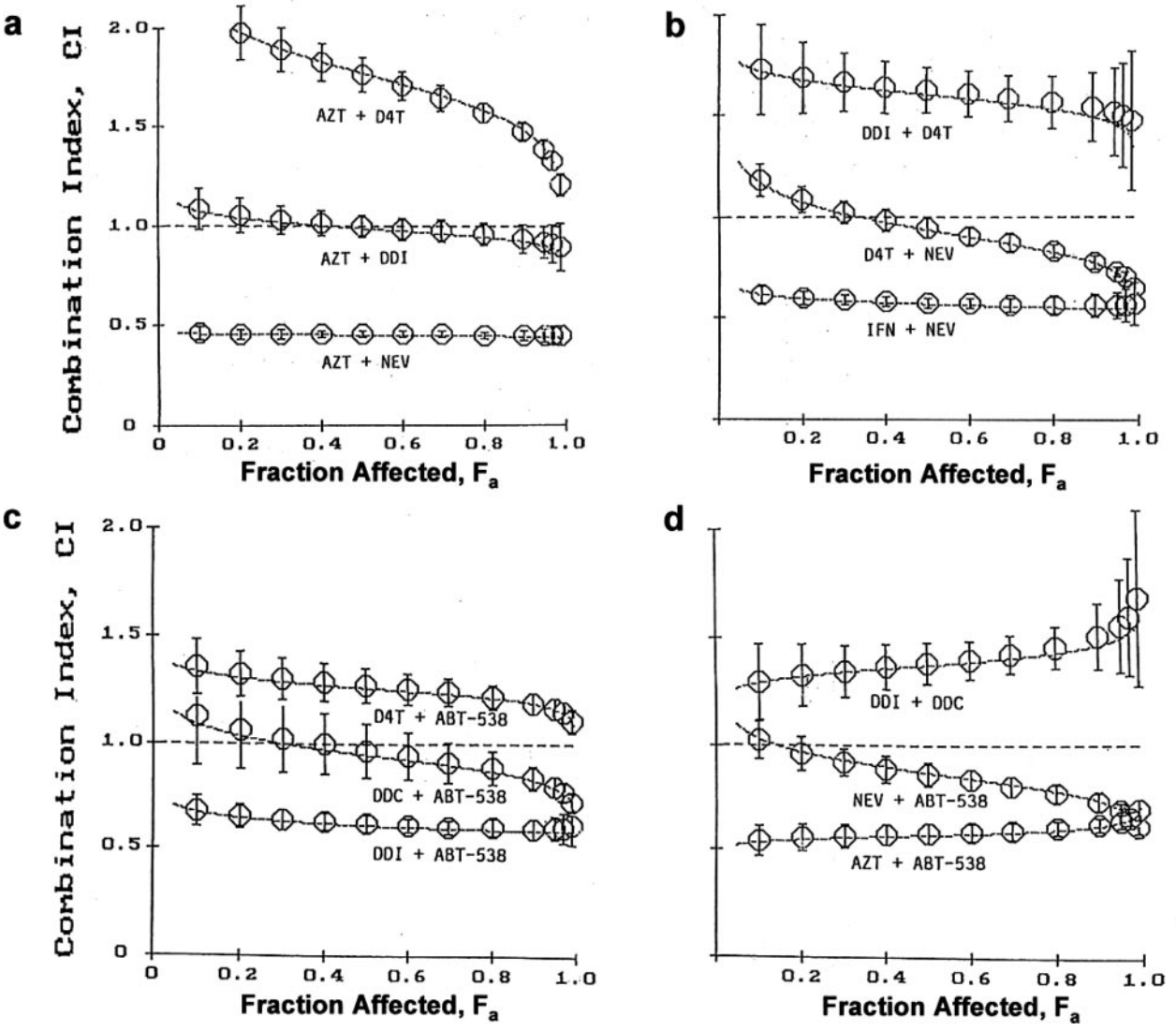

FIG. 12. Examples of F_a-CI plot of 12 sets of two-drug combinations in Table 21, which are divided into four subgroups: a, b, c, and d. The CI is plotted as a function of the fractional inhibition (f_a) by computer simulation from f_a = 0.10 to 0.95. CI < 1, = 1, and > 1 indicate synergism, additive effect, and antagonism, respectively. The vertical bars indicate 95% confidence intervals based on SDA using custom-made software by T. C. Chou and H. Kim. Similar graphics can also be generated by using CompuSyn (Chou and Martin, 2005), but the vertical bars are located on the experimental combination data points in this figure.

are from in vitro studies, unless otherwise specifically indicated, in the case of in vivo or animal studies.

A. Cited Methods and Evaluation of Single Drug and Drug Discovery

For the evaluation of pharmacological properties of a new compound in vitro or in vivo for potential drug development, the median-effect equation and plot provide three pieces of basic information in terms of quantitative parameters: 1) the D_m value signifies "potency," such as IC_{50}, ED_{50}, and LD_{50} (see Fig. 3); 2) the m value signifies the "shape" of dose-effect curve with $m = 1$, > 1, and < 1 indicating hyperbolic (such as the Michaelis-Menten kinetics or simple receptor binding), sigmoidal (such as allosteric enzyme kinetics or oxygen-hemoglobin kinetics), and flat sigmoidal (such as negative cooperativity in allosteric kinetic systems), respectively; and 3) the r value signifies the "conformity" of the data set to the median-effect principle of the mass-action law. These three parameters can be automatically obtained using the computer software, CompuSyn (Chou and Martin, 2005) or an earlier version of the software (Chou and Chou, 1985; Chou and Hayball, 1997), after entry of doses and the corresponding effects. The algorithm for the parameter determination is that the antilog of the x-intercept of the median-effect plot gives the D_m value, whereas the slope of the median-effect plot gives the m value, and the linear correlation coefficient of the median-effect plot gives the r value.

This method is distinct from other methods in biomedical literature by having the following features: 1) Is uses quantitative parameters for potency, shape, and conformity. 2) It may use a smaller number of data points for a dose-effect curve. This feature is particularly useful for cost-effective and ethical considerations for animal studies (see sections VI.A.1. and VI.D.1.; for detailed illustrations, see Supplemental Data Appendices II–IV). 3) All data points are equally weighted, without emphasis on the points on the curve nearest to the median-effect dose. 4) It allows calculation of the dose for any given effect (eq. 8) or calculation of the effect for any given dose (eq. 9) by using a pocket calculator or CompuSyn software. The dose calculated in the form of concentration (e.g., micromolar) for a desired effect (e.g., for 95% or 99% inhibition) provides an estimation of whether the desired plasma or tissue drug concentrations are feasible to achieve at the intended dose or at a MTD in animals or humans.

Researchers in the author's laboratory have used the MEP and its software for evaluating new compounds for the Drug Discovery/Development Program at Memorial Sloan Kettering Cancer Center (MSKCC) and for collaborative research with other institutions during the past 20 years. It is estimated that >20,000 sets of dose-effect data have been subjected to the MEP method of data analysis. Excellent conformity results have been obtained and published, including results for chemicals, drugs, biomodifiers, carcinogens, and radiation. This fact alone attests to the general applicability and usefulness of the MEP method for evaluating efficacy and toxicity of a drug, or drugs, or entities. In conjunction with colleagues at the Bio-Organic Chemistry Laboratory at MSKCC and the organic chemistry laboratories elsewhere, our work has resulted in the discovery of many potentially useful new compounds, as indicated by U.S. patents 5,053,431 (1991) for chrysophanol; 5,340,818 (1994) for plant ingredients; 5,354,864 (1994) for acridinylanilines; 5,476,952 (1995) for cyclopentanthraquinones; 5,622,958 (1997) for enediynequinones; 5,939,428 (1999) for acridinylamino-5-hydroxymethylanilines, 6,147,076 (2000) for ardeemins. 6,204,388 (2001), 6,242,469 (2001), 6,284,781 (2001), 6,300,355 (2001), 6,369,234 (2002), 6,656,961 (2003), 6,656,961 (2003), 6,723,854 (2004), and 6,828,340 (2004) for epothilone derivatives; and 6,355,639 (2002) for the reverse prenyl compounds. Some of the epothilones are in phase I and phase II clinical trials in cancer patients. Some are in different stages of preclinical developments. One of the most remarkable compounds discovered through this process of evaluations is fludelone (26-trifluoro-9,10-dehydro-12,13-desoxyepothilone B), a microtubule targeted stabilization epothilone that allows the first fully documented report of a "therapeutic cure" against human mammary and colon carcinoma xenografts in nude mice with complete tumor remission without any relapse for >6 months (Chou et al., 2005b).

Examples of specific applications of the MEP method for single drugs (Chou, 1976) are given below.

1. Exploration of Potency, Toxicity, Parameters, and Structure-Activity Relations for New Compounds.
   a. Cytotoxic anticancer agents
      i. Antimetabolites: Galivan et al. (1989), Su et al. (1993).
      ii. DNA topoisomerase inhibitors: Kong et al. (1992a), Su et al. (1992a), Su and Chou (1994), Conti et al. (1996), Scarborough et al. (1996), Luo et al. (1996), Josien et al. (1997).
      iii. DNA intercalculating agents: Koyama et al. (1989), Su et al. (1995, 1999), Rastogi et al., (2002), Chang et al. (2003).
      iv. Alkylating agents: Kong et al. (1992a), Kohler et al. (1993), Shair et al. (1994, 1996); Kim et al. (1996), Shan et al. (1999), Vijayaraghavan et al. (2003), Bacherikov et al. (2004), Liang et al. (2004), Su et al. (2005).
      v. Microtubule depolymerization agents: Shan et al. (1999).
      vi. Microtubule stabilization agents: Balog et al. (1997), Su et al. (1997a,b), Meng et al. (1997), Chou et al. (1998a,b, 2001, 2003,

2005b), Stachel et al. (2000), Lee et al. (2000), Rivkin et al. (2003, 2005).

vii. Protein synthesis inhibitors: Su et al. (1992b).

viii. Inhibitors of protein kinase and other enzymes: Steckel et al. (1983), Link et al. (1996).

b. Antiviral agents

i. Anti-HSV/HBV agents: Kong et al. (1992c), Prochaska et al. (1993).

ii. Anti-HSV agents: Chou et al. (1987), Fox et al. (1988), Kong et al. (1992b).

iii. Antihuman hepatitis B virus agents: Fox et al. (1988).

iv. Anticytomegalovirus agents: Yang et al. (1990).

v. Antisimian varicella virus agents: Soike et al. (1987, 1990).

vi. Anti-Epstein-Barr virus agents: Lin et al. (1989).

c. Cytodifferentiating agents: Kong et al. (1987, 1988), Breitman and He (1990), Laneuville et al. (1994).

d. α_1-Adrenergic blockers: Somers et al. (1989), Breslin et al. (1993a,b).

e. Immunosuppressants: Vathsala et al. (1990, 1991), Zucker et al. (1997).

f. Insecticides: Chou and Talalay (1983, 1984), Alzogaray et al. (1998).

g. Hormones and modulators: Sharom et al. (1998).

h. Antifungal, antimalarial, and anthelmintic agents: Young et al. (1992), Berger et al. (1995, 1996, 1997), Gebre-Hiwot and Frommel (1993).

i. Tumor promotors: Kopelovich and Chou (1984), Ramel (1986), Porter et al. (1997).

j. Radiation, radioimmunoassay, and magnetic field: Maisin et al. (1987), Cohen et al. (1991), Griffon-Etienne et al. (1996), Liang et al. (1997).

k. Photodynamic agents: Rezzoug et al. (1998).

l. Enzyme-ligand interactions: Kremer et al. (1980), Steckel et al. (1983), Rahier et al. (1989), Barrie et al. (1989), Chou and Chou (1990), Huang et al. (1992), Conner et al. (1992), Dawson et al. (1995), Trzaskos et al. (1995), Jez et al. (1996).

m. Antiasthmatic and antiallergic agents: Matsushita et al. (1998).

n. Receptor-ligand and interactions: Friedman and Skehan (1980), Finotti and Palantini (1981), Zahniser and Molinoff (1983), Clark et al. (1988), Bylund et al. (1988), Bylund and Ray-Prenger (1989), Baker et al. (1986, 1988), Munson and Rodbard (1988), Dewar et al. (1989), Schoepp et al. (1990, 1992, 1994, 1996, 1997), Breslin et al. (1993), Jin et al. (1994), Katz et al. (1994), Zuckerman et al. (1999), Boileau et al. (1998, 1999).

o. Antiangiogenic agents: Qian et al. (2004), Vucenik et al. (2004).

p. Thermo effects: Hegedus and Khachatourians (1996).

q. Environmental contaminants: Vogiatzis and Loumbourdis (1998).

2. Low-Dose Risk Assessment for Carcinogens and Radiation: Chou (1980, 1981, 1991), Chou and Talalay (1984, 1987) (for more information, see sections VI.B.1 through VI.B.2).

3. Calculation of K_i from the IC_{50} Value: Chou (1974, 1977), Chou and Talalay (1981), Murphy and Snyder (1982), Baker and Posner (1986), Goldstein and Barrett (1987), Bylund et al. (1988), Bylund and Ray-Prenger (1989), Price et al. (1989), Clark et al. (1989), Schoepp and Johnson (1989a,b, 1993), Schoepp et al. (1996), Boileau et al. (1998). For more information, see section VI.B.6.

4. Exclusive and Nonexclusive Inhibitors and Topology of Binding Sites: Chou (1974, 1977a), Steckel et al. (1983), Chou and Chou (1988, 1990a), Lombardini et al. (1989) (for more information, see section VI.A.2).

5. Drug Resistance Evaluation and Other Applications: Chou et al. (1998a, 2005c), Chang et al. (2006).

6. Cellular Pharmacological Studies: Chou et al. (1977, 1982, 1983, 1984, 1994, 1996, 1998a,b, 2003, 2005a,b,c), Long et al. (1982), Kufe et al. (1984), Takemura et al. (1985), Chang et al. (1985), Colombani et al. (1989), Fykse et al. (1989), Dewar et al. (1989), Christensen et al. (1990), Gonzales et al. (1991), Traversa et al. (1994), Cheng et al. (1995), Schultz et al. (1998), Vaskinn et al. (1999).

7. Tissue Pharmacological Studies: Chou et al. (1977), Sharma and Klein (1988), Puig et al. (1988), Seo et al. (1989), Chu et al. (1989), Gonzales and Moerschbaecher (1989), Schoepp and Johnson (1989a,b), Wiener and van Os (1989), Zemelman et al. (1989), Woodward and Gonzales (1990), Woodward and Blair (1991), Woodward and Harms (1992), Noonan et al. (1992), Woodward and Cueto (1993), Schoepp et al. (1995, 1996), Desai et al. (1995), Mathis et al. (1999).

8. Cardiovascular Pharmacological Studies: Sharma and Klein (1988), Dong et al. (1988), Herman et al. (1989), Lyu et al. (1992), Heim et al. (1995).

9. Pharmacological Studies on Animals: Chou et al. (1975, 1981, 1998a,b, 2001, 2005a,b,c), Schinazi et al. (1986).

10. Behavioral Studies: Lakhdar-Ghazal et al. (1986), Altman et al. (1987), Barrie et al. (1997), Jin et al. (1994), Katz et al. (1994), Schoepp et al. (1995), Ryan-Moro et al. (1996), Zuckerman et al. (1999).

11. Cancer Prevention Agents: Dinkova-Kostova et al. (2005), triterpenoid analogs.

B. Examples of Cited Applications in Drug Combinations

The combination index method that involves both the median-effect equation (Chou, 1976) and the multiple drug-effect equation (Chou and Talalay, 1984; Chou 1991) has been widely used in biomedical research. One review article alone by Chou and Talalay (1984) has been cited in >1294 scientific papers. These applications are most noticeable in the three areas of biomedical research. The first area is anticancer drug combinations. Many of these studies were carried out at MSKCC and other academic medical institutions in North America, the United Kingdom, Germany, France, Italy, the Netherlands, Spain, Japan. and many other countries. The second area is antiviral agent combinations, especially for anti-HIV agents. Many of these studies were carried out in Prof. Martin S. Hirsch's laboratory at Massachusetts General Hospital (MGH), Harvard Medical School. During the 19 years of research collaboration between Hirsch and the author, 21 articles have been published, which covered most of the new anti-HIV agents, shortly after their introduction (see below). These studies have helped generate information that led to the discovery of anti-HIV cocktails by Prof. David Ho, who was a former trainee in Hirsch's laboratory at MGH (Fischl et al., 1995; Perelson et al., 1997; Cameron et al., 1999; Zhang et al., 1999). In attempts to establish animal models and to develop anti-HIV vaccines, researchers in Prof. Ruth M. Ruprecht's laboratory at Dana-Faber Cancer Institute, Harvard Medical School, have conducted many studies on multiclade MAbs combinations in vitro and in vivo in macaques. Since the mid-1980s, the combination index method has made impacts in AIDS clinical trials, as indicated by the publications by the MGH group and others (Mildvan et al., 1990; Fischl et al., 1995; D'Aquila et al., 1996; Chou and Zhu, 1997). During the 16 years of research collaboration between Prof. Ruprecht and the author, they have published 12 articles, which include combinations of as many as four monoclonal antibodies (see below). The third area is immunosuppressants combinations. Many of these studies were carried out in Prof. Barry D. Kahan's laboratory at the Division of Organ Transplantation, Department of Surgery, University of Texas at Houston. During Prof. Kahan's 16 years of research collaboration with the author, 19 articles have been published, which covered mostly new and some old immunosuppressants in in vitro and in vivo studies, including heart, kidney, and small intestine transplantations in rodents (see below).

Applications of the MEP-CI method for combination studies have also been reported in other areas, such as molecular biology, gene therapy, cancer prevention, insecticides, radiation, drug combinations in animals, and clinical protocol design. Some examples of specific applications that have been published are given below. Also given below are sample articles that highlight the observation of strong antagonism, a phenomenon that has been rarely reported. A report that highlights the strong antagonism between AZT and ribavirin (Vogt et al., 1987) was published in *Science,* before these drugs were used in AIDS patients. The applications of the CI-isobol method of Chou and Talalay are also categorized and presented below. Most in vivo studies were not carried out to the full extent and were based on the in vitro findings by using CI-isobol methods. Chou et al. (2005a) carried out full in vivo therapeutic studies in xenograft tumor-bearing nude mice. They were able to demonstrate dose-effect parameters and construct the F_a-CI plots and isobolograms. With the constant ratio diagonal design (Table 5), only 50 nude mice were used for each in vivo xenograft drug combination studies. Both antitumor effect and toxicity were analyzed for synergism and/or antagonisms in vivo.

1. Anticancer Agent Combinations.
   a. Cytotoxic agents (CAs).
      i. Two CA combinations: Chou et al. (1993), edatrexate + cisplatin; Koechli et al. (1993), paclitaxel (Taxol) + doxorubicin (Adriamycin); Figul et al. (2003), temozolomide + didox; Balzarotti et al. (2004), temozolomide + other cytotoxic agents; Honore et al. (2004), discodermolide + paclitaxel; Horvath et al. (2004), didox + carmustine; Chauhan et al. (2005), oral proteosome inhibitor + bortezomib; Tanaka et al. (2005a,b), oxaliplatin + CPT-11; Shanks et al. (2005), gemcitabine + various antitumor agents; Fischel et al. (2001), irinotecan, 5-FU, and oxaliplatin ternary combination; Harris et al. (2005a,b), XR 5944 + carboplatin or doxorubicin.
      ii. Two-drug and three-drug combinations with different mechanisms of action: Chou et al. (1994), paclitaxel (Taxol), topotecan, cisplatin, vincristine, and VP-16 (polygonograms were used; see detailed sample analysis in section Ii.e. for two- and three-drug combinations of anticancer agents and Supplemental Data Appendix II for details and the CompuSyn printout); Fischel et al. (2001), irinotecan + 5-FU + oxaliplatin.
      iii. CAs + cytodifferentiating agent: Kong et al. (1988).
      iv. CAs + MDR-reversing agents: Perez et al. (1994), carboplatin resistance; Chou et al. (1998a), MDR and multidrug resistance protein resistance reversal by ardeemins;

Chang and Chou (2000) and Chou and Chang (2002), MDR; Chou et al. (2005c), MDR reversal by ningalins; Chang et al. (2006), nordihydroguaiaretic acids + doxorubicin or paclitaxel.

v. CAs + modulators: Sacks et al. (1995), retinoic acid; Finch et al. (2000) GCSF + LiCl/all-*trans*-retinoic acid; Muller-Tidow et al. (2003), IFN_α + lovastatin/bcr-abl$^+$ cells.

vi. CA + virus: Bennett et al. (2004), mitomycin C + oncolytic herpes virus.

vii. CA + enzyme: Romanini et al. (1989), trimetrexate + carboxypeptidase G_2.

b. Modulator combinations or modulator + hormone: Bregman and Meyskens (1986), difluoromethylornithine + biological modifiers; Durand and Goldie (1987), etoposide + cisplatin, in spheroid model; Triozzi et al. (1989), IFN + steroids; Durand (1990), cisplatin + CCNU in spheroid cells (oxygen tension and distance from spheroid surface); Raje et al. (2004), rapamycin + thalidomide analog; Whitmore et al. (2004), poly-rI:rC + CpG-oligodeoxynucleotides; Algur et al. (2005), radiation + zoledronic acid; Bozec et al. (2005), dual anti-EGFR + radiation; Cosaceanu et al. (2005), radiation + insulin-like growth factor receptor inhibitor; Dai et al. (2005), paclitaxel (Taxol) + amifostine (a normal tissue protection agent); Gemmill et al. (2005), Iressa + rapamycin; Horvath et al. (2005), free-radical scavenger + Ara-C; Mohammed et al. (1995), platinum drugs + tamoxifen.

c. Radiation combinations: Leonard et al. (1996), paclitaxel (Taxol) + radiation; Donson et al. (1999), tamoxifen + radiation and radiation + virus; Adusumilli et al. (2004) ionizing radiation + oncolytic virus.

d. Cancer prevention combinations and cell differentiation combinations.

i. Khafif et al. (1998), epigallocatechin-3-gallate + curcumin.

ii. Soriano et al. (1999), chemopreventive agents + cytotoxic agents.

iii. Finch et al. (2000), GCSF/retinoic acid receptor α + LiCl/all-*trans*-retinoic acid-treated cells.

2. Antiviral Agent Combinations.

a. Anti-HIV agent combinations: For crude data analytical illustrations, see Kong et al. (1991). For a large-scale anti-HIV drug combination study (Chou and Zhu, 1997) involving two- to five-drug combinations of seven anti-HIV agents, see section VI.C.3. Details of the CompuSyn report (90 pages) are found in Supplemental Data (http://pharmrev.aspetjournals.org/cgi/content/full/pr.58.3.10/DC1). For other applications, see Hartshorn et al. (1986, 1987), $rIFN_\alpha$ + phosphonoformate and AZT-$rIFN_\alpha$, the first anti-HIV combinations; Vogt et al. (1987, 1988), DDC + $rIFN_\alpha$; Johnson et al. (1990, 1991, 1992), three-drug combination of AZT + CD4 + IFN_α and AZT + DDI or IFN_α for HIV-1/AZT, protease inhibitor RO-131 + AZT, DDC, or IFN_α for HIV/AZT; Richman et al. (1991), BI-RG-587 +AZT for HIV/AZT; Chou et al. (1991), oligonucleotide S-dC28 + AZT, IFN, or dextran sulfate; Kong et al. (1991), two-drug and three-drug combinations, AZT, phosphonoformate, and 3′-azido-3′-deoxythymidine; Pan et al. (1992), three-drug combination, 3′-fluoro-3′-deoxythymidine, CD4, and IFN_α; Tilley et al. (1992), hMAb combinations; Eron et al. (1992), AZT + DDC for HIV-1/AZT and schedule dependence; Merrill et al. (1996), two-drug and three-drug combinations, lamivudine, stavudine, and AZT; Zhu et al. (1996), AZT, stavudine, and nevirapine for HIV/AZT; Deminie et al. (1996), protease inhibitors + reverse transcriptase inhibitors; Tremblay et al. (1999, 2000, 2002), two-drug and three-drug combinations or protease inhibitors for HIV-resistant isolates and fusion inhibitor T-20 + CXCR4 blocker AMD-3100; CCR5 antagonist SCH-C + other anti-HIV agents; Hostetler et al. (2000), phosphonoformate analogs + AZT; Xu et al. (2001), hMAbs (clade B) combinations against HIV (clade C); Kollmann et al. (2001), nevirapine + efavirenz; Kitabwalla et al. (2003), hMAbs (clade B) combinations against HIV (clades A and D), a four-drug combination; Zhang et al. (2005), MAbs as anti-HIV vaccine.

b. Antisimian-human HIV combinations: Li et al. (1997, 1998), human anti-HIV-1 envelope MAb, globulin combination against simian immunodeficiency virus/HIV-1; Baba et al. (2000) hMAbs of IgG1 combinations against simian-human immunodeficiency virus.

c. Prevention of HIV infection in vivo: Ruprecht et al. (1990), AZT + IFN against retroviral viremia in mice; Baba et al. (2000) hMAbs of IgG1 combinations against simian-human immunodeficiency virus infection; Hofmann-Lehmann et al. (2001a,b), passive immunization combinations against oral AIDS virus transmission, three-drug combinations of hMAbs against oral simian-human immunodeficiency virus in macaques.

d. Anti-HSV combinations: Schinazi et al. (1986), in vitro and in vivo combinations; Gong et al. (2004), betulin + acyclovir.

e. Anticytomegalovirus agent combinations: Yang et al. (1990), two-drug combinations against

guinea pig cytomegalovirus in vitro. Manion et al. (1996), two-drug combinations.

f. Anti-Epstein Barr virus agent combinations: Lin et al. (1989), IFN_{α}, IFN_{γ} + AZT against Epstein-Barr virus in vitro.

g. Antisimian varicella virus combinations: Soike et al. (1987, 1990), guanine analog + IFN_{β} and 1-(2-deoxy-2-fluoro-1-*b*-D-arabinosyl)-5-ethyluracil + IFN_{β} against simian varicella virus infection in monkeys.

3. Immunosuppressant Combinations for Organ Transplantations.
   a. In vitro studies.
      i. Bone marrow transplant by purging progenitor cells: Chang et al. (1985), 4-hydroperoxycyclophosphamide + etoposide; Chang et al. (1987), combinations of various cytotoxic agents.
      ii. Cyclosporine (C_SA), rapamycin (Rapa, Sirolimus), FK-506 (tacrolimus) combinations: Kahan et al. (1991a,b), C_SA + Rapa; Vathsala et al. (1991), C_SA + Rapa; Kahan et al. (1993), combinations in vitro and in vivo, brequinar + C_SA or + Rapa, two-drug and three-drug combinations; Knight et al. (1994) C_SA + MAb.
      iii. Schedule-dependent combinations: Candinas et al. (1997), leflunomide + C_SA or + FK506; Podder et al. (2001), sirolimus + C_SA.
   b. In vivo combinations and organ transplantations.
      i. Heart transplantation: Stepkowski et al. (1994), C_SA, Rapa, and brequinar combinations, mice cardiac allografts; Kaji et al. (1994), 15-desoxyspergualin + C_SA, rat cardiac allografts; Tu et al. (1995), C_SA, Rapa, and brequinar combinations, mice cardiac allografts; Hamashima et al. (1995), donor antigen + C_SA or + C_SA/sirolimus, rats heart allografts.
      ii. Kidney transplantations: Kahan et al. (1993), in vitro and in vivo, brequinar + C_SA or + Rapa, two-drug and three-drug combinations; Chou et al. (1994), C_SA and other combinations; Kahan et al. (1993), C_SA and other combinations.
      iii. Small intestine transplantations: Wang et al. (1996), brequinar + C_SA, and brequinar + MAb, rat small intestine allografts; Stepkowski et al. (1996), oral sirolimus + C_SA, rat heart allografts; Grochowicz et al. (1997), castanospermine + tacrolimus, rat cardiac allografts; Stepkowski et al. (1997), sirolimus + C_SA, rat heart and kidney allografts; Candinas et al. (1997), leflunomide + C_SA or FK-506, rat cardiac allografts.
      iv. Islet transplantation: Gores et al. (1994), 15-desoxyspergualin + C_SA, rat islet allografts.
      v. Immunosuppressant combination reviews: Kahan et al. (1992); Chou et al. (1994), protocol design; Chou and Kahan (2001), book chapter.
4. Schedule Dependence of Combinations.
   a. Antitumor combination schedules.
      i. In vitro combinations: Chang et al. (1987), α-difluoromethylornithine + CisPt; Perez et al. (1993), edatrexate + CisPt; Chandrasekaran et al. (1995), AZT + 5-FU, cell-cycle dependence; Chou et al. (1996), paclitaxel (Taxol) or docetaxel (Taxotere) + edatrexate; Takahashi et al. (2002), schedule of ecteinascidin-743 + paclitaxel (Taxol); Hubeek et al. (2004), sequential combinations of GCSF, fludarabine, and Ara-C; De Luca et al. (2004), gemcitabine + vinorelbine; Levis et al. (2004), FLT-3 inhibitor + cytotoxic agents; Tanaka et al. (2005a,b), paclitaxel (Taxol) + oxaliplatin; Fischel et al. (2005a,b), docetaxel + capecitabine/5′-deoxy-5-fluorouridine; Harris et al. (2005a,b), XR5944 + irinotecan or 5-FU.
      ii. In vivo combinations: Rigas et al. (1999), paclitaxel (Taxol) + edatrexate, Phase I trials; Takahashi et al. (2002) schedule of ecteinascidin-743 + paclitaxel (Taxol).
   b. Antiviral combination schedules.
      i. In vitro combinations: Mazzulli et al. (1994), various anti-HIV combinations.
      ii. In vivo combinations: Schinazi et al. (1986), various anti-HSV agent combinations.
5. Drug Combinations That Highlight Antagonism.
   a. Antitumor combinations: Kong et al. (1988), cytodifferentiating agent + cytotoxic agents, Ara-C, Adriamycin (doxorubicin), and harringtonine; Chou et al. (1994), paclitaxel (Taxol) + vincristine, CisPt + VP-16; paclitaxel (Taxol) + vincristine + VP-16, in polygonograms; De Luca et al. (2004), gemcitabine + vinorelbine.
   b. Anti-HIV combinations: Vogt et al. (1987), AZT + ribavirin; Chou et al. (1991), various agent combinations; Merrill et al. (1997), protease inhibitors, indinavir, saquinavir.
   c. Immunosuppressant combinations: Vathsala et al. (1991), low-dose FK-506 + C_SA.
6. Topological Analysis of Multiligand Bindings.
   a. Chou (1974), the distribution equation for ligand-binding sites.
   b. Chou (1977a), availability of ligand-binding sites in a steady-state system.

c. Chou and Chou (1988), ligand exclusivity and competitiveness.
d. Lombardini et al. (1989), binding site combination kinetics.
e. Chou and Chou (1990), topological assessment with the aid of a computer.

7. Selectivity of Synergism.
   a. Berman et al. (1989), HIV versus normal bone marrow progenitor cells.
   b. Chang et al. (1985, 1987), sequential versus reverse sequential administration.
   c. Chou et al. (1996), sequential dependence.
   d. Chang et al. (1987), leukemic cells versus normal hematopoietic precursors.
   e. Peters et al. (1991), cisplatin plus 4-hydroperoxycyclophosphamide, influence of glutathione.
   f. Durand and Goldie (1987), etoposide + cisplatin, spheroids; Durand (1990), cisplatin + CCNU, effects of distance and oxygen tension on multicell spheroids.
   g. Duffy et al. (1998), anticancer drugs + nonsteroidal anti-inflammatory drugs, effect of multidrug resistance protein.
   h. Norberg and Wahlstrom (1986), hexobarbital + thiopental, age-specific, in vivo.
   i. Martin and Symonds (2002), toremifene + IFN_{α} dependence on IFN_{α} subtype.
   j. Pei et al. (2004), flavopiridol + Bcl-2 inhibitor, free radical and Jun NH_2-kinase-dependent.
   k. Konecny and Pegram (2004) gemcitabine + trastuzumab or cisplatins with HER2 overexpression cells.

8. Gene Therapy or Molecular Biology by Combinations.
   a. Aghi et al. (1998), ganciclovir/TK and 5-fluorocytosine/cytidine deaminase.
   b. Aghi et al. (1999), oncolytic virus/oxazaphosphorine/cytochrome + ganciclovir/HSV-TK.
   c. Rainov et al. (2001), temozolomide + ganciclovir/HSV-TK.
   d. Singh et al. (2002), p53 induction/zinc + phosphatidylinositol 3′-kinase inhibition/LY294002.
   e. Formento et al. (2004), Iressa + trastuzumab.
   f. Kaliberov et al. (2004), gene therapy mediated via adenovirus + radiations.
   g. Lee et al. (2004), insulin-like growth factor binding protein-3 + farnesyl transferase inhibitor.
   h. Qian et al. (2004), antiangiogenics + antihistone deacetylase.
   i. Park et al. (2004), Iressa + paclitaxel (Taxol).
   j. Yee et al. (2004), FLT-3 inhibitor + cytarabine or + daunorubicin.
   k. Yen et al. (2004), Targretin + paclitaxel (Taxol).
   l. David et al. (2005), farnesyl transferase inhibitor + proteosome inhibitor.
   m. Fischel et al. (2005a), Iressa + cetuximab.
   n. Gu et al. (2005), imatinib + mycophenolic acid.
   o. Lunghi et al. (2005), arsenic trioxide + mitogen-activated protein kinase kinase-1 inhibitor.
   p. Mullerad et al. (2005), oncolytic HSV + mitomycin C.
   q. Rahmani et al. (2005), heat shock protein-90 inhibitor + histone deacetylase inhibitor.
   r. Tseng et al. (2005), imatinib + phosphoinositide-dependent.
   s. Van Schaeybroeck et al. (2005), gefitinib + cytotoxic agents.
   t. Aghi et al. (2006), alkylating temozolomide + oncolytic HSV, in vitro and in vivo.
   u. Bruzzese et al. (2006), EGFR kinase inhibitor + gefitinib or + IFN_{α}, in vitro and in vivo.
   v. Kaliberov et al. (2006), adenoviral-directed enzyme/prodrug + immunotherapy, in vitro and in vivo.
   w. Zhou et al. (2006), combinations targeting EGFR and ErbB2 simultaneously, in vitro and in vivo.

9. Combinations of Other Anti-Infectious Disease Agents.
   a. Anticryptosporidium combinations: You et al. (1998), paromomycin + lasalocid.
   b. Antifungal combinations: Kullberg et al. (2004), antifungals + cytokines.
   c. Mycotoxin combinations: Koshinsky et al. (1991), toxin combination against CO_2 release in yeast.
   d. Antimalarial combinations: Coutaux et al. (1994), chloroquine + monoamine reuptake inhibitors.
   e. Antisevere acute respiratory syndrome-coronavirus combination: Morgenstern et al. (2005), ribavirin + IFN_{β}.
   f. Antibovine viral diarrhea virus combination: Yanagida et al. (2004), mizoribine + IFN_{α} against bovine viral diarrhea virus

10. Cardiovascular Drug Combinations: Bennett et al. (1984), aorta/relaxation drug combinations.
11. Combination for Animal Growth: Nakagawa et al. (1996), synthetic growth hormone releasing peptide + growth hormone inducer.
12. Anesthetic Combinations: Norberg and Wahlstrom (1986), hexobarbital + thiopental in vivo; Bansinath et al. (1992), ketamine + halothane, in vitro; Naguib (1994), rocuronium bromide + mivacurium chloride, neuromuscular relaxants.
13. Radiation and Drug Combinations: Potmesil et al. (1986), radiation + doxorubicin analogs in vitro; Seo et al. (2006), combination of radiosensitizers in vitro.
14. Antiparasitic Combination: Davoudi et al. (2005), antileishmania vaccine using HSV-TK conferring increased sensitivity to ganciclovir and 5-fluorocytosine.
15. Segmental Reviews for Median-Effect Principle and Combination Index Methods.

a. Journal review articles.
   i. Chou (1980), on carcinogen risk assessment.
   ii. Chou and Talalay (1983), on a new look at a very old problem.
   iii. Chou et al. (1994), on clinical protocol design.
   iv. Chou et al. (2006), on MDR reversal and clinical protocol design.
b. Monograph chapters.
   i. Chou and Talalay (1984), a state-of-the-art overview of MEP and CI.
   ii. Chou and Talalay (1987), on drug combination in chemotherapy.
   iii. Chou (1991), a updated overview of MEP and CI.
   iv. Chou (1994), on clinical perspectives.
   v. Chou et al. (1994), on immunosuppressants combinations.
   vi. Chou and Kahan (2001), on modern immunosuppressives and therapy.
   vii. Chou and Chang (2002) and Chang et al. (2006), on MDR reversal and clinical protocol design.
c. Encyclopedia chapters.
   i. Chou and Fanucchi (1988), in *Encyclopedia of Medical Devices and Instrumentation*, on computer software as a medical device.
   ii. Chou et al. (1991a, 1997), in *Encyclopedia of Human Biology,* a brief overview on MEP and CI.
   iii. Bertino and Chou (1997), in *Encyclopedia of Cancer,* a brief overview on drug combinations.
d. Editorial: Chou (1998), "Drug Combinations: From Laboratory to Practice."
e. Computer Software and Users' Guides.
   i. Chou and Chou (1985), for Apple II computer.
   ii. Chou and Chou (1988), for IBM-PC.
   iii. Chou (1991a) and Chou JH (1991), review, theory, and equations.
   iv. Chou and Hayball (1997), CalcuSyn for PC Windows.
   v. Chou and Martin (2005), CompuSyn for PC Windows interface, CD-ROM, Web browser, graphic improvements, statistic updates, and polygonograms.

VI. Illustrations of Real Data Analysis with Mass-Action Law-Based Computer Software

A. Single-Drug, Two-Drug, and Three-Drug Combination Analysis with Computer Software

1. Single-Drug Analysis and Two-Drug Combinations.
   a. Inhibition of alcohol dehydrogenase with ADP using Yonetani and Theorell (1964) data. Data given in Table 8 are analyzed for ADP as a single drug (points [1]–[5]). After entry of dose and effect, dose$_2$ and effect$_2$, . . . , the computer-generated report indicates that m = 1.0423, D_m = 1.6561 μM, and r = 0.99964. These results indicate excellent conformity to the mass-action law principle. Other single drugs in the table, such as ADP-R and *o*-phenanthrolene, can be analyzed similarly.
   b. Inhibition of alcohol dehydrogenase with ADP and ADP-R in nonconstant ratio combinations, using "all data points" in Table 8 with constant ratio and nonconstant ratios.
   c. Inhibition of alcohol dehydrogenase with ADP and ADP-R in a constant ratio (1:180) using diagonal data points [1]~[5] only. For details of the CompuSyn analysis on section VI.A.1.a.–c., see Supplemental Data Appendix II.
   d. Inhibition of alcohol dehydrogenase with ADP and *o*-phenanthrolene (Table 9). For details of the CompuSyn analysis on section VI.A.1.d., see Supplemental Data Appendix II.
   e. Conclusions and comments for section IV.A.1.a.–d.:
      i. In entering experimental data (Yonetani and Theorell, 1964) into the derived multiple drug-effect equations (Chou and Talalay, 1981), using manual calculations in 1981 (before the computer software for these became available), there was excellent conformity between the median-effect equation and the multiple drug-effect equation from the laboratory of a highly esteemed Nobel Laureate, Axel Hugo Theodor Theorell (Chou and Talalay, 1981).
      ii. In the present computerized analysis for either one of three compounds (ADP, ADP-R, or *o*-phenanthrolene), the r values ranged from 0.99 to 0.999 and for their constant ratio combinations (points [4]–[5] in Tables 8 and 9), the r values ranged from 0.99 to 0.999. Again, the experimental results conformed to the mass-action law excellently.
      iii. The m values are nearly 1, indicating that both inhibitors and their combinations follow first-order kinetics, which is exactly what was presented by Michaelis-Menten kinetics (Dixon and Webb, 1964).
      iv. The computerized CI analysis indicates that ADP and ADP-R have an additive effect, whereas ADP and *o*-phenanthrolene exhibit a synergistic effect. Most importantly, Supplemental Data Appendices II and III both indicate that virtually identical conclusions can be reached when data analyses are executed in the following ways:
         (1) Using the full contents of the data in a checkerboard (or Latin square) (i.e., in both Tables 8 and 9, there are 36 data

points, 5 for D_1, 5 for D_2, and 25 for D_1 + D_2 in various ratios, plus a control).

(2) Using only the constant ratio design: Table 8, points [1]–[5] in 1:190; and Table 9, points [1]–[5] in 1:17.4.

(3) Using only the various partial data for the combination analysis, either in a constant ratio or nonconstant ratios.

(4) Using only one single data point of combination. Still we can obtain a nearly identical conclusion. However, this single dose design for combination is not recommended as a common practice, since most biological studies are not as accurately measured as enzyme assays.

The above results indicate that *by using the combination index method, we can still reach a nearly identical conclusion, even though the data from different experimental designs or very few data points were used, provided that the data obtained are from accurate measurements.* However, it is recommended that the constant ratio design (i.e., the diagonal design in Tables 8 and 9, for points [1]–[5], excluding the two triangles in the tables) is the most efficient and economic way to conduct drug combination studies, since, as shown in the above examples, it saves 80% of data points (in two triangles) in the table and yet it allows computerized simulation of the F_a-CI plot and the F_a-DRI plot with the full scope of effects and the construction of an isobologram at any desired effect level. It also allows construction of a classic polygonogram if the experiment is expanded to three or more drugs. The saving of data points for a combination study can be translated into saving animals, saving costs, and saving time in in vivo studies (Chou et al., 2005a) (see also section VI.D.). The prerequisite of using this method is to conduct reliable and accurate assays, both for single drugs and their combination(s).

2. Topological Analysis for the Multiple Ligand Sites in the Steady-State System.

a. By application of the Lineweaver-Burk plot, ADP and ADP-R are known to be competitive inhibitors with NAD, and *o*-phenanthrolene is known to be a noncompetitive inhibitor (Yonetani and Theorell, 1964). By contrast, the median-effect plots for ADP and ADP-R and (ADP + ADP-R) at a constant ratio yield three parallel lines, indicating that the bindings for ADP and ADP-R are "mutually exclusive." The median-effect plots for ADP, as well as those for *o*-phenanthrolene, yield parallel lines. However, ADP + *o*-phenanthrolene at a constant ratio yields a steeper and slightly concave upward curve, indicating that the bindings for ADP and *o*-phenanthrolene are "mutually nonexclusive" (Chou and Talalay, 1981). Note that competitiveness can be determined by the Lineweaver-Burk plot (Lineweaver and Burk, 1934) plot, whereas exclusiveness can be determined by the median-effect (Chou, 1976) plot. These plots have somewhat different meanings, with the latter having topological implications (Chou, 1974, 1977a; Chou and Chou, 1988, 1990a). These topological analyses are useful for simple systems, such as enzymes or receptors. Some complexity is expected in conditions with combinations of three or more ligands.

b. The availability of the ligand-binding site of an enzyme or receptor in the steady state can be described by eq. 3, $K_i/I_{50} = E_x/E_t$ (Chou, 1974, 1977a), where K_i can be determined with the Lineweaver-Burk plot (1934), and the IC_{50} value can be determined by the median-effect plot (Chou, 1976) (see also Fig. 3). A method of topological analysis for the binding of two or more inhibitors has been proposed (Chou and Chou, 1988, 1990a). This proposed method for the steady equilibrium state is illustrated in Fig. 13. By contrast, the tight bindings can be analyzed by physical-mechanical means, such as cofraction in chromatography and cozoning of electrophoresis.

3. Two- and Three-Drug Combinations against Cancer Cell Growth and the Construction of Polygonograms.

a. Crude data: Numerical crude data are obtained from a study reported in Chou et al. (1994) on inhibition of teratocarcinoma cell growth by paclitaxel (Taxol), cisplatin, topotecan, vincristine, and etoposide individually and in their two- and three-drug combinations (Table 10). These experiments used a constant ratio design. All five drugs that have been studied have different pharmacological mechanisms of action. The polygonogram was used for the first time; however, this term was not formally introduced until 4 years later (Chou and Chou, 1998).

b. Computer printouts: The full computer printout using the CompuSyn software for analysis of data in Table 10 is shown in Supplemental Data Appendix IV. Computer printouts for (A) paclitaxel (Taxol), (B) cisplatin, (C) topotecan, and A + B, B + C, A + C, and A + B + C in a constant ratio of A:B:C = 1:100:10 and for their two-drug components are included. Printouts for other combinations using (D) etoposide and (E) vincristine, such as A + D, A + E, B + D, B + E, A + B + D, and A + B + E are not shown in Supplemental Data Appendix IV, because of the size of the report, but the conclusions can be found in the original article (Chou et al., 1994).

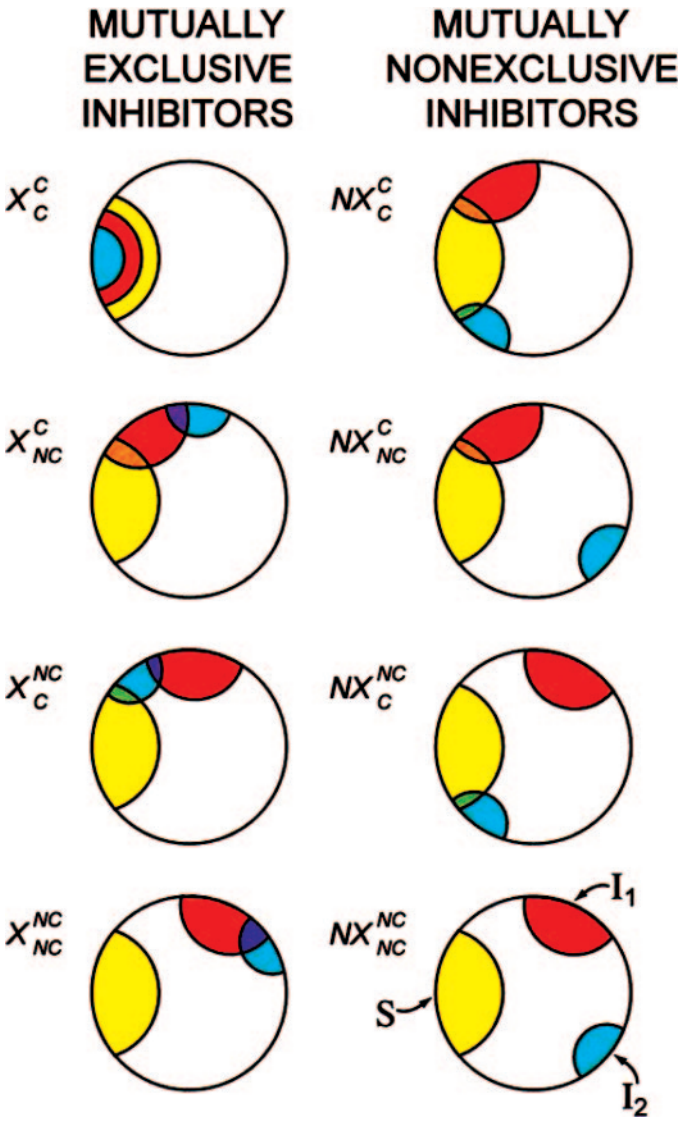

FIG. 13. Topological analysis of receptor-binding sites. The binding sites are S, substrate (yellow); inhibitor I_1 (red) and I_2 (blue); X, mutually exclusive between I_1 and I_2 bindings (overlapping); NX, mutually nonexclusive between I_1 and I_2 bindings (nonoverlapping); C, competitive inhibition; NC, noncompetitive inhibition. Competitiveness can be determined by the Lineweaver-Burk plot (Lineweaver and Burk, 1934), and exclusivity can be determined by the median-effect plot (Chou, 1976). The availability of a ligand-binding site can be determined by $K_i/IC_{50} = E_x/E_t$, where E_t is the total enzyme and E_x is the proportion of enzyme that is available for the inhibitor binding (Chou, 1974). Enzyme can be considered as a receptor, S can be the primary ligand or agonist, and I can be inhibitor, antagonist, or suppressor (see also Chou and Chou, 1988, 1990a).

c. Summary, conclusions, and comments for the above examples: Table 11 gives a brief summary of the results for paclitaxel (Taxol), cisplatin, and topotecan combinations on the CI and DRI values at ED_{50}, ED_{75}, ED_{90}, and ED_{95}. Conclusions are the following:
   i. Overall, the dose-effect relationships for single drugs (r = 0.905–0.993) (Table 9) and for combinations (r = 0.984–0.999) (Table 8) follow the mass-action principle excellently.
   ii. The in vitro cellular studies usually have $m > 1$; however, for animal studies $m \gg 1$ is common (e.g., see Tables 11–13).
   iii. It has been reported that paclitaxel (Taxol) is a microtubule stabilizer, vincristine is microtubule depolymerizer, and topotecan is a DNA topoisomerase I inhibitor, whereas etoposide is a DNA topoisomerase II inhibitor and cisplatin is an alkylation agent. The CI results shown in Tables 8 and 10 clearly indicate that, in most cases, there is no way to predict synergism or antagonism from the mechanisms of drug actions. Synergism or antagonism needs to be determined and not be predicted.
   iv. In this study, we frequently observed antagonism occurring at low effect levels and synergism occurring at high effect levels for a given combination. For cancer chemotherapy, we need to kill cancer cells 90, 99, or 99.9%. Synergism at high effect levels should be more relevant to therapy than those at low effect levels. It should be noted that the synergism scale of CI is from 0 to 1, and the antagonism scale of CI is from 1 to infinity. The F_a-log (CI) plot places synergism and antagonism on symmetrical and equal footings.

B. Other Applications of the Median-Effect Principle of the Mass-Action Law

1. Estimating Low-Dose Risk of Carcinogens.
   a. Introduction: Estimating the effect of a very low dose of carcinogen that may affect only [1/10,000] or [1/100,000] of a population is difficult to accomplish without extrapolation. The extrapolation process involves a great deal of magnification on a mathematical scale and in one's imagination. Ideally, extrapolation should be based on sound principles, and one should not merely rely on arbitrary mechanical tools or visual inspection. Because carcinogenic data conform to the mass-action law excellently, as indicated by the r values (i.e., $r \approx 1$), it is therefore proposed that the median-effect equation of the mass-action law be used for a low-dose risk assessment. Thus, in 1980, Chou applied the median-effect equation using a pocket calculator and analyzed two sets of experimental data for chronic carcinogenic exposure from Peto (1974) and Peto et al. (1975) and three sets of experimental data of acute carcinogenic exposure from Bryan and Shimkin (1943). Later, these data were analyzed using computer software (Chou and Chou, 1985; Chou and Talalay, 1987). These data have now been further ana-

TABLE 10

*Example of experimental design and dose-effect relationships of paclitaxel, cisplatin, and topotecan and their two- and three-drug combinations on growth inhibition of 833K teratocarcinoma cells after 96 h of exposure (modified from Chou et al., 1994, J Natl Cancer Inst **86:**1517–1524)*

Experimental data were subjected to automated calculation of m, D_m, and r parameters as well as plots simulations using CompuSyn (Chou and Martin, 2005). For detailed CompuSyn analysis, see Supplemental Data Appendix IV (http://pharmrev.aspetjournals.org/cgi/content/full/pr.58.3.10/DC1).

Drug			Fractional Inhibition, f_a	Parameter[a]			CI[b]
Paclitaxel	Cisplatin	Topotecan		m	D_m	r	
μM					μM		
$(D)_1$							
0.002			0.429				
0.004			0.708				
0.005			0.761				
0.01			0.882				
0.02			0.932	1.248	0.00217	0.990	
	$(D)_2$						
	0.05		0.055				
	0.1		0.233				
	0.2		0.301				
	0.5		0.559				
	1.0		0.821				
	2.0		0.953	1.458	0.320	0.986	
		$(D)_3$					
		0.01	0.069				
		0.02	0.213				
		0.05	0.373				
		0.1	0.785				
		0.2	0.940				
		0.5	0.991	1.855	0.0462	0.991	
$(D)_1 + (D)_2$ (1:100)[c]							
0.001	0.1		0.450				0.900
0.002	0.2		0.701				0.815
0.005	0.5		0.910		0.0001147		0.681[d]
0.01	1.0		0.968	1.572	+ 0.11471		0.602
$(D)_2 + (D)_3$ (100:10)							
	0.05	0.005	0.304				0.445
	0.1	0.01	0.413				0.658
	0.2	0.02	0.675				0.669
	0.5	0.05	0.924		0.1053		0.561
	1.0	1.0	0.977	1.588	+ 0.01053	0.989	0.522
$(D)_1 + (D)_3$ (1:10)							
0.001		0.01	0.274				1.373
0.002		0.02	0.579				1.078
0.005		0.05	0.901		0.00166		0.719
0.01		0.1	0.965	1.891	+ 0.01661	0.999	0.681
$(D)_1 + (D)_2 + (D)_3$ (1:100:10)							
0.001	0.1	0.01	0.456				1.121
0.002	0.2	0.02	0.806		0.001162		0.729
0.003	0.3	0.03	0.947		+ 0.11616		0.403
0.005	0.5	0.05	0.995	3.363	+ 0.011612	0.984	0.136

[a] The parameters m, D_m, and r are the slope, antilog of the x-intercept, and the linear correlation coefficient of the median-effect plot, which signifies the shape of the dose-effect curve, the potency (IC_{50}), and the conformity of the data to the mass-action law, respectively. D_m and m values are used for calculating the CI values.

[b] CI < 1, CI = 1, and CI > 1 indicate synergism, additive effect, and antagonism, respectively. As based on the classic isobologram equation, CI can be calculated by eq. 16: $CI = [(D)_1/(D_x)_1] + [(D)_2/(D_x)_2]$, where $D_x = D_m[f_a/(1 - f_a)]^{1/m}$ (eq. 8).

[c] The drug mixture was serially diluted and added to incubation mixture at 0 h. The combination ratio was approximately equal to the D_m ratio of the component drugs (i.e., close to their equipotency ratio).

[d] Sample pocket calculator calculation of the CI value of 0.005 μM paclitaxel + 0.5 μM cisplatin that inhibited 833K cell growth by 91.0% (f_a = 0.910). On the basis of eq. 8, for paclitaxel alone to inhibit cell growth by 91% would require $[D_{0.91}]_{paclitaxel} = (D_m)_{paclitaxel}[0.91/(1 - 0.91)]^{1/1.248} = 0.00217\ \mu M \times 6.385 = 0.01385\ \mu M$ and for cisplatin alone to inhibit cell growth by 91% would require $[D_{0.91}]_{cisplatin} = (D_m)_{cisplatin}[0.91/(1 - 0.91)]^{1/1.458} = 0.320\ \mu M \times 4.888 = 1.564\ \mu M$. Therefore, CI = (0.005 μM/0.01385 μM) + (0.5 μM/1.564 μM) = 0.681 at 91% inhibition.

lyzed with CompuSyn (Chou and Martin, 2005)and along with the calculated parameters are given in Table 12.

b. Analytical conclusions: For "chronic exposure" to the skin of Swiss albino female mice (using benzo[*a*]pyrene as a carcinogen), starting at 10 weeks and starting at 55 weeks (Peto et al., 1975), there was little difference in carcinogenic effect, with D_m = 39.469 and 41.120 weeks, respectively. There were also no significant differences in the m values of 4.5693 ± 0.0630 and 4.6225 ± 0.1337, respectively; which both showed very steep (i.e., very sigmoidal) dose-effect curves. Remarkably, both give excellent conformity to the mass-action law with r = 0.9981 and r = 0.9917, respectively.

For "acute exposure" of C3H male mice via subcutaneous injection with benzo[*a*]pyrene and methylcholanthrene and dibenz[*a,h*]anthracene (Bryan and Shimkin, 1943), it yielded somewhat less sigmoidal shapes for the three carcinogens (m = 1.3879, 1.930, and 1.7720, respectively) than chronic exposure, as indicated above. Again, excellent conformity to the mass-action law with

TABLE 11

Sample illustration of computer-simulated CI and DRI values for paclitaxel, cisplatin, and topotecan combinations at 50, 75, 90, and 95% inhibition of 833K teratocarcinoma cell growth (for experimental data, see Table 10)

Incubation was carried out for 96 h under conditions described in Chou et al. (1994). Data analysis was carried out for parameters (D_m and m) and statistics (r) by using CompuSyn.

Drug Combination	Combination Ratio	CI Values[a] at Inhibition of				DRI Values[b] at inhibition of			
		50%	75%	90%	95%	50%	75%	90%	95%
Paclitaxel + cisplatin	1:100	0.887	0.781	0.690	0.636	1.89	2.27	2.72	3.07
						2.79	2.94	3.11	3.22
Cisplatin + topotecan	10:1	0.557	0.562	0.570	0.577	3.04	3.23	3.43	3.58
						4.39	3.97	3.59	3.36
Paclitaxel + topotecan	1:10	1.126	0.923	0.772	0.692	1.31	1.76	2.38	2.91
						2.78	2.81	2.85	2.87
Paclitaxel + cisplatin + topotecan	1:100:10	1.150	0.738	0.480	0.361	1.87	3.25	5.65	8.23
						2.76	4.22	6.46	8.63
						3.98	5.19	6.77	8.11

[a] CI values are based on the combination index isobologram equations (eq. 16 for two drugs and eq. 20 for three drugs).
[b] DRI represents the order of magnitude (fold) of dose reduction that is allowed in combination for a given degree of effect compared with the dose of each drug alone (TC Chou, 1991; JH Chou, 1991). Upper values are for the first drug and lower values are for the second drug.

r values of 0.9973, 0.9992, and 0.9984, respectively, have been observed (Fig. 14). Even at low doses, there is no apparent tendency for a systematic deviation from linearity. This conformity to the median-effect principle provides a rationale for low-dose risk assessment for carcinogens.

By using the benzo[a]pyrene data from both chronic and acute exposure in Table 12 as examples, it is possible to estimate the risk of a low-dose carcinogen (e.g., 0.5–0.001 D_m) for both acute and chronic exposures, as shown in Table 13. These findings have interesting and divergent implications for risk at low and high doses. For a given low total dose of carcinogen, chronic exposure is much less hazardous than an acute single injection. Thus, at 0.1 and 0.01 D_m, chronic exposure is 10^{-3} and 10^{-6} times less hazardous, respectively. In contrast, extrapolation to high (cumulative or single) doses indicates that chronic exposure is more hazardous than a single injection. The median-effect plots indicate that both the D_m values and m values are greatly affected by the mode or route of exposure. The m value, which describes the increment of dose versus the increment of effect, is a reflection of the basic intrinsic characteristics of the dose-effect relation of a carcinogen (Chou, 1976, 1980). Although these analyses have been carried out for single carcinogens only, similar methods using the multiple drug equation are apparently applicable to the effects of multiple carcinogens (including cocarcinogens) and the analysis of their interactions (e.g., synergism, additive effect, or antagonism).

2. Risk Assessment for Radiation.
   a. Crude data: Data for radiation-induced leukemia incidence among Hiroshima atom bomb survivals during 1950 to 1957 (Heyssel et al., 1960; Upton, 1961) were subjected to MEP analysis (Chou and Chou, 1985). These data, as shown in Table 14, have now been further analyzed with CompuSyn (Chou and Martin, 2005).
   b. Analytical conclusions and comments.
      i. The following parameters were obtained: m = 0.8956, a slightly flat dose-effect curve suggesting a negative cooperativity or repair process; D_m = 2,769,289 (rad), the dose required to induce leukemia in one half of a million people; and r = 0.98963, a very good correlation coefficient despite the fact that it was obtained from vivo human studies.
      ii. From these parameters, we can get an estimated risk at a very low dose by using eq. 9: $f_a = 1/[1 + (D_m/D)^m]$, thus:

Radiation Dose	Estimated Risk in Population
rad	*incidence per 10^x per year*
10,000	6.4536×10^{-3}
5,000	3.4794×10^{-3}
1,000	8.2538×10^{-4}
100	1.0504×10^{-4}
10	1.3360×10^{-5}
1	1.6986×10^{-6}

      iii. Similarly, we can calculate the required dose for producing a given low risk, e.g., 1×10^{-6}, 1×10^{-5}, 1×10^{-4} by eq. 8: $D_x = D_m [f_a/(1 - f_a)]^{1/m}$, thus:

Risk of Leukemia	Estimated Dose Required
incidence per 10^x per year	*rad*
10^{-6} (f_a = 0.000001)	0.55352
10^{-5} (f_a = 0.00001)	7.2390
10^{-4} (f_a = 0.0001)	94.6807

3. Therapeutic Index and Safety Margin
   a. Introduction: Depending on the type of drugs and type of experiments, the therapeutic index is usually defined as the ratio of LD_{50}/ED_{50} or TD_{50}/ED_{50}, and the safety margin can be defined as TD_{10}/ED_{90} or, more restrictively, TD_5/ED_{95}, where L, E, and T represent lethal, therapeuti-

TABLE 12

Dose-effect relationships of carcinogenic hydrocarbons in mice with chronic and acute exposure: an analysis by the median-effect equation

Reproduced from Chou TC, "Comparison of Dose-Effect Relationships Following Low-Dose Chronic Exposure and High-Dose Single Injection: An Analysis by the Median-Effect Principle," *Carcinogenesis*, 1980, volume 1, pp 203–213, by permission of Oxford University Press. Table also used by permission of Oxford University Press in Chou and Talalay (1987).

Experiment and Source of Data	Carcinogen	Weeks of Treatment[a]	Cumulative Fraction of Tumorless ($1 - f_a$)[b]	Slope (m)[c]	Median-Effect Dose (D_m)[c]
Chronic exposure (Peto et al., 1975)[d]					
Starting age: 10 weeks	Benzo[a]pyrene	42	0.99216	4.5693 ± 0.0630 (r = 0.9981)	39.469 weeks
		44	0.98425		
		46	0.96851		
		48	0.95276		
		50	0.93701		
		52	0.88977		
		54	0.87402		
		56	0.85040		
		58	0.77166		
		60	0.70867		
		62	0.66862		
		64	0.65212		
		66	0.57060		
		68	0.51354		
		70	0.43841		
		72	0.37033		
		74	0.30933		
		76	0.30037		
		78	0.26339		
		80	0.22507		
		82	0.19507		
		84	0.13265		
Starting age: 55 weeks	Benzo[a]pyrene	42	0.99024	4.6225 ± 0.1337 (r = 0.9917)	41.120 weeks
		44	0.98010		
		46	0.97316		
		48	0.96597		
		50	0.95489		
		52	0.95109		
		54	0.92644		
		56	0.88793		
		58	0.84308		
		60	0.78719		
		62	0.71539		
		64	0.66450		
		66	0.60643		
		68	0.53731		
		70	0.46268		
		72	0.40959		
		74	0.36449		
		76	0.35503		
		78	0.28518		
		80	0.18780		
		82	0.17147		
		84	0.17147		

Experiment and Source of Data	Carcinogen	Dose	Fraction Affected (f_a)[e]	Slope (m)[c]	Median-Effect Dose (D_m)[c]
		μg / mouse			
Acute (point) exposure[f] (Bryan and Shimkin, 1943)					
Starting age: 6–13 weeks	3-Methylchoanthrene	125	0.973	1.9330 ± 0.040 (r = 0.9992)	20.663 μg/mouse
		62	0.881		
		31	0.668		
		15.6	0.379		
		7.8	0.146		
		3.9	0.036		
	Dibenz [a,h]anthracene	62.5	0.912	1.7720 ± 0.0502 (r = 0.9984)	16.208 μg/mouse
		31.2	0.748		
		15.6	0.494		
		7.81	0.242		
		3.90	0.083		
		1.95	0.019		
	Benzo[a]pyrene	2000	0.988	1.3879 ± 0.0455 (r = 0.9973)	98.857 μg/mouse
		1000	0.960		
		500	0.888		
		250	0.756		
		125	0.565		
		62	0.358		
		31	0.186		

[a] Weeks of exposure minus 28 weeks (the latent period from initiation of tumor to tumor growth of 10 mm diameter) to obtain the effective exposure period of carcinogen as indicated by Peto et al (1975).

[b] Cumulative incidence of tumorless (i.e., cumulative $1 - f_a$) is calculated by the life-table procedure as used by Peto et al. (1975) See original study for details.

[c] The median-effect plot was carried out by plotting $\log [f_a/(1 - f_a)]$ vs. $\log D$, where m is the slope and $\log D_m$ is the intercept of the plot at the median-effect axis (i.e., at $\log [f_a/(1 - f_a)] = 0$). Both m and D_m are obtained from least-square regression analysis and D_m = antilog ($-y$-intercept/m). The range of m values is given as mean ± S.E. and r is the linear regression coefficient.

[d] Benzo[a]pyrene was applied twice weekly to skin of Swiss albino female mice. Animals with epithelial tumors of 10 mm diameter were scored.

[e] Statistically calculated values obtained by Bryan and Shimkin (1943) are used. Tumor incidences of 100% and <1% have been excluded from analysis.

[f] Carcinogenic hydrocarbons were injected s.c. into C3H male mice. Animals with spindle cell sarcoma during life-time were scored.

TABLE 13

Influence of the mode of exposure on the low-dose carcinogenic risk assessment of benzo[a]pyrene in mice[a]

Reproduced from Chou TC, "Comparison of Dose-Effect Relationships Following Low-Dose Chronic Exposure and High-Dose Single Injection: An Analysis by the Median-Effect Principle," *Carcinogenesis*, 1980, volume 1, pp 203–213, by permission of Oxford University Press. Table also used by permission of Oxford University Press in Chou and Talalay (1987).

Parameters of the Median-Effect Plot[b]	Acute Experiments[b,c]	Chronic Experiments[b,d]
m	1.3879 ± 0.0455	4.5693 ± 0.0630
D_m	98.857 (μg/mouse)	1578.8[e] (μg)
r	0.9973	0.9981

For a Given Dose (in D_m)	Acute Experiments		Chronic Experiments	
	Calculated Dose	Calculated Risk f_a	Calculated Cumulative Dose	Calculated Risk f_a
	μg/mouse		μg	
0.001	0.0988	1.85×10^{-5}	1.579	1.96×10^{-14}
0.01	0.988	1.67×10^{-3}	15.79	7.28×10^{-10}
0.1	9.886	3.93×10^{-2}	157.9	2.70×10^{-5}
0.5	49.43	2.77×10^{-1}	789.5	4.03×10^{-2}
1	98.86	0.50	1578.8	0.50
2	197.71	0.7234	3157.6	0.9596

[a] Risk (f_a) at a given dose was calculated from eq. 9: $f_a = 1/[1 + (D_m/D)^m]$.
[b] Parameters calculated are given in Table 12.
[c] Data from Bryan and Shimkin (1943) are used. C3h male mice were injected subcutaneously with a single dose of benzo[a]pyrene. Tumor incidence at the site of injection was histologically confirmed, spindle-cell sarcoma. Statistically calculated values reported by the original authors are used. Tumor incidence of 100% and <1% has been excluded from analysis.
[d] Data from Peto et al. (1975) are used. Benzo[a]pyrene (20 μg) in 0.25 ml of acetone, twice a week, was applied to the skin of Swiss albino female mice at 10 weeks old, treated for 100 weeks. Mice with epithelial tumors exceeding 10 mm in diameter were killed for histological examinations. The raw tumor incidence data were refined by the original authors in accordance with the life-table procedure.
[e] The total cumulated doses over a period of 39.469 weeks as calculated previously (Chou, 1980, 1981) (i.e., 20 μg/wk × 2 × 39.469 weeks = 1578.8 μg).

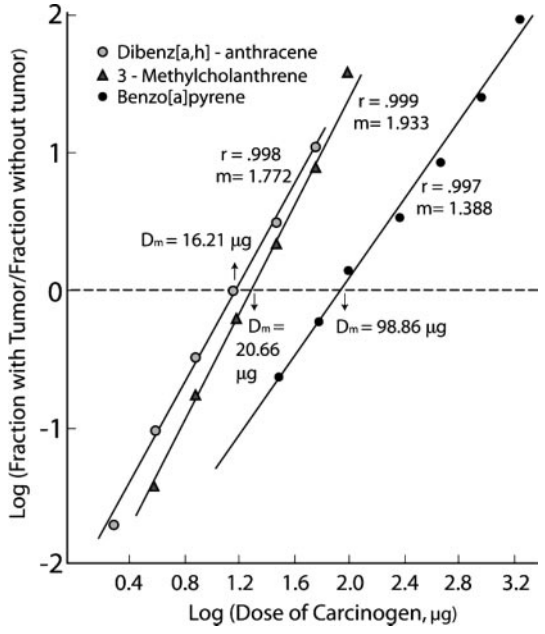

FIG. 14. The median-effect plot for carcinogenic polycyclic hydrocarbons in mice after an acute single dose by subcutaneous injections [original data from Bryan and Shimkin (1943), which were analyzed by Chou and Talalay (1981); see Table 12 for details].

TABLE 14

Dose-effect relationship in radiation-induced cancer: leukemia in Hiroshima atomic bomb survivors, 1950 to 1957

Data from Heyssel et al. (1960) [see also Upton (1961)].

Dose in Rad (D)	Incidence per 10^6 per Year ($f_a/10^{-6}$)
2620	1790
1060	950
430	355
177	230
77	69

cally effective, and toxicity, respectively. The requirement of these indexes for beneficial therapy is usually low for cytotoxic anticancer agents (e.g., therapeutic index = 2–10) and very high for drugs that are used for treating non-life-threatening diseases. The endpoint of the measurements can also influence the magnitude of an index. Although the endpoint for lethality (for LD) is clear-cut and universal, the choice of endpoints for therapeutic effect (for ED) and for the toxic effect (for TD) are somewhat arbitrary and circumstantial. For a less quantitative context, the therapeutic index is called the therapeutic window.

The doses (in the same unit) and fractional effect pairs (for the therapeutic and the toxic effects) are needed to calculate m and D_m (and r) parameters. These parameters are then used to calculate the D_x values by using the median-effect equation.

b. Crude data: An antitumor agent has been studied in mice bearing L1210 leukemia. The fractional leukemic cell survival is calculated from a calibration curve for increasing the size of leukemic cell inoculation and life-span shortening as proposed by Skipper (1974). These data are given in Table 15.

c. Analytical conclusions: The parameters for therapeutic effect are m = 9.7139, an extremely steep dose-effect curve (i.e., a very highly sigmoidal shape); D_m = 3.19097; and r = 0.9940 and for lethality to the host are m = 7.3700, an extremely steep dose-effect curve; D_m = 47.4524; and r =

TABLE 15
Ratio of therapeutic dose versus lethal dose against L1210 leukemia in mice: for calculation of therapeutic index or safety margin

Therapeutic Effect			Lethal Toxicity	
Dose of Therapy(D)	Fractional Leukemic Cell Survival (f_u)[a]	Fractional Leukemic Cell Kill ($f_a = 1 - f_u$)	Dose of Treatment (D)	Fractional Lethality to the Host (f_a)
			mg/kg	
0 mg/kg	1	0	36.4	0.1
4.0 mg/kg	$10^{-1.05}$	0.9109	40	0.2
5.3 mg/kg	$10^{-2.37}$	0.99573	44	0.5
7.1 mg/kg	$10^{-3.24}$	0.9994246	53	0.7
9.5 mg/kg	$10^{-4.30}$	0.99994988	59	0.8
12.6 mg/kg	$10^{-5.61}$	0.999997545		
16.9 mg/kg	$10^{-7.37}$	0.9999999573		

[a] Calculated from calibration curve for increasing size of leukemic cell inoculation and lifespan shortening as proposed by Skipper (1974).

0.9757. By using the above parameters and eq. 8, $D_x = D_m [f_a/(1 - f_a)]^{1/m}$.

CompuSyn will provide D_x values at any f_a levels. Thus,

$$\text{Therapeutic index} = LD_{50}/ED_{50} = 47.452/3.1909 = 14.870$$

$$\text{Safety margin} = LD_{10}/ED_{90} = 35.219/4.0009 = 8.803$$

Similarly,

$$LD_5/ED_{95} = 31.8237/4.3326 = 7.345$$

$$LD_1/ED_{99} = 25.438/5.1211 = 4.967$$

4. Age-Specific Cancer Incidence Rate Analysis.
   a. Introduction: The application of MEP to the age-specific cancer incidence or mortality rate in humans was not originally planned since the derivation of the median-effect equation at a steady state and at equilibrium state did not include a time factor. However, it is reasonable to assume that carcinogenic insults are proportional to age (Chou, 1978; Chou and Miller, 1980). The proportionality is implicated in the m value, which is the slope of the dose-effect curve. Chou and Chou (1985) have used the U.S. Third National Cancer Survey from 1975 and have randomly selected age-specific colon cancer incidence data among U.S. white males, 1969 to 1971, as an example for an analysis (Table 16). These data have now been further analyzed with CompuSyn (Chou and Martin, 2005). Remarkably, the r value is 0.9958, which shows excellent conformity between data and theory and thus points to useful epidemiological applications.
   b. Crude data and analytical results: The analysis has used eq. 9: $(f_a) \times 10^5 = [1 + (D_m/\text{age})^m]^{-1} \times 10^5$ (for a population of 100,000). Sample data are given in Table 16. The median-effect plot yields $m = 4.982 \pm 0.137$, a very high m value (i.e., a highly sigmoidal shape); $D_m = 254.92$ (years), calculated by $D_m = \text{antilog}\ (-y_{\text{intercept}}/m)$; and $r = 0.9958$. As shown in the last two columns of Table 16, the observed incidence per 10^5 population $[(f_a)_{obs} \times 10^5]$ and the calculated incidence per 10^5 population $[(f_a)_{cal} \times 10^5]$ are in close agreement.

TABLE 16
Colon cancer incidences (excluding rectum cancer) among white American males, 1969 to 1971
Source: Third National Cancer Survey (1975)

Age Group in Years	Median of the Age Group	Observed Incidence per 10^5 Population $[(f_a) \times 10^5]$	Calculated Incidence per 10^5 Population $[(f_a)_{cal} \times 10^5]$[a]
20–24	22	0.7	0.5
25–29	27	1.6	1.4
30–34	32	2.9	3.2
35–39	37	4.7	6.7
40–44	42	9.5	12.6
45–49	47	20.0	22.0
50–54	52	32.1	36.4
55–59	57	58.1	57.4
60–64	62	95.6	87.3
65–69	67	146.2	128.4
70–74	72	213.1	183.7
75–79	77	288.0	256.4
80–84	82	346.0	350.5

[a] Based on the median-effect principle of the mass-action law, the regression line slope for $\log[[(f_a)^{-1} - 1]^{-1}]$ vs. log (age) is $m = 4.982 \pm 0.137$; the y-intercept is $y_{int} = 11.988$, and the correlation coefficient is $r = 0.9958$. The median-effect value is $D_m = \text{antilog}\ (-y_{int}/m) = 254.92$ (years). The age-specific incidence rate is calculated by eq. 9; therefore, $(f_a)_{cal} \times 10^5 = [1 + (D_m/\text{age})^m]^{-1} \times 10^5$.

From the parameters and the equation above, it can be calculated that at age 65, a U.S. white male would have a 1.103×10^{-3} chance of getting colon cancer. At the age of 80, the chance of colon cancer among U.S. white males would be increased to 3.098×10^{-3} (a 2.8-fold increase, although age increased only 23%).

5. Epidemiological Applications (Chou, 1978; Chou and Miller, 1980): The median-effect equation and parameters have also been applied to other epidemiological data for trend studies:
   a. Epidemiological trend analysis for different time periods, e.g., different decades for various diseases can be analyzed in terms of mass-action law parameters.
   b. Social and economic effect analysis, e.g., changes in the population who smoke are reflected in the m values (e.g., decreased smoking leads to decreased m values and increased D_m values) for lung cancer among males and females and among racial groups.

c. Physiological status effect analysis, e.g., sudden changes in the m value (e.g., a break) are seen in breast cancer in females at the time of menopause.
d. Other applications, e.g., the use of the median-effect equation for the analysis of the environmental factor effects.
e. Changes in the mass-action law parameters for the cancer mortality rate at different decades may reflect therapeutic improvement and/or the early detection of cancer over decades for trend analysis.
f. The above analyses will be quantitative, not only qualitative.

6. Calculation of K_i from IC_{50}.
a. Introduction: During the early stages of deriving the median-effect equation, Chou (1972, 1974) used a systematic approach to derive equations in enzyme kinetic systems. The following relationship was derived (Chou, 1974).

$$IC_{50}/K_i = 1 + (A/K_A) = E_t/E_x$$

or

$$K_i = IC_{50}/[1 + (A/K_A)] \quad (24)$$

for the competitive inhibition of a single substrate (A) in a first-order reaction, where K_A is the enzyme-substrate dissociation constant (K_m) and E_x is the proportion of total enzyme (E_t) that is available for inhibitor binding. This relationship also indicates that the K_i (the inhibitor-enzyme dissociation constant) can never be greater than IC_{50}.

Apparently eq. 24 can be used for calculating K_i from IC_{50} in receptor binding system, which yields

$$K_i = IC_{50}/[1 + (L/K_D)] \quad (25)$$

where L is the primary or substrate ligand concentration and K_D is the ligand-receptor dissociation constant. K_D can be determined by the Scatchard (1949) plot and IC_{50} (for the inhibitor or secondary ligand) can be determined by the median-effect plot. Currently, eq. 25 is one of the most widely cited methods in the biomedical literature, especially in neuroscience and pharmacology. The following is an example for analysis.

By using an illustrative inhibitor dose-effect relationship given in Table 17, the m, D_m, and r parameters for an inhibitor can be determined with the median-effect plot. These, in conjunction with K_D determination using the Scatchard plot at the fixed concentration of a primary ligand, the K_i values can be determined from the IC_{50} (i.e., the D_m value) by using eq. 24 (Cheng and Prusoff, 1973; Chou, 1974), as illustrated in the footnote of Table 17. Many other examples for calculating K_i from IC_{50} are given in section V.A.3.

TABLE 17
Example for determination of K_i for receptor-inhibitor binding affinity
If we have determined K_D from the Scatchard plot to be 0.85 μM and if the present inhibition study is carried out in the presence of a constant concentration of the primary ligand at 1 μM, then the dose-effect relationship in Table 17 can be analyzed with CompuSyn to yield D_m = 5.5202 μM, m = 0.73226, and r = 0.9903. Thus, based on eq. 24, $K_i = IC_{50}/[1+ (A/K_A)] = 5.5202\ \mu M/[1+ (1/0.85)] = 2.5363\ \mu M$.

Inhibitor Concentration	Primary Ligand Binding	Fractional Inhibition (f_a)
	dpm	
0 (control)	10,000	
1 μM	7500	0.25
3 μM	6000	0.4
10 μM	5000	0.5
30 μM	2000	0.8
100 μM	1000	0.9
300 μM	500	0.95

C. Sample Analysis of Drug Combination Data with Computerized Summaries

1. Synergism of Two Insecticides on Houseflies. Le Pelley and Sullivan (1936) studied the lethality of rotenone, pyrethrins, and their mixture on houseflies. In this study, 900 to 1000 adult flies were used for each dose of these drugs at five dose levels. These data, as shown in Table 18, are of historical interest, since during the past 70 years, researchers from at least five different laboratories (Finney, 1947, 1952; Chou and Talalay, 1987; among others) have attempted to answer the question of whether or not there is synergism between these insecticides. A complete CompuSyn report (printout) for both 1:5 and 1:15 combinations is given in Supplemental Data Appendix V (http://pharmrev.aspetjournals.org/cgi/content/full/pr.58.3.10/DC1).

Table 18 reveals that the r values are greater than 0.993 and nearly 1.0, indicating that the applicability of the MEP method to these in vivo data is excellent. The LD_{50} values for rotenone, pyrethrins, and their 1:5 mixture calculated from the median-effect plot are 0.1505, 0.8932; and 0.4497 mg/ml, respectively (Table 18; see also Supplemental Data Appendix V for details). These values are in close agreement with those obtained from the probit analysis by Finney (1952), who obtained 0.156, 0.918, and 0.455 mg/ml, respectively.

The original authors interpreted their results as indicating no striking antagonistic or synergistic effect of the mixture. Richardson, quoted by Finney (1952), used a method for the mixture equivalent to the similar action law and asserted that there was pronounced synergism. Bliss, as indicated by Finney, supported Richardson's conclusion, and Finney after a new analysis of data, also agreed that there was evidence of synergism (Finney, 1952). The present analysis of the same data with the combination index equation and with the computer simulation (Table 18; Supplemental Data Appendix V) indicates that rotenone and pyrethrins (1:5) yielded nearly an additive effect with slight synergism (the CI values from ED_{50} to ED_{95} are 0.9176–0.9152). The 1:15 combination yielded slightly less synergism than the 1:5 combination since the former yielded CI values from ED_{50} to ED_{95}, which ranged from 0.9543 to 0.9187. CompuSyn generated a F_a-CI plot [and F_a-log (CI) plot] and a F_a-DRI plot [and F_a-log (DRI) plot]; the classic isobolograms for rotenone and pyrethrins are given in Supplemental Data Appendix V.

TABLE 18

Toxicity of rotenone and pyrethrins to houseflies: original data and computer-analyzed summary of results

Modified from "Quantitative Analysis of Dose-Effect Relationships: The Combined Effects of Multiple Drugs or Enzyme Inhibitors," *Advances in Enzyme Regulation*, volume 22, pp 27–55. Copyright 1984 with permission from Elsevier.

Original Data[a]			CompuSyn-Generated Results[b]									
Compound or Mixture	Concentration	% Kill[c]	Dose-Effect Parameters			Combination Index at:				Dose-Reduction Index at:			
			m	D_m	*r*	ED_{50}	ED_{75}	ED_{90}	ED_{95}	ED_{50}	ED_{75}	ED_{90}	ED_{95}
	μg/ml												
Rotenone (R)	0.1	26.0											
	0.15	47.5											
	0.20	67.5	2.626	0.151	0.907								
	0.25	81.5											
	0.35	89.5											
Pyrethrins (P)	0.5	21.5											
	0.75	39.5											
	1.0	54.0	2.387	0.893	0.995								
	1.5	75.0											
	2.0	89.0											
Rotenone + pyrethrins (1R:5P)	0.3	27.0								2.01	1.97	1.94	1.92
	0.45	53.0											
	0.60	64.0	2.519	0.450	0.994					2.38	2.44	2.50	2.54
	0.875	82.0		(0.075									
	1.175	93.0		+ 0.375)		0.9176	0.9163	0.9155	0.9152				
Rotenone + pyrethrins (1R:15P)	0.4	23.0								3.70	3.64	3.59	3.55
	0.6	48.0											
	0.8	61.0	2.533	0.652	0.983					1.46	1.50	1.54	1.57
	1.2	76.0		(0.041									
	1.6	93.0		+ 0.611)		0.9543	0.9465	0.9274	0.9187				

[a] Original data from Le Pelley and Sullivan (1936), retrieved and analyzed by Finney (1952), and analyzed by Chou and Talalay (1987).
[b] Further analyzed by CompuSyn (Chou and Martin, 2005). The full computer printouts are given in Supplemental Data Appendix III (http://pharmrev.aspetjournals.org/cgi/content/full/pr.58.3.10/DC1).
[c] Data for rotenone or pyrethrins alone were the average of two series of experiments.

2. Antagonism between Methotrexate and Arabinosylcytosine. The inhibition of the incorporation of [^{3}H]dUrd into DNA of L1210 leukemic cells by methotrexate (MTX) and Ara-C antimetabolites was analyzed by Chou and Talalay (1984). The experiment was carried out in a constant molar ratio of 1:0.782, and the data are given in Table 19.

TABLE 19

Inhibition of [^{3}H]dUrd incorporation into DNA in L1210 leukemic cells by MTX and Ara-C alone and in (1:0.782) combination

L1210 murine leukemic cells (8×10^6 cells) were incubated in Eagle's basal medium in the presence and absence of various concentrations of MTX and Ara-C and their mixture (molar ratio, 1:0.782) at 37°C for 20 min and then incubated with 0.5 μM (1 μCi) of [6-^{3}H]dUrd at 37°C for 30 min. Fractional inhibition (f_i or f_a) of [6-^{3}H]dUrd incorporation into perchloric acid-insoluble DNA fraction was then measured. All measurements were made in duplicate. Modified from "Quantitative Analysis of Dose-Effect Relationships: The Combined Effects of Multiple Drugs or Enzyme Inhibitors," *Advances in Enzyme Regulation*, volume 22, pp 27–55. Copyright 1984 with permission from Elsevier.

MTX		Fractional Inhibition (f_a) at [Ara-C] of:						
	0	0.0782	0.156	0.313	0.625	1.25	2.5	5.0
					μM			
0	0	0.582	0.715	0.860	0.926	0.955	0.980	0.993
0.1 μM	0.0348	0.405						
0.2 μM	N.D.[a]		0.587					
0.4 μM	N.D.			0.775				
0.8 μM	0.140				0.878			
1.6 μM	0.415					0.943		
3.2 μM	0.573						0.970	
6.4 μM	0.755							N.D.

[a] Result not used because of large variation between duplicates.

The computerized analysis of these data yields the following results. For MTX, $m = 1.091$, $D_m = 2.554$ μM, and $r = 0.9842$; for Ara-C, $m = 1.0850$, $D_m = 0.06245$ μM, and $r = 0.9966$. For the combination of MTX and Ara-C (1:0.782): $m = 1.1296$, $D_m = 0.2496$ μM, and $r = 0.9995$. The combination index shows an antagonism at all effect levels with the CI value at IC_{50} to IC_{90} ranging from 1.809 to 1.626.

3. Seven-Drug Combination against Human Immunodeficiency Virus and Their Polygonograms.

a. Introduction. In this large scale experiment, seven anti-HIV agents were used for two-, three-, four-, and five-drug combination to compare the results under the standarized conditions with P-24 enzyme-linked immunosorbent assays in MT4 cells infected with HIV-1-III_B. The preliminary results of this study were disclosed earlier (Chou and Zhu, 1997). In all, 21 sets of two-drug combinations, 20 sets of three-drug combinations, 10 sets of four-drug combinations and 2 sets of five-drug combinations have been analyzed using CalcuSyn (Chou and Hayball, 1997). The purposes of this study were 1) to rank synergism and antagonism within the group and among the groups for the degrees of synergism and antagonism in terms of CI values, 2) to compare the DRI values within the group and among the groups for the benefit of dose reduction at different effect levels, 3) to illustrate the automated

construction of a polygonogram for a large-scale experiment, 4) to demonstrate the usefulness of a polygonogram when presenting a massive amount of results, semiquantitatively, for a simple visual inspection, and 5) to predict the synergism or antagonism, semiquantitatively, of a higher number of drugs in combinations (that have not yet been carried out) from the CI results of the lower number of drugs in combinations.

The CompuSyn (Chou and Martin, 2005)-generated computer report for two- to five-drug combination anti-HIV studies consists of 90 pages of printout, which is available as Supplemental Data (http://pharmrev.aspetjournals.org/cgi/content/full/pr.58.3.10/DC1). Both software programs yielded vertically identical results except for slight differences after several digits of the decimal point. These slight differences are due to the slight differences in digits of the decimal points used for data entries. Using CalcuSyn, data sets need to be divided into many groups for analysis, whereas CompuSyn can handle large-scale data sets at once, as shown in Supplemental Data. In addition, CompuSyn has better graphics, new features such as polygonograms. and more flexible options (see section IV.).

TABLE 20
Dose-effect relationship parameters of the seven drugs used singly against HIV-1 IIIB replication in MT4 cells

The original data of Chou and Zhu (1997) were analyzed by CalcuSyn (Chou and Hayball, 1997). The dose-effect relationship parameters for potency, shape (sigmoidicity), and conformity are represented by D_m, m, and r, respectively, where D_m (EC_{50}) is the x-intercept (antilog), m is the slope of the median-effect plot that signifies the shape of the dose-effect curve ($m = 1$, > 1, and < 1 indicate hyperbolic, sigmoidal, and negative sigmoidal curve, respectively), and r is the linear correlation coefficient of the median-effect plot (Chou, 1976, 1991). The ranges of values given are the mean of two separate experiments; each experiment consists of seven concentrations for each drug.

Drugs	Parameters		
	D_m[a]	m	r
	μM		
AZT	0.00109 ± 0.00005	2.535 ± 0.0093	0.983 ± 0.001
DDI	2.743 ± 0.0245	1.929 ± 0.066	0.963 ± 0.001
DDC	0.1235 ± 0.0396	2.111 ± 0.113	0.983 ± 0.007
D4T	0.0142 ± 0.0015	2.458 ± 0.267	0.997 ± 0.001
IFN	0.0616 ± 0.0212	1.317 ± 0.249	0.989 ± 0.001
NEV	0.0568 ± 0.0033	2.406 ± 0.022	0.991 ± 0.006
ABT-538	0.0073 ± 0.0009	3.157 ± 0.299	0.974 ± 0.004

[a] The IC_{50} concentration (D_m) for each drug was in μM except for IFN, which was in kU/ml.

b. Summaries of results. The mass-action law parameters for each drug alone are given in Table 20. The CI values for 21 sets of two-drug combinations at ED_{50}, ED_{75}, ED_{90}, and ED_{95} are given in Table 21; the CI values for 20 sets of three-drug, 10 sets of four-drug, and two sets of five-drug combinations at ED_{50}, ED_{75}, ED_{90}, and ED_{95} are given in Table 22. The selected examples for the relationship of CIs and DRIs in the two- to five-drug combinations are given in Table 22. As expected from eq. 16, DRI and CI are somewhat inversely related. However, DRI for each drug can be influenced by the combination ratios of the experimental design. The polygonograms for two-drug combinations of the seven drugs are given in Fig. 9a.

c. Conclusions. Conclusions are as follows:

1. The rank orders of potency based on IC_{50} values (in micromolar concentrations, except for IFN in kallikrein units per milliliter) (Table 20) are AZT > ABT-538 > D4T > NEV > IFN > DDC ≫ DDI. The combination ratios for these seven drugs that

TABLE 21
CI values of two-drug combinations against HIV-1 III_a replication in MT4 cells

CI < 1, = 1, and > 1 indicate synergism, additive effect, and antagonism, respectively, as described by Chou and Talalay (1984).

Drug Combinations[a]	CI Values at:				Weighted Average CI Values[b]	Assigned Symbol[c]
	EC_{50}	EC_{75}	EC_{90}	EC_{95}		
AZT + DDC	1.469	1.321	1.189	1.107	1.211	− −
AZT + DDI	0.992	0.956	0.925	0.907	0.931	±
AZT + D4T	1.772	1.622	1.485	1.399	1.567	− − −
AZT + IFN	0.897	0.920	0.954	0.982	0.953	±
AZT + NEV	0.455	0.451	0.446	0.444	0.447	+ + +
AZT + ABT-538	0.580	0.603	0.628	0.647	0.626	+ + +
DDI + DDC	1.377	1.421	1.466	1.498	1.461	− − −
DDI + D4T	1.606	1.551	1.499	1.464	1.506	− − −
DDI + NEV	0.770	0.685	0.611	0.566	0.624	+ + +
DDI + IFN	0.619	0.711	0.819	0.905	0.812	+ +
DDI + ABT-538	0.619	0.602	0.594	0.593	0.598	+ + +
DDC + D4T	1.152	1.049	0.956	0.899	0.971	±
DDC + NEV	1.064	0.946	0.842	0.778	0.859	+
DDC + ABT-538	0.952	0.890	0.833	0.798	0.842	+ +
DDC + IFN	0.890	0.842	0.808	0.791	0.816	+ +
D4T + NEV	1.189	1.075	0.973	0.909	0.989	±
D4T + IFN	0.940	0.850	0.774	0.730	0.782	+ +
D4T + ABT-538	1.263	1.225	1.188	1.163	1.193	−
IFN + NEV	0.575	0.563	0.555	0.553	0.558	+ + +
IFN + ABT-538	0.921	0.778	0.673	0.617	0.696	+ + +
NEV + ABT-538	0.876	0.807	0.744	0.705	0.754	+ +

[a] The combination ratios are designed to approximate the IC_{50} ratios in which the seven drugs and their corresponding constituent components have the combination ratio of AZT/DDI/DDC/IFN/D4T/NEV/ABT-538 = 1:1600:50:16:10:40:4.

[b] Because the high degrees of effects are more important to the chemotherapy than the low degrees of effects, the weighted CI value was designed as $CI_{wt} = [CI_{50} + 2CI_{75} + 3CI_{90} + 4CI_{95}]/10$.

[c] Degrees of synergism (+ signs) or antagonism (− signs) are based on the ranges of CI values as described in Table 4.

TABLE 22

CI values of three- to five-drug combinations against HIV-1 IIIB replication in MT4 cells

CI < 1, = 1, and > 1 indicate synergism, additive effect, and antagonism, respectively, as described by Chou and Talalay (1984).

Drug Combinations[a]	CI values at:				Weighted Average CI values[b]	Assigned Symbol[d]
	EC_{50}	EC_{75}	EC_{90}	EC_{95}		
Three-drug combinations						
AZT + DDC + D4T	1.904	1.672	1.472	1.350	1.506	− − −
AZT + DDC + NEV	1.227	1.040	0.883	0.789	0.911	±
AZT + DDC + ABT-538	1.529	1.295	1.098	0.982	1.134	−
AZT + DDI + NEV	0.719	0.623	0.541	0.493	0.566	+ + +
AZT + DDI + IFN	0.715	0.771	0.838	0.891	0.834	+ +
AZT + DDI + ABT-538	0.638	0.651	0.669	0.684	0.668	+ + +
AZT + D4T + NEV	1.420	1.268	1.132	1.049	1.155	−
AZT + D4T + ABT-538	1.335	1.312	1.290	1.276	1.293	− −
AZT + IFN + NEV	0.368	0.371	0.377	0.381	0.377	+ + +
AZT + IFN + ABT-538	0.447	0.494	0.551	0.597	0.548	+ + +
AZT + NEV + ABT-538	1.224	1.042	0.887	0.796	0.915	±
AZT + NEV + ABT-538	0.602	0.574	0.548	0.532	0.552	+ + +
DDC + D4T + NEV	1.338	1.178	1.039	0.955	1.063	±
DDC + D4T + ABT-538	1.335	1.198	1.077	1.003	1.097	±
DDC + NEV + ABT-538	0.899	0.808	0.727	0.678	0.741	+ +
DDI + IFN + NEV	0.407	0.475	0.558	0.625	0.553	+ + +
DDI + IFN + ABT-538	0.682	0.646	0.623	0.613	0.630	+ + +
DDI + NEV + ABT-538	0.687	0.625	0.573	0.543	0.583	+ + +
D4T + NEV + ABT-538	1.254	1.122	1.005	0.932	1.024	±
IFN + NEV + ABT-538	0.714	0.648	0.596	0.566	0.606	+ + +
Four-drug combinations						
AZT + DDC + D4T + NEV	1.390	1.248	1.120	1.042	1.141	−
AZT + DDC + D4T + ABT-538	2.045	1.834	1.613	1.525	1.665	− − −
AZT + DDC + NEV + ABT-538	1.340	1.135	0.967	0.812	0.976	±
AZT + DDI + IFN + NEV	0.866	0.729	0.616	0.551	0.638	+ + +
AZT + DDI + IFN + ABT-538	0.498	0.488	0.478	0.479	0.482	+ + +
AZT + DDI + NEV + ABT-538	0.701	0.648	0.609	0.586	0.617	+ + +
AZT + D4T + NEV + ABT-538	1.756	1.524	1.322	1.202	1.358	− −
AZT + IFN + NEV + ABT-538	0.426	0.420	0.418	0.416	0.418	+ + +
DDC + D4T + NEV + ABT-538	1.532	1.322	1.143	1.037	1.175	−
DDI + IFN + NEV + ABT-538	0.410	0.388	0.371	0.364	0.376	+ + +
Five-drug combinations						
AZT + DDC + D4T + NEV + ABT-538	1.440	1.291	1.149	1.064	1.173	−
AZT + DDI + IFN + NEV + ABT-538	0.609	0.539	0.485	0.455	0.495	+ + +

[a] The combination ratios are designed to approximate the IC_{50} ratios in which the seven drugs and their corresponding constituent components have the combination ratio of AZT/DDI/DDC/IFN/D4T/NEV/ABT-538 = 1:1600:50:16:10:40:4.

[b] Because the high degrees of effects are more important to the chemotherapy than the low degrees of effects, the weighted CI value was designed as $CI_{wt} = [CI_{50} + 2CI_{75} + 3CI_{90} + 4CI_{95}]/10$.

[c] Degrees of synergism (+ signs) or antagonism (− signs) are based on the ranges of CI values as described in Table 4.

have been used in experiments are 1:4:10:16:40:50:1600, respectively.

2. For two-drug combinations, the rank orders for synergism based on the weighted CI values in Table 21 are AZT + NEV > IFN + NEV ≥ DDI + ABT-538 > DDI + NEV ≥ AZT + ABT-538, IFN + ABT-538. The rank orders for antagonism based on weighted CI values are AZT + D4T > DDI + D4T ≥ DDI + DDC > AZT + DDC.
3. For three-drug combinations in Table 22, the rank orders for synergism are AZT + IFN + NEV > DDI + IFN + NEV ≥ AZT + IFN + ABT-538 ≥ AZT + NEV + ABT-538 ≥ AZT + DDI + NEV > DDI + NEV + ABT-538 ≥ DDI + IFN + ABT-538 ≥ AZT + DDI + ABT-538. The ranks for antagonism are AZT + DDC + D4T ≥ AZT + D4T + ABT-538.
4. For four-drug combinations in Table 22, the synergism rank orders are DDI + IFN + NEV + ABT-538 > AZT + IFN + NEV + ABT-538 ≥ AZT + DDI + IFN + ABT-538 ≥ AZT + DDI + IFN + NEV. The rank orders for antagonism are AZT + DDC + D4T + ABT-538 > AZT + D4T + IFN + ABT-538.
5. For five-drug combinations in Table 22, the synergism is AZT + DDI + IFN + NEV + ABT-538 and the slight antagonism is AZT + DDC + D4T + NEV + ABT-538.
6. Results in Table 23 indicate that two-, three- four- and five-drug combinations all showed favorable dose-reduction from ED_{50} to ED_{95}. The higher number of drugs in combination yields more favorable dose reduction than the lower number of drugs in combination.
7. The polygonogram (Fig. 9a) for two-drug combinations of seven drugs provide semiquantitative simple predictions of synergism or antagonism in three-, four- and five-drug combinations as indicated in the experimental observations in Table 22.
8. The results in Table 21 for two-drug combinations offer good predictions for synergism or antagonism for the three-, four-, and five- drug combinations in Table 22. There are 120 possible combinations for 7 drugs and 21 combinations for two-drug combinations in Table 21 and yet the software produced a great deal of predictive power for combinations in-

TABLE 23
Typical example of changes in DRI values and their relationship to CI values in two- to five-drug combinations

Drug Combinations	DRI[a] Values at:				CI[b] Values at:			
	EC_{50}	EC_{75}	EC_{90}	EC_{95}	EC_{50}	EC_{75}	EC_{90}	EC_{95}
AZT +	3.87	3.85	3.83	3.82	0.455	0.451	0.446	0.444
NEV (1:40)	5.09	5.24	5.40	5.50				
AZT +	5.43	5.12	4.89	4.74				
NEV +	7.08	6.97	6.86	6.79	0.368	0.371	0.377	0.381
IFN (1:40:16)	24.36	30.76	38.90	45.57				
AZT +	3.80	4.14	4.33	4.56				
NEV +	5.06	5.57	6.14	6.55	0.602	0.574	0.548	0.532
ABT-538 (1:40:4)	6.87	6.61	6.38	6.20				
AZT +	6.0	6.0	6.0	6.05				
NEV +	7.81	8.16	8.52	8.79	0.426	0.420	0.418	0.416
ABT-538 +	10.61	9.68	8.87	8.33				
IFN (1:40:4:16)	26.89	36.00	48.26	58.93				
AZT +	5.18	5.80	6.29	6.62				
NEV +	6.99	7.84	8.79	9.51				
ABT-538 +	9.50	9.28	9.13	9.00	0.609	0.539	0.485	0.455
IFN +	23.95	34.65	49.83	63.78				
DDI (1:40:4:16:1600)	7.90	9.77	12.09	13.97				

[a] The DRI provides a measure of how much (fold) the dose of each drug in a synergistic combination may be reduced at a given effect level compared with the doses of each drug alone. The relationship of CI and DRI is depicted in eq. 16.
[b] CI values are obtained from Tables 21 and 22.

volving three, four, and five drugs. The results for three-drug combinations also provided good predictions for the outcomes of four- and five-drug combinations.

9. AZT, DDC, DDI, and D4T are nucleoside analogs that are known to inhibit HIV reverse transcriptase whereas NEV is a non-nucleoside reverse transcriptase inhibitor. ABT-538 is known to be a HIV-associated protease inhibitor, and IFN possesses rather complex mechanisms. The results in Tables 21 and 22 suggest that combinations consisting of different classes of anti-HIV agents (e.g., attacking different stages of the HIV life cycle) are more likely to produce better synergism than those consisting of several anti-HIV agents from the same class.

D. Approaches for the Conservation of Laboratory Animals

Millions after millions of animals have been used annually for biomedical research in academia and industry for dose-effect studies of drug efficacy, toxicity, and drug combinations. During the past decades, much attention has been focused on humane treatment of animals as indicated in federal legislation and regulations (*U.S. Department of Agriculture Animal Welfare Act and Regulations,* 2002; *U.S. Public Health Service Policy on Humane Care and Use of Laboratory Animals,* 2002). It should be stressed, however, that attaining research aims with a reduced number of animals or avoiding the necessary use of animals is not only economically cost-effective but also an ethical blessing for humanity. The cost of using animals in preclinical research not only involves animal purchasing, maintenance, facilities, and equipment but also involves personnel time and their efforts, in addition to frequently unavoidable pain, discomfort, suffering, or death of the laboratory animals. The popular methods in the 1940s to the 1960s for determining LD_{50} values using a large number of animals for the sake of fulfilling statistical requirements is no longer considered necessary or ethical, especially when using large animals.

During past decades, Chou JH, Chou, and Talalay, (Chou JH et al., 1983, 1984) had advocated reducing the numbers of animal used by scientific means, such as improving experimental design and using a computer and software based on the mass-action law. A featured special report on Chou's computer approach in saving animal's lives was presented by Cusack (1983) that highlighted the team of father and son's crusade of saving animals with a cartoon.

Conservation of laboratory animals can be achieved by these and other means. We repeatedly advocated use of the median-effect principle (MEP) of the mass-action law, its efficient experimental design, and computer simulation as well as SDA and polygonogram methods (Chou and Chou, 1985, 1989; Chou and Hayball, 1997; Chou and Martin, 2005). These aims can be illustrated on several fronts, as indicated below:

1. The Median-Effect Principle. With the median-effect principle [i.e., the median-effect equation (eqs. 7–9) and the median-effect plot], we are using animal data to "conform" the fundamental mass-action law. We are not using animal data to "fit" an empirical and unfounded dose-effect curve. These are illustrated by the theoretical analysis given in Figs. 3 and 11, as well as by actual experimental data in vitro given in Tables 8 through 11 and 20, and the in vivo data given in Tables 12 through 16 and 18, and in Fig. 14 (and their computerized analysis, parameters, and graphic printouts). There is no doubt (i.e., from their r values) that the experimental data, both in vitro and in vivo, conform to the MEP excellently. At the theoretical extreme, we can even obtain a dose-effect curve from only two data points, but this requires accurate measurements and uses of uniformed test subjects. By using fewer data

points (either theoretical or experimental, in vitro and in vivo), virtually identical results or conclusions can actually be verified by arbitrarily deleting one, two, or even three data points from the existing data points, rerunning the analysis by using a computer, and compare the resulting conclusions. The results and conclusions are usually similar (see Supplemental Data Appendices II–V). For the study of microtubule stabilization of epothilones as antitumor agents, we have used only three to six nude mice for each dose against various xenograft tumors and depending on the experiment purposes, we have used a very few doses (e.g., three to four doses for the dose-effect relationships in vivo) (Chou et al., 1998a,b, 2001, 2005a,b,c).

2. Experimental Design. For drug combination studies, there are different ways to combine the drugs. I recommend using a constant ratio combination (e.g., equipotent combination, such as IC_{50} or ED_{50} ratios) as illustrated in Tables 5 and 19 and Fig. 10. This type of diagonal scheme design for in vivo studies can easily save 60 to 80% or more animals than the checkerboard design and yet allows the determination of potency, shape, and conformity parameters (D_m, m, and r, respectively) as well as automated construction of dose-effect curves, median-effect plots, the F_a-CI plot, the F_a-DRI plot, and isobolograms. Remarkably, before use of the combination index method and formal derivation of the isobologram equation, earlier scholars, such as Le Pelley and Sullivan (1936) (see Table 18 and Supplemental Data Appendix V) had already used 1:5 and 1:15 constant combination ratios for rotenone and pyrethrins against houseflies (800–1000 houseflies/dose). Equally remarkable, Yonetani and Theorell (1964) carried out elegant studies on alcohol dehydrogenase with outstanding accuracy (as manifested by r values) and had also used inhibitors in combination at constant ratio(s) (see Tables 8 and 9 and Supplemental Data Appendices II and III).

In vivo anticancer drug combination studies were carried out by Chou et al. (2005a) on the basis of the combination index method and the constant ratio experimental design. Taxotere and T-900607 were combined at 1:2 ratios against a human mammary carcinoma MX-1 xenograft in nude mice. There were three doses for each drug alone and in combination. Each dose was tested in five mice. A total of 60 mice, 50 mice for the drug combination experiment [15 mice each for the single drug alone and its combination (three groups) and 5 mice for the untreated control group] plus 10 mice for the preliminary exploratory studies, had been used, and the authors were able to obtain the above-mentioned parameters (including ED_{50}) and plots (e.g., dose-effect curves, median-effect plots, F_a-CI plots, F_a-DRI plots, and isobolograms).

3. Serial Deletion Analysis. In the dose-effect relationship studies, there is no fixed rule as to how many doses should be used for a given drug. Usually, for in vitro studies, we used five to eight concentrations and for in vivo studies we used three to five doses. As indicated above, the median-effect plot can generate a dose-effect curve and calculate mass-action law parameters with two or more doses. For example, for pyrethrins in Table 18, 5 doses, 0.5, 0.75, 1, 1.5, and 2 μg/ml, were used, for which the generated effect yielded $m = 2.387$, $D_m = 0.893$ μg/ml, and $r = 0.995$ (see Supplemental Data Appendix V). If we rerun these data by deleting one dose each time, a series of m, D_m, and r values to subject to statistical treatments can be obtained. Similarly, the same principle can be applied for rotenone. Each corresponding D_m and m value for each drug can be introduced into the combination index equation for a series of CI determinations, which can also be subjected to statistical treatment. Thus, the mass law-based equation has unique properties that allow treating one experiment as if it were several experiments for maximal utilization of data. Consequently, intelligent design and analysis may reduce experimental size, reduce time and effort needed for experiments, and reduce animal usage for both single drug and drug combination studies.

4. Polygonogram. Although, testing of extra large-scale drug combinations are difficult to carry out in animals for practical and economical considerations, theoretically, as shown in Fig. 8a, seven drugs may have 120 different drug combinations. Inspection of a polygonogram with only 20 sets of two-drug combinations of seven anti-HIV agents allows semiquantitative prediction of what would happen to the combinations with higher number of drugs before the experiments are actually carried out. The usefulness of these predictions has been largely confirmed by experiments that are actually carried out for three-, four-, and five-drug combinations. This predictive utility can be translated to fewer experiments, less time and effort, and less animal usage when the experiments are carried out in vivo.

Appendix I: Derivation of the Multiple Drug-Effect Equation

Detailed descriptions for the derivation of multiple drug-effect equation based on the median-effect principle (Chou, 1976) have been given in Chou and Talalay (1977, 1981, 1984). This process has been outlined in Fig. 2. The early steps of the derivations can be summarized as the following, which can then lead to the combination index equation (Chou and Talalay, 1983).

A. Summation of the Effects

The summation of the effects (additive effects) of multiple inhibitors of various types on the initial velocity of enzyme systems obeying Michaelis-Menten kinetics is described by the general relation (Chou and Talalay, 1977):

$$\frac{1}{v_{1,2,3\ldots n}} = \sum_{i=1}^{n} \frac{1}{v_1} - \frac{n-1}{v_0} \qquad \text{(A1)}$$

wherein $v_{1,2,3...n}$ is the velocity of reaction in the simultaneous presence of n inhibitors, v_i is the velocity observed in the presence of each individual inhibitor, and v_0 is the velocity in the absence of inhibition. The derivation is based on the assumption that each enzyme species can combine with no more than one of the inhibitors (i.e., the inhibitors are mutually exclusive). The above relationship holds irrespective of the number of inhibitors, the type of inhibition (competitive, noncompetitive, or uncompetitive), or the kinetic mechanism (sequential, ping-pong, or random) of the enzyme reaction under consideration. Derivations from this equality define synergism or antagonism of inhibitors, depending on whether the value on the left side of the above equation is greater or smaller than the right side, respectively. Knowledge of the kinetic constants for substrates and inhibitors is not required.

If we define f_v = fractional velocity = v_n/v_0 and f_i, the fractional inhibition, = $(1 - f_a)$, then the analysis can proceed as below:

B. Alternative Equations for Multiple Inhibitors in First-Order Systems

These can be obtained, and several useful forms of eq. A1 can be derived as follows. Because the fractional velocity (f_v) is v_n/v_0 and the fractional inhibition (f_i) is $(1 - f_v)$, then multiplying both sides of eq. A1 by v_0 and taking the reciprocal, we obtain

$$(f_v)_{1,2...n} = \left[\sum_{j=1}^{n} (f_v)_j^{-1} - (n-1)\right]^{-1} \quad \text{(A2)}$$

Because by definition $f_i + f_v = 1$, eq. A2 can be converted to

$$(f_v)_{1,2...n} = \frac{1}{1 + \sum_{j=1}^{n} \frac{(f_i)_j}{(f_v)_j}} \quad \text{(A3)}$$

Again, because by definition $(f_i)_{1,2...n} = 1 - (f_v)_{1,2...n}$; therefore

$$\frac{(f_i)_{1,2...n}}{(f_v)_{1,2...n}} = \sum_{j=1}^{n} \frac{(f_i)_j}{(f_v)_j} \quad \text{(A4)}$$

Based on the distribution equation of enzyme species, it was shown by Chou (1974) that the fractional velocity of Michaelis-Menten-type enzyme reactions with different number of substrates, different reaction mechanisms (e.g., sequential or ping-pong), and different types and mechanisms of inhibition (e.g., competitive, noncompetitive, or uncompetitive) by a single inhibitor, which binds to a given enzyme species, can be expressed by

$$f_v = \frac{1}{1 + (I/K_i)(E_x/E_t)} \quad \text{(A5)}$$

where E_t is the total amount of enzyme and E_x is the fractional availability of the enzyme species with which the inhibitor may combine.

Furthermore, the availability of the ligand-binding site, E_x/E_t, can be described by the distribution equation (Chou, 1974, 1977)

$$E_x/E_t = K_i/I_{50} \quad \text{(A6)}$$

where I_{50} is the median-effect concentration of the inhibitor, i.e., that required to inhibit the enzyme reaction by 50%.

Hence, eq. A6 can be transformed to

$$f_v = \frac{1}{1 + (I/I_{50})} \quad \text{(A7)}$$

and

$$f_i = \frac{1}{1 + (I_{50}/I)} \quad \text{(A8)}$$

Note that eq. A8, which is derived for a reference ligand (e.g., inhibitor), has the same form as the Michaelis-Menten (1913) equation for a primary ligand (e.g., substrate).

Equations A7 and A8 give

$$f_i/f_v = I/I_{50} \quad \text{(A9)}$$

which is the median-effect equation for first-order kinetics (Chou, 1975, 1976).

In the presence of N inhibitors, a combination of eqs. A3 and A9, gives

$$(f_v)_{1,2...n} = \frac{1}{1 + \sum_{j=1}^{n} \frac{(I)_j}{(I_{50})_j}} \quad \text{(A10)}$$

From eqs. A4, A5, and A10, we obtain (Chou and Talalay, 1981)

$$\frac{(f_i)_{1,2...n}}{(f_v)_{1,2...n}} = \sum_{j=1}^{n} \frac{(f_i)_j}{(f_v)_j} = \sum_{j=1}^{n} \frac{(I)_j}{(K_i)_j} \cdot \frac{(E_x)_j}{E_t} = \sum_{j=1}^{n} \frac{(I)_j}{(I_{50})_j} \quad \text{(A11)}$$

C. Inhibition of Higher-Order Kinetic Systems by a Single Inhibitor

If we consider the case where m molecules of inhibitor, I, interact with one molecule of an enzyme species to form a complex, then by extending the first-order median-effect equation to higher orders, the following relationship is obtained (Chou, 1975, 1976):

$$f_i/f_v = (I/I_{50})^m \quad \text{(A12)}$$

The validity of eq. A12 is independent of the mechanism of inhibition and of the mechanisms of the enzyme or the nature of the enzyme species that binds to the inhibitor. An explicit and formal derivation for eq. A12 is given in Chou (1976) and Chou and Talalay (1981, Appendix II).

Because $f_i + f_v = 1$, an alternative form of eq. A12 is

$$f_i = \frac{1}{1 + (I_{50}/I)^m} \quad \text{(A13)}$$

By definition of terms:

$$f_i/f_v = [(f_i)^{-1} - 1]^{-1} = (f_v)^{-1} - 1 = (v_0 - v_n)/v_n \quad \text{(A14)}$$

Thus, the logarithmic form of the median-effect equation (eq. A12) may be written as

$$\log[(f_i)^{-1} - 1]^{-1} = m \log I - m \log I_{50} \quad \text{(A15)}$$

A graphic representation of eq. A15 for different m values and $IC_{50} = 1$ is given in Fig. 5. The slope of each line represents m and the median-effect axis, where log $[(f_i)^{-1} - 1]^{-1} = 0$ (i.e., $f_i = 0.5$), intersects each line at the I_{50} value. This plot is designated as the "median-effect plot."

This equation for the "reference ligand" (such as inhibitor) is arithmetically similar to the currently formulated versions of the Hill equation for the "primary ligand" (S):

$$\log[v/(V - v)] = n \log S - \log K \quad \text{(A16)}$$

where n is the Hill coefficient and K is a constant that was undefined. A comparison of the median-effect equation and the Hill equation is given in Table 2.

D. Inhibition of the Higher-Order Kinetic Systems by Mutually Exclusive Inhibitors

In the presence of n inhibitors, each with m binding sites and if interactions follow Hill-type kinetics (i.e., the inhibitor binds to the enzyme sites in one step only), the general equation can be obtained by relating the first-order (eq. A11) to the mth order relationship of $f_i/f_v = (I/I_{50})^m$ (eq. A12) or $(f_i/f_v)^{1/m} = I/I_{50}$ to give (Chou and Talalay, 1981)

$$\frac{(f_i)_{1,2\ldots n}}{(f_v)_{1,2\ldots n}} = \left[\sum_{j=1}^{n} \frac{(I)_j}{(I_{50})_j}\right]^m$$

Taking the mth root gives

$$\left[\frac{(f_i)_{1,2\ldots n}}{(f_v)_{1,2\ldots n}}\right]^{1/m} = \sum_{j=1}^{n} \frac{(I)_j}{(I_{50})_j} = \sum_{j=1}^{n} \left[\frac{(f_i)_j}{(f_v)_j}\right]^{1/m} \quad \text{(A17)}$$

When $m = 1$, eqs. A17 and A11 become the same. The usefulness of the median-effect concentration (I_{50}) in analyzing the effect of multiple inhibitors is apparent from eq. A17, because when $(f_i)_{1,2\ldots n} = (f_v)_{1,2\ldots n} = 0.5$, the left term of the equation is equal to unity for any value of m and even when the m values for the inhibitors are different.

An alternative form of eq. A17 is

$$(f_v)_{1,2\ldots n} = \frac{1}{1 + \left\{\sum_{j=1}^{n} \left[\frac{(f_i)_j}{(f_v)_j}\right]^{1/m}\right\}^m} = \frac{1}{1 + \left[\sum_{j=1}^{n} \frac{(I)_j}{(I_{50})_j}\right]^m} \quad \text{(A18)}$$

The behavior of two mutually exclusive inhibitors in a second-order system ($m = 2$) may now be presented graphically, e.g., a plot of f_i with respect to the concentration of inhibitor(s) or the median-effect plot of log $[(f_i)^{-1} - 1]^{-1}$ with respect to log (I).

E. Multiple Inhibitions by Mutually Nonexclusive Inhibitors

1. First Order. In an earlier study (Chou and Talalay, 1977), we reported that multiple inhibitions of (first-order) Michaelis-Menten kinetic systems with noncompetitive, mutually nonexclusive inhibitors in single substrate reactions may be described by

$$(f_v)_{1,2\ldots n} = (f_v)_1 \cdot (f_v)_2 \ldots \cdot (f_v)_n \quad \text{(A19)}$$

By using the general principles described above, we can develop a simple shorthand method for deriving equations for multiple inhibitions by mutually nonexclusive inhibitors in first-order and the simplified higher-order kinetic systems. To illustrate this procedure, it is convenient to first consider a mutually exclusive case by examining the distribution of enzyme species and then extending the analysis to mutually nonexclusive cases, as shown below.

a. Case 1. I_1 and I_2 are mutually exclusive inhibitors that bind to the enzyme to form the following species: E + EI_1 + EI_2 (but not EI_1I_2). From the median-effect equation (eq. A11), we obtain

$$\frac{(f_i)_{1,2\ldots n}}{(f_v)_{1,2\ldots n}} = \frac{(I)_1}{(I_{50})_1} + \frac{(I)_2}{(I_{50})_2} = \frac{(f_i)_1}{(f_v)_1} + \frac{(f_i)_2}{(f_v)_2}$$

or, rearranging and substituting for $f_i = 1 - f_v$,

$$(f_v)_{1,2} = \frac{1}{1 + \frac{(I)_1}{(I_{50})_1} + \frac{(I)_2}{(I_{50})_2}} = \frac{1}{1 + \frac{(f_i)_1}{(f_v)_1} + \frac{(f_i)_2}{(f_v)_2}} \quad \text{(A20)}$$

Now, by analogy to the inductive reasoning of the distribution of enzyme species, it becomes apparent that the terms in the denominator of eq. A20: 1, $(I)_1/(I_{50})_1$, and $(I)_2/(I_{50})_2$; or 1, $(f_i)_1/(f_v)_1$, and $(f_i)_2/(f_v)_2$ correspond to the species E, EI_1, and EI_2, respectively. It should be noted that this is valid irrespective of the type of inhibition exerted by I_1 and I_2.

b. Case 2. I_1 and I_2 are mutually nonexclusive inhibitors that bind to the enzyme to form the following species: E + EI_1 + EI_2 + EI_1I_2. The enzyme species E, EI_1, EI_2, and EI_1I_2 should correspond to the terms of 1, $I_1/(I_{50})_1$, $I_2/(I_{50})_2$, and $I_1I_2/(I_{50})_1(I_{50})_2$, respectively. Therefore,

$$\frac{(f_i)_{1,2}}{(f_v)_{1,2}} = \frac{(f_i)_1}{(f_v)_1} + \frac{(f_i)_2}{(f_v)_2} + \frac{(f_i)_1(f_i)_2}{(f_v)_1(f_v)_2}$$

or, rearranging and substituting for $f_i = 1 - f_v$,

$$(f_v)_{1,2} = \frac{1}{1 + \frac{(f_i)_1}{(f_v)_1} + \frac{(f_i)_2}{(f_v)_2} + \frac{(f_i)_1(f_i)_2}{(f_v)_1(f_v)_2}} = \frac{1}{1 + \frac{(I)_1}{(I_{50})_1} + \frac{(I)_2}{(I_{50})_2} + \frac{(I)_1(I)_2}{(I_{50})_1(I_{50})_2}} \quad \text{(A21)}$$

This relationship permits us to compare graphically the effects of mutually exclusive and nonexclusive inhibitors in higher-order systems. At all concentrations, the mixtures of mutually nonexclusive inhibitors have more inhibition than the exclusive inhibitors, and at high concentrations, there is more inhibition than with the parent components (i.e., the concave upward dose-effect curves) (Chou and Talalay, 1981).

2. Multiple Inhibitions by Inhibitors with Different Kinetic Orders. The assumption has been made that all nonexclusive inhibitors follow the same kinetic order, m. As already pointed out (Chou and Talalay, 1981), when $(f_v)_{1,2...n} = (f_i)_{1,2...n} = 0.5$ (i.e., when the combination of n nonexclusive inhibitors produces the median effect), then eq. A21 can be given by

$$\frac{(I)_1}{(I_{50})_1} + \frac{(I)_2}{(I_{50})_2} + \frac{(I)_1(I)_2}{(I_{50})_1(I_{50})_2} = 1 \quad \text{(A22)}$$

Because $f_i + f_v = 1$; therefore, $f_i/f_v = (1/f_v) - 1$. Thus, eq. A21 becomes

$$\frac{1}{(f_v)_{1,2}} - 1 = \left[\frac{1}{(f_v)_1} - 1\right] + \left[\frac{1}{(f_v)_2} - 1\right] + \left[\frac{1}{(f_v)_1} - 1\right]\left[\frac{1}{(f_v)_2} - 1\right]$$

which is identical to eq. A19 (at $n = 2$); i.e., $(f_v)_{1,2} = (f_v)_1 \cdot (f_v)_2$. Proof of $(f_v)_{1,2} = (f_v)_1 \cdot (f_v)_2$ for case 2 can also be conveniently obtained by $(v_i)_{1,2}/v_0 = (v_i)_1/v_0 \cdots (v_i)_2/v_0$, as shown by Chou and Talalay (1977).

Further examples of cases involving more than two nonexclusive inhibitors and mixtures of exclusive and nonexclusive inhibitors are analyzed in the appendix of Chou and Talalay (1981). All of these analyses provide inductive proof that the combined effects of mutually nonexclusive inhibitors can be described by the product of the fractional velocities observed in the presence of the component inhibitors; i.e.,

$$(f_v)_{1,2...n} = \prod_{j=1}^{n} (f_v)_j$$

3. Higher-Order Multiple Mutually Nonexclusive Inhibitors. As indicated in eqs. A21 and A22, the third term (product) will result in a concave upward curve compared with the parent compounds. In calculating the CI value, this will have an additional (product) term and thus yield a greater CI value than the mutually exclusive assumption of CI calculation. Consequently, the mutually nonexclusive assumption will project somewhat less synergism (or more antagonism) and hence was termed a "conservative" estimation, since this "intrinsic synergism" has already been taken into account in the overall synergism (Chou and Talalay, 1981). The earlier software (Chou and Chou, 1985; Chou and Hayball, 1997) automatically calculated CI values and generated the F_a-CI plot under both mutually exclusive and nonexclusive assumptions, since exclusivity of two drugs, in most cases, can be determined by the median-effect plot. However, with three or more drug combinations, especially at kinetic order $m \neq 1$, (e.g., $m \gg 1$, $m \ll 1$), there can be partial exclusivity or mixed situations that make the complexity of equations beyond practical analysis. To be consistent with the classic isobologram and its equation, we decided that all drug combinations will be analyzed with mutually exclusive assumptions under the same universal standard.

This practice has been manifested in most drug combination studies in the past. The recent software CompuSyn no longer automatically provides CI analysis under mutually nonexclusive assumption (Chou and Martin, 2005). Thus, intrinsic synergy due to nonexclusivity is incorporated into the overall synergism calculation.

Glossary

Additive effect (CI = 1): The combined effect predicted by the mass-action law principle in the absence of synergism or antagonism.

Antagonism (CI >1): Smaller than expected additive effect based on the mass-action law.

Classic isobol: An equipotent graph with the doses of $Drug_1$ and $Drug_2$ on x- and y-axes, respectively.

Combination index (CI): A quantitative measure based on the mass-action law of the degree of drug interaction in terms of synergism and antagonism for a given endpoint of the effect measurement (Chou and Talalay, 1981).

CompuSyn: A computer software for PCs developed by Chou and Martin (2005) that can be used for dose-effect analysis for single drugs using the median-effect equation and for multiple drug combinations using both the median-effect equation and the combination index equation.

Dose-reduction index (DRI): A measure of how many -fold the dose of each drug in a synergistic combination may be reduced at a given effect level compared with the doses of each drug alone (Chou and Chou, 1988).

F_a-CI plot: A plot of CI on the y-axis as a function of effect level (f_a) on the x-axis. The computer-simulated F_a-CI plot displays synergism or antagonism for the entire spectrum of effect levels (e.g., f_a = 0.01–0.99) (Chou and Talalay, 1981, 1984).

F_a-DRI plot: A plot of DRI on the y-axis as a function of effect level (f_a) on the x-axis (Chou and Chou, 1988).

Isobologram (ED_{50} isobol, ED_{75} isobol, ED_{90} isobol, etc.): A graph indicating the equipotent combinations of various doses of two drugs. It can be used to illustrate additive effect, synergism, or antagonism, at different dose levels.

***m* value:** The shape parameter for the dose-effect curve. The *m* value is the slope of the median-effect plot. $m = 1$, $m > 1$, and $m < 1$ indicate hyperbolic, sigmoidal, and flat sigmoidal, respectively (Chou, 1976).

Median-effect dose (D_m): The dose that produces 50% effect such as IC_{50}, ED_{50}, or LD_{50}. It is a potency parameter, and it is obtained from the antilog of the *x*-intercept of the median-effect plot (Chou, 1976).

Median-effect equation: $f_a/f_u = (D/D_m)^m$; a general equation for dose-effect relationship derived from the mass-action law principle that takes into account both the potency (D_m) of a dose (D) and the shape (m) of dose-effect curve, where f_a and f_u are the fractions affected and unaffected, respectively. $m = 1$, $m > 1$, and $m < 1$ indicate hyperbolic, sigmoidal, and flat sigmoidal shape, respectively (Chou, 1976).

Median-effect plot: A plot $x = \log (D)$ versus $y = \log (f_a/f_u)$, where $f_a + f_u = 1$ and $f_u = 1 - f_a$. This plot linealizes all dose-effect curves that followed the mass-action law principle. The slope gives the *m* value, and the *x*-intercept antilog gives the D_m value (Chou, 1976).

MEP: The median-effect principle of the mass-action law (Chou, 1976, 1991). This includes the median-effect equation and plot and its parameters, as well as the interconversion of dose and effect.

Mutually exclusive drugs: Two (or more) drugs with similar basic modes of action are considered mutually exclusive drugs. The mutually exclusive condition is the general assumption of the classic isobologram and its equations are accepted as the golden standard for calculating the CI and DRI values.

Mutually nonexclusive drugs: Two (or more) drugs with totally independent modes of action analogous to the binding of one ligand to the receptor will not affect the binding of other ligands at different sites. In the ideal situation, even if D_1 and D_2 alone give parallel lines on the median-effect plot, $D_1 + D_2$ in combination will give a nonparallel slightly concave upward curve. Thus, $D_1 + D_2$ in combination contain an element of "intrinsic synergism," which may contribute to the overall synergism. If a mutually nonexclusive condition is assumed for the CI calculation, it will contain the third term (i.e., the product of the first two terms) in the CI equation. Consequently, the CI value will be greater (i.e., synergism will be less), and thus it was termed "conservative synergism" (Chou and Talalay, 1984). In real life, partial exclusivity may occur that would be difficult to quantitize. This is especially so if the combination includes more than two drugs, since different pairs of drugs could have different degrees of exclusivity. To be consistent with the classic isobologram assumption and for simplicity of calculation, the present software uses only the mutually exclusive assumption and does not use the mutually nonexclusive assumption for drug combinations (i.e., intrinsic synergism, if it exists, is included in the overall synergism in drug combination analysis).

Normalized isobol: An equipotent graph with the normalized dose of $Drug_1$ as $[D_1/(D_x)_1]$ and $Drug_2$ as $[D_2/(D_x)_2]$ on the *x*- and *y*-axes, respectively. Both *x*- and *y*-axes are scaled to 1 (Chou and Talalay, 1984).

Polygonogram: A polygonal graphic representation depicting synergism (solid line in red tone), additive effect (thin line in pink tone), and antagonism (broken line in blue tone) for three (triangular), four (tetrahedral), five (pentagonal), or more drug combinations. The degree of boldness (thickness) of the line represents the degree of synergism or antagonism. The "component drugs" in pairs or triplets, etc., in the polygonogram may be considered dissectional components presented in the same graph. This method was first used by Chou et al. (1994), and the term was formally named as "polygonogram" by Chou and Chou (1998). In the current software (Chou and Martin, 2005), each drug pair is represented in the polygonogram. That is, only combinations (at a constant ratio) with two component drugs are shown on the polygonogram. Three-drug component combinations, if carried out, can be manually drawn with triangles; four-drug component combinations can be drawn with rectangles or squares, etc. The polygonogram provides a simple visual presentation for complicated multidrug combinations. It also provides a rational for projecting the outcome of synergism or antagonism for the multidrug combination experiments that have not yet been conducted.

Potentiation: A condition in which one of the two drugs is not effective by itself, but increases the effect of the other drug. It is usually described by percent potentiation or -fold potentiation, a synonym of augmentation or enhancement. No CI can be determined without *m* and D_m values due to an ineffective drug.

***r* value:** The conformity parameter for goodness of fit to the median-effect principle (MEP) of the mass-action law. It is the linear correlation coefficient of the median-effect plot, where $r = 1$ indicates a perfect conformity.

Sequential deletion analysis (SDA): An iterative sequential deletion of one dose (or concentration) of a drug at a time for repetitive CI calculations. This is followed by calculating the mean ± 95% confidence interval at each specified effect levels of the F_a-CI plot (Chou and Martin, 2005).

Synergism (CI < 1): Greater than expected additive effect based on the mass-action law.

Acknowledgments. I express my deepest gratitude to my Ph.D. thesis mentor, Professor and American Cancer Society Chair Robert E. Handschumacher of Yale University College of Medicine, and my postdoctoral mentor, Professor and John Jacob Abel Chair Paul Talalay of The Johns Hopkins University School of Medicine, for allowing me, then as a student and junior scientist, to have a free

spirit for independent exploration in the research field that is only tangential to theirs. Their generosity and kindness transcended to their continued support of a series of my early theoretical works and encouraged me to be the solo author. Even long after I left Johns Hopkins for the Sloan-Kettering Institute, Prof. Talalay kindly joined me for the work that led to the current combination index theorem. I also thank Professor and Eugene Higgins Chair Lenard J. Savage of Yale Statistics Department, the coauthor of *Inequalities for Stochastic Processes: How to Gamble If You Must*. During the last 2 years of his life, Prof. Savage helped me solve some combinatorial and number theory problems and served as an examiner in my Ph.D. thesis defense 36 years ago.

This article is dedicated to my mother, Sheng-Mei Chen, for her guidance and loving care after my father died when I was six; to my wife, Dorothy, for her understanding, patience, and support for this multidecade-long project; and to my son, Joseph, for helping me to write the first computer software ever for the mass-action law-based dose-effect analysis and for the drug combinations when he was 13 (before personal computers became available), and for signing an agreement with Elsevier-Biosoft, Cambridge, UK, for the software publication.

REFERENCES

Adusumilli PS, Stiles BM, Chan MK, Chou TC, Rusch VW, and Fong Y (2004) TSDA Award paper: stress response conferred by ionizing radiation potentiates oncolytic viral therapy efficacy in the treatment of lung cancer. *Ann Thoracic Surg* ATS #039503.

Aghi M, Chou TC, Suling K, Breakefield XO, and Chiocca EA (1999) Multimodal cancer treatment mediated by a replicating oncolytic virus that delivers the oxazaphosphorine/rat cytochrome P450 2B1 and ganciclovir/herpes simplex virus thymidine kinase gene therapies. *Cancer Res* **59:**3861–3865.

Aghi M, Kramm CM, Chou TC, Breakefield XO, and Chiocca A (1998) Synergistic anticancer effects of the ganciclovir/thymidine kinase and 5-fluorocytosine/cytidine deaminase gene therapies. *J Nat Cancer Inst* **90:**370–380.

Aghi M, Rabkin S, and Martuza RL (2006) Effect of chemotherapy-induced DNA repair on oncolytic herpes simplex viral replication. *J Natl Cancer Inst* **98:**38–50.

Algur E, Macklis RM, and Hafeli UO (2005) Synergistic cytotoxic effects of zoledronic acid and radiation in human prostate cancer and myeloma cell lines. *Int J Radiat Oncol Biol Phys* **61:**535–542.

Altman HJ, Stone WS, and Ogren SO (1987) Evidence for a possible functional interaction between serotonergic and cholinergic mechanisms in memory retrieval. *Behav Neural Biol* **48:**49–62.

Alzogaray RA, Picollo MI, and Zerba EN (1998) Independent and joint action of *cis*- and *trans*-permethrin in *Triatoma infestans* (Hempitera: Reduviidae) *Arch Insect Biochem Phys* **37:**225–230.

Ariens EJ, Simonis AM, and van Rossum JM (1964) *Molecular Pharmacology*, vol 1 (Ariens EJ ed) pp 287–324, Academic Press, New York.

Armitage P and Doll R (1954) The age distribution of cancer and a multi-stage theory of carcinogenesis. *Br J Cancer* **8:**1–12.

Ashford JR (1981) General models for the joint action of mixtures of drugs. *Biometrics* **37:**457–474.

Baba TW, Liska V, Hofman-Lehmann R, Vlasak J, Xu W, Ayehunie S, Cavacini LA, Posner MR, Katinger H, Stigler G, et al. (2000) Human neutralizing monoclonal antibodies of the IgG1 subtype completely protect against mucosal simian-human HIV infection. *Nat Med* **6:**200–206.

Bacherikov VA, Chou TC, Dong HJ, Chen CH, Lin YW, Tsai TJ, and Su TL (2004) Potent antitumor N-mustard derivatives of 9-anilinoacridine: synthesis and antitumor evaluation. *Bioorg Med Chem Lett* **14:**4719–4722.

Baker SP and Posner P (1986) Irreversible binding of acetylethylcholine mustard to cardiac cholinergic muscarinic receptors. *Mol Pharmacol* **30:**411–418.

Baker SP, Standifer KM, Kalberg CJ, Pitha J, and Sumners C (1988) Irreversible binding and recovery of the norepinephrine uptake system using an alkylating derivative of norepinephrine. *J Neurochem* **50:**1044–1052.

Balog A, Bertinato P, Su DS, Meng D, Sorensen E, Danishefsky SJ, Zheng YH, Chou TC, He L, and Horwitz SB (1997) Stereoselective synthesis and evaluation of compounds in the 8-desmethylepothilone A series: some surprising observations regarding their chemical and biological properties. *Tetrahedron Lett* **38:**4529–4532.

Balzarotti M, Ciusani E, Calatozzolo C, Croci D, Boiardi A, and Salmaggi A (2004) Effect of association of temozolomide with other chemotherapeutic agents on cell growth inhibition in glioma cell lines. *Oncol Res* **14:**325–330.

Bansinath M, Warner W, Tang CK, Turndorf H, and Puig MM (1992) On the mechanism of the interaction of ketamine and halothane in vitro. *Gen Pharmacol* **23:**1183–1187.

Barrie SE, Haynes BP, Potter GA, Chan FC, Goddard PM, Dowsett M, and Jarman M (1997) Biochemistry and pharmacokinetics of potent non-steroidal cytochrome P450(17α) inhibitors. *J Steroid Biochem Mol Biol* **60:**347–351.

Barrie SE, Rowlands MG, Foster AB, and Jarman M (1989) Inhibition of 17α-hydroxylase/C17–C20 lyase by bifluranol and its analogues. *J Steroid Biochem* **33:**1191–1195.

Bennett BM, Tam GS, Van Alstyne K, Brien JF, Nakatsu K, and Marks GS (1984) Effect of 5-isosorbide mononitrate on isosorbide dinitrate-induced relaxation of rabbit aortic rings. *Can J Physiol Pharmacol* **62:**1194–1197.

Bennett JJ, Adusumilli P, Petrowsky H, Burt BM, Roberts G, Delman KA, Zager JS, Chou TC, and Fong Y (2004) Up-regulation of GADD34 mediates the synergistic anticancer activity of mitomycin C and γ_1 34.5 deleted oncolytic herpes virus (G207). *FASEB J* **10:**1–21.

Berenbaum MC (1977) Synergy, additivism and antagonism in immunosuppression: a critical review. *Clin Exp Immunol* **28:**1–18.

Berenbaum MC (1981) Criteria for analysing interactions between biologically active agents. *Adv Cancer Res* **35:**269–335.

Berenbaum MC (1989) What is synergy? *Pharmacol Rev* **41:**93–141.

Berger BJ, Carter NS, and Fairlamb AH (1995) Characterisation of pentamidine-resistant *Trypanosoma brucei brucei. Mol Biochem Parasitol* **69:**289–298.

Berger BJ, Dai WW, Cerami A, and Ulrich P (1997) Studies on the mechanism of antimalarial action of a novel arylene bis(methylketone). *Biochem Pharmacol* **54:**739–742.

Berger BJ, Paciorkowski A, Suskin M, Dai WW, Cerami A, and Ulrich P (1996) Antimalarial activity of novel arylene bis(methylketone) compounds. *J Infect Dis* **174:**659–662.

Berman E, Duigou-Osterndorf R, Krown SE, Fanucchi MP, Chou J, Hirsch MS, Clarkson BD, and Chou TC (1989) Synergistic cytotoxic effect of azidothymidine and recombinant interferon α on normal human bone marrow progenitor cells. *Blood* **74:**1281–1286.

Berkson J (1946) Approximation of chi-square by "probits" and by "logits." *J Am Stat Assoc* **41:**70–74.

Bertino JR and Chou TC (1997) Chemotherapy: synergism and antagonism, in *Encyclopedia of Cancer,* vol 1 (Bertino JR ed) pp 368–379, Academic Press, San Diego.

Bliss CI (1939) The toxicity of poisons applied jointly. *Ann Appl Biol* **26:**585–615.

Boileau AJ, Evers AR, Davis AF, and Czajkowski C (1999) Mapping the agonist binding site of the GABAA receptor: evidence for a β-strand. *J Neurosci* **19:**4847–4854.

Boileau AJ, Kucken AM, Evers AR, and Czajkowski C (1998) Molecular dissection of benzodiazepine binding and allosteric coupling using chimeric γ-aminobutyric $acid_A$ receptor subunits. *Mol Pharmacol* **53:**295–303.

Bothamley J (2002) *Dictionary of Theories.* Barnes & Noble, New York.

Bozec A, Formento P, Ciccolini J, Fanciullino R, Padovani L, Murraciole X, Fischel JL, and Milano G (2005) Response of endothelial cells to a dual tyrosine kinase receptor inhibition combined with irradiation. *Mol Cancer Ther* **4:**1962–1971.

Bregman MD and Meyskens FL Jr (1986) Difluoromethylornithine enhances inhibition of melanoma cell growth in soft agar by dexamethasone, clone A interferon and retinoic acid. *Int J Cancer* **37:**101–107.

Breitman TR and He RY (1990) Combinations of retinoic acid with either sodium butyrate, dimethyl sulfoxide, or hexamethylene bisacetamide synergistically induce differentiation of the human myeloid leukemia cell line HL60. *Cancer Res* **50:**6268–6273.

Breslin D, Fields DW, Chou TC, Marion DN, Kane M, Vaughan ED Jr, and Felsen D (1993) Medical management of benign prostatic hyperplasia: a canine model comparing the in vivo efficacy of α-1 adrenergic antagonists in the prostate. *J Urol* **149:**395–399.

Bruzzese F, Di Gennaro E, Avallone A, Pepe S, Arra C, Caraglia M, Tagliaferri P, and Budillon A (2006) Synergistic antitumor activity of epidermal growth factor receptor tyrosine kinase inhibitor gefitinib and IFN-α in head and neck cancer cells in vitro and in vivo. *Clin Cancer Res* **12:**617–625.

Bryan WR and Shimkin MB (1943) Quantitative analysis of dose-response data obtained in strain C3H mice. *J Natl Cancer Inst* **3:**503–531.

Bylund DB and Ray-Prenger C (1989) Alpha-2A and alpha-2B adrenergic receptor subtypes: attenuation of cyclic AMP production in cell lines containing only one receptor subtype. *J Pharmacol Exp Ther* **251:**640–644.

Bylund DB, Ray-Prenger C, and Murphy TJ (1988) Alpha-2A and alpha-2B adrenergic receptor subtypes: antagonist binding in tissues and cell lines containing only one subtype. *J Pharmacol Exp Ther* **245:**600–607.

Cameron DW, Japour AJ, Xu Y, Hsu A, Mellors J, Farthing C, Cohen C, Poretz D, Markowitz M, Follansbee S, et al. (1999) Ritonavir and saquinavir combination therapy for the treatment of HIV infection. *AIDS* **13:**213–224.

Candinas D, Mills C, Lee S, Dalgic A, Antoniou E, Germenis A, Stavropoulos C, Chou TC, McMaster P, and D'Silva M (1997) Effect of combination schedules of leflunomide with cyclosporine or FK506 in rat cardiac allograthing. *Cardiovasc Eng* **2:**143–153.

Carter WH Jr, Gennings C, Staniswalis JG, Campbell ED, and White KL Jr (1988) A statistical approach to the construction and analysis of isobolograms. *J Am Coll Toxicol* **7:**963–973.

Chandrasekaran B, Kute TE, and Duch DS (1995) Synchronization of cells in the S phase of the cell cycle by 3′-azido-3′-deoxythymidine: implications for cell cytotoxicity. *Cancer Chemother Pharmacol* **35:**489–495.

Chang BK, Gutman R, and Chou TC (1987) Schedule-dependent interaction of α-difluoromethylornithine and cis-diammine-dichloroplatinum(II) against pancreatic cancer cell lines. *Cancer Res* **47:**2247–2250.

Chang CC, Liang YC, Klutz A, Hsu CI, Lin CF, Mold DE, Chou TC, Lee YC, and Huang RCC (2006) Reversal of multidrug resistance by two nordihydroguaiaretic acid derivatives, M_4N and maltose-M_3N, and their use in combination with doxorubicin or paclitaxel. *Cancer Chemother Pharmacol* **58:**640–653.

Chang JY, Lin CF, Pan WY, Bacherikov V, Chou TC, Chen CH, Dong HJ, Cheng SY, Tsai TJ, Lin YW, et al. (2003) New analogues of AHMA as potential antitumor agents: Synthesis and biological activity. *Bioorg Med Chem* **11:**4959–4969.

Chang TT and Chou TC (2000) Rational approach to the clinical protocol design for drug combinations: a review. *Acta Paediatr Taiwan* **41:**294–302.

Chang TT, Gulati SC, Chou TC, Vega R, Gandola L, Ibrahim S, Yopp J, Colvin M, and Clarkson B (1985) Synergistic effect of 4-hydroperoxycyclophosphamide and etoposide on HL-60 myelogenous leukemia cell line demonstrated by computer analysis. *Cancer Res* **45:**2434–3439.

Chang TT, Gulati SC, Chou TC, Colvin M, and Clarkson B (1987) Comparative

cytotoxicity of various drug combinations for human leukemic cells and normal hematopoietic precursors. *Cancer Res* **47:**119–122.
Chauhan D, Catley L, Li G, Podar K, Hideshima T, Velankar M, Mitsiades C, Mitsiades N, Yasui H, Letai A, et al. (2005) A novel orally active proteasome inhibitor induces apoptosis in multiple myeloma cells with mechanisms distinct from Bortezomib. *Cancer Cell* **8:**407–419.
Cheng J, Standifer KM, Tublin PR, Su W, and Pasternak GW (1995) Demonstration of κ3-opioid receptors in the SH-SY5Y human neuroblastoma cell line. *J Neurochem* **65:**170–175.
Cheng YC and Prusoff WH (1973) Relationship between the inhibition constant (K_i) and the concentration of inhibitor which causes 50 per cent inhibition (I_{50}) of an enzymatic reaction. *Biochem Pharmacol* **22:**3099–3108.
Chou JH (1991) Quantitation of synergism and antagonism of two or more drugs by computerized analysis, in *Synergism and Antagonism in Chemotherapy* (Chou TC and Rideout DC eds) pp 223–244, Academic Press, New York.
Chou JH, Chang TT, and Chou TC (2006) Models for drug development and drug resistance, in *Cancer Handbook* (Alison MR ed) John Wiley & Sons, Ltd, West Sussex, UK. In press.
Chou JH and Chou TC (1985) *Dose-Effect Analysis with Microcomputers: Quantitation of ED_{50}, ID_{50}, Synergism, Antagonism, Low-Dose Risk, Receptor Ligand Binding and Enzyme Kinetics: Computer Software for Apple II Series.* Elsevier-Biosoft, Cambridge, UK.
Chou JH and Chou TC (1988) Computerized simulation of dose reduction index (DRI) in synergistic drug combinations. *Pharmacologist* **30:**A231.
Chou JH and Chou TC (1989) *Dose-Effect Analysis with Microcomputers: Quantitation of ED_{50}, ID_{50}, Synergism, Antagonism, Low-Dose Risk, Receptor Ligand Binding and Enzyme Kinetics, Computer Software for the IBM PC Series*. Elsevier-Biosoft, Cambridge, UK.
Chou JH, Chou TC, and Talalay P (1983) Computer simulation of drug effects: quantitation of synergism, summation and antagonism of multiple drugs. *Pharmacologist* **25:**175.
Chou JH, Chou TC, and Talalay P (1984) Conservation of laboratory animals by improved experimental design, generalized equations and computer analysis. *Fed Proc* **43:**576.
Chou TC (1970) *L-Asparagine Biosynthesis and Its Control*. Ph.D. thesis, Yale University, New Haven, CT.
Chou TC (1972) Combinatorial analysis of multiple substrate-multiple product enzyme reactions. *J Theor Biol* **35:**285–297.
Chou TC (1974) Relationships between inhibition constants and fractional inhibition in enzyme-catalyzed reactions with different numbers of reactants, different reaction mechanisms, and different types and mechanisms of inhibition. *Mol Pharmacol* **10:**235–247.
Chou TC (1975) A general procedure for determination of median-effect doses by a double logarithmic transformation of dose-response relationships. *Fed Proc* **34:** 228.
Chou TC (1976) Derivation and properties of Michaelis-Menten type and Hill type equations for reference ligands. *J Theor Biol* **59:**253–276.
Chou TC (1977a) On the determination of availability of ligand binding sites in steady-state systems. *J Theor Biol* **65:**345–356.
Chou TC (1977b) Comparison of the mass-action law with the power law, the probit law and the logit law in dose-effect analysis. *Pharmacologist* **19:**165.
Chou TC (1978) Analysis of age specific mortality rates of different causes by the median-effect equation. *Fed Proc* **37:**882.
Chou TC (1980) Comparison of dose-effect relationships of carcinogens following low-dose chronic exposure and high-dose single injection: an analysis by the median-effect principle. *Carcinogenesis* **1:**203–213.
Chou TC (1981) Carcinogenic risk assessment by a mass-action law principle: application to large scale chronic feeding experiment with 2-acetylaminofluorene (2-AAF). *Proc Am Assoc Cancer Res* **22:**141.
Chou TC (1987) Quantitative dose-effect analysis and algorithms: a theoretical study. *Asia Pac J Pharmacol* **2:**93–99.
Chou TC (1991) The median-effect principle and the combination index for quantitation of synergism and antagonism, in *Synergism and Antagonism in Chemotherapy* (Chou TC and Rideout DC eds) pp 61–102, Academic Press, San Diego.
Chou TC (1994) Assessment of synergistic and antagonistic effect of chemotherapeutic agents in vitro, in *Chemosensitivity Testing in Gynecologic Malignancies and Breast Cancer* (Koechli OR, Sevin BU, and Haller U eds) vol 19. pp 91–107, Karger-Verlag, Basel.
Chou TC (1998) Drug combinations: from laboratory to practice (Editorial). *J Lab Clin Med* **132:**6–8.
Chou TC, Burchenal JH, Schmid FA, Braun TJ, Su TL, Watanabe KA, Fox JJ, and Philips FS (1982) Biochemical effects of 2′-fluoro-5′-methyl-1-beta-D-arabinofuranosyluracil and 2′-fluoro-5-iodo-1-beta-D-arabinofuranosylcytosine in mouse leukemic cells sensitive and resistant to 1-beta-D-arabinofuranosylcytosine. *Cancer Res* **42:**3957–3963.
Chou TC and Chang TT (2002) Models for drug development and drug resistance, in *Cancer Handbook* (Haier J and Nicolson GL eds) vol 2, pp 1041–1054, Nature Publishing Corp., London.
Chou TC and Chou JH (1988) Distinction between multiple ligand exclusivity and competitiveness in receptor binding topology. *FASEB J* **2:**A1778.
Chou TC and Chou JH (1990a) Determination of availability of ligand binding site at steady state for topological assessment of receptors with the aid of microcomputers. *Eur J Pharmacol* **183:**921.
Chou TC and Chou JH (1990b) The median-effect equation: a unified form for Michaelis-Menten, Hill, Scatchard and Henderson-Hasselbalch equations. *FASEB J* **6:**A824.
Chou TC and Chou JH (1992) Theoretical basis and equations for three dimensional isobolograms for three drug combinations. *FASEB J* **6:**A1590.
Chou TC and Chou JH (1998) Computerized indexing of drug combinations: prediction of synergism and antagonism of more than two drugs by polygonogram (Abstract). *FASEB J* **12:**A832.
Chou TC, Depew KM, Zheng YH, Safer ML, Chan D, Helfrich B, Zatorska DA, Bornmann W, and Danishefsky SJ (1998a) Reversal of anticancer multidrug resistance by the ardeemins. *Proc Natl Acad Sci USA* **95:**8369–8374.
Chou TC, Dong HJ, Rivkin A, Yoshimura F, Gabarda AE, Cho YS, Tong WP, and Danishefsky SJ (2003) Design and total synthesis of epothilone analogues which eliminate xenograft tumors to a non-relapsable state. *Angew Chem Int Ed* **42:** 4761–4767.
Chou TC, Dong HJ, and Timmermans PBMWM (2005a) Design, experimentation and computerized automated data analysis of synergistic drug combinations against xenograft tumors by Taxotere and T-900607. *Proc Am Assoc Cancer Res* **46:**1167.
Chou TC, Dong HJ, Zhang XG, Tong WP, and Danishefsky SJ (2005b) Therapeutic cure against human tumor xenografts in nude mice by a microtubule stabilization agent, fludelone, via parenteral or oral route. *Cancer Res* **65:**9445–9454.
Chou TC and Fanucchi MP (1988) Chemotherapy, in *Encyclopedia of Medical Devices and Instrumentation* (Webster JG ed) vol 2, pp 660–670, John Wiley & Sons, New York.
Chou TC, Guan Y, Soenen DR, Danishefsky SJ, and Boger DL (2005c) Potent reversal of multidrug resistance by ningalins and its use in drug combination against human colon carcinoma xenografts in nude mice. *Cancer Chemother Pharmacol* **56:**379–390.
Chou TC and Hayball MP (1997) *CalcuSyn for Windows: Multiple-Drug Dose-Effect Analyzer and Manual.* Biosoft, Cambridge, UK.
Chou TC, Hirano I, Chou J, Chang TT, Gulati SC, Clarkson B, and Talalay P (1986) Computer simulation of combined effects of anticancer agents in vitro: determination of optimal combination dose ratio for maximal synergy. *Proc Am Assoc Cancer Res* **27:**376.
Chou TC and Kahan BD (2001) A rigorous approach to the diagnosis of immunosuppressive synergy combination therapy, in *Modern Immunosuppressives: Milestones in Drug Therapy* (Schuurman HJ ed) pp 183–200, Birkhauser, Switzerland.
Chou TC, Kong XB, Fanucchi MP, Cheng YC, Takahashi K, Watanabe KA, and Fox JJ (1987) Synthesis and biological effects of 2′-fluoro-5-ethyl-1-β-D-arabinofuranosyluracil. *Antimicrob Agents Chemother* **31:**1355–1358.
Chou TC, Lopez C, Colacino JM, Feinberg A, Watanabe KA, Fox JJ, and Philips FS (1984) Metabolic competition studies of 2′-fluoro-5-iodo-1-β-D-arabino-furanosylcytosine in vero cells and herpes simplex type 1-infected vero cells. *Mol Pharmacol* **26:**587–593.
Chou TC and Martin N (2005) *CompuSyn for Drug Combinations: PC Software and User's Guide: A Computer Program for Quantitation of Synergism and Antagonism in Drug Combinations, and the Determination of IC_{50} and ED_{50} and LD_{50} Values.* ComboSyn, Paramus, NJ.
Chou TC and Miller DG (1980) A two-parameter method for analyzing cancer incidence trends, in *Proceedings of the Fourth Annual Meeting of the American Society of Preventive Oncology*, Mar 6–7, Chicago, IL. p. 10.
Chou TC, Motzer RJ, Tong Y, and Bosl GJ (1994) Computerized quantitation of synergism and antagonism of Taxol, topotecan, and cisplatin against human teratocarcinoma cell growth: a rational approach to clinical protocol design. *J Natl Cancer Inst* **86:**1517–1524.
Chou TC, O'Connor OA, Tong WP, Guan YB, Zhang XG, Stachel SJ, Lee S, and Danishefsky SJ (2001) The synthesis, discovery and development of a highly promising class of microtubule stabilization agents: curative effects of desoxyepothilones B and F against human tumor xenografts in nude mice. *Proc Natl Acad Sci USA* **98:**8113–8118.
Chou TC, Otter G, and Sirotnak FM (1996) Schedule-dependent synergism of Taxol or Taxotere with edatrexate against human breast cancer cells in vitro. *Cancer Chemother Pharmacol* **37:**222–228.
Chou TC, Rideout D, Chou J, and Bertino JR (1991a) Chemotherapeutic synergism, potentiation, and antagonism, in *Encyclopedia of Human Biology* (Dulbecco R ed) vol 2, pp 371–379, Academic Press, New York.
Chou TC, Rideout D, Chou J, and Bertino JR (1997) Chemotherapeutic synergism, potentiation, and antagonism, in *Encyclopedia of Human Biology*, 2nd ed (Dulbecco R ed) vol 2, pp 675–683, Academic Press, New York.
Chou TC, Schmid FA, Feinberg A, Philips FS, and Han J (1983) Uptake, initial effects, and chemotherapeutic efficacy of harringtonine in murine leukemic cells sensitive and resistant to vincristine and other chemotherapeutic agents. *Cancer Res* **43:**3074–3079.
Chou TC, Stepkowski SM, and Kahan BD (1994) Computerized quantitation of immunosuppressive synergy for clinical protocol design, in *Cyclosporine: The Ten-Year Experience* (Kahan BD ed) pp 3043–3045, Appleton & Lange, Norwalk, CT.
Chou TC and Talalay P (1977) A simple generalized equation for the analysis of multiple inhibitions of Michaelis-Menten kinetic systems. *J Biol Chem* **252:**6438–6442.
Chou TC and Talalay P (1981) Generalized equations for the analysis of inhibitions of Michaelis-Menten and higher-order kinetic systems with two or more mutually exclusive and nonexclusive inhibitors. *Eur J Biochem* **115:**207–216.
Chou TC and Talalay P (1983) Analysis of combined drug effects: a new look at a very old problem. *Trends Pharmacol Sci* **4:**450–454.
Chou TC and Talalay P (1984) Quantitative analysis of dose-effect relationships: the combined effects of multiple drugs or enzyme inhibitors. *Adv Enzyme Regul* **22:** 27–55.
Chou TC and Talalay P (1987) Applications of the median-effect principle for the assessment of low-dose risk of carcinogens and for the quantitation of synergism and antagonism of chemotherapeutic agents, in *New Avenues in Developmental Cancer Chemotherapy* (Harrap KR and Connors TA eds) pp 37–64, Academic Press, New York.
Chou TC, Tan QH, and Sirotnak FM (1993) Quantitation of the synergistic interaction of edatrexate and cisplatin in vitro. *Cancer Chemother Pharmacol* **31:**259–264.
Chou TC, Zhang XG, Balog A, Su DS, Meng D, Savin K, Bertino RJ, and Danishefsky SJ (1998b) Desoxyepothilone B: an efficacious microtubule-targeted antitumor

agent with a promising in vivo profile relative to epothilone B. *Proc Natl Acad Sci USA* **95:**9642–9647.
Chou TC, Zhang XG, Harris CR, Kuduk SD, Balog A, Savin K, and Danishefsky SJ (1998) Desoxyepothilone B is curative against human tumor xenografts that are refractory to paclitaxel. *Proc Natl Acad Sci USA* **95:**15798–15802.
Chou TC and Zhu QY (1997) How to pick the best cocktail against HIV (Invited speech), in *Proceedings of the 4th Sino-American Infectious Disease Symposium*, 1997 Oct 23–24, Shanghai.
Chou TC, Zhu QY, and Stein CA (1991b) Differential alteration of the anti-HIV effect of phosphorthioate oligonucleotide S-dC28 by AZT, interferon-alpha and dextran sulfate. *AIDS Res Human Retrovir* **7:**943–951.
Christensen H, Fykse EM, and Fonnum F (1990) Uptake of glycine into synaptic vesicles isolated from rat spinal cord. *J Neurochem* **54:**1142–1147.
Chu SH, Ely IG, and Walker WA (1989) Age and cortisone alter host responsiveness to cholera toxin in the developing gut. *Am J Physiol* **256:**G220–G225.
Clark JA, Houghten R, and Pasternak GW (1988) Opiate binding in calf thalamic membranes: a selective mu 1 binding assay. *Mol Pharmacol* **34:**308–317.
Clark JA, Liu L, Price M, Hersh B, Edelson M, and Pasternak GW (1989) Kappa opiate receptor multiplicity: evidence for two U50, 488-sensitive kappa 1 subtypes and a novel kappa 3 subtype. *J Pharmacol Exp Ther* **251:**461–468.
Clark WM (1928) *The Determination of Hydrogen Ions*, 3rd ed, Williams & Wilkins, Baltimore.
Cleland WW (1963) The kinetics of enzyme-catalyzed reactions with two or more substrates or products. *Biochim Biophys Acta* **67:**173–196.
Cohen NA, Egorin MJ, Snyder SW, Ashar B, Wietharn BE, Pan SS, Ross DD, and Hilton J (1991) Interaction of *N,N′,N′*-triethylenethiophosphoramide and *N,N′,N′*-triethylenephosphoramide with cellular DNA. *Cancer Res* **51:**4360–4366.
Colombani PM, Bright EC, Wells M, and Hess AD (1989) Drug-drug interaction between cyclosporine and agents affecting calcium-dependent lymphocyte proliferation. *Transplant Proc* **21:**840–841.
Conner JW, Yuan ZM, and Callery PS (1992) Active-site directed irreversible inhibition of diamine oxidase by a homologous series of aziridinylalkylamines. *Biochem Pharmacol* **44:**1229–1232.
Conti JA, Kemeny N, Saltz LB, Huang Y, Tong W, Chou TC, Pulliam S, and Gonzalez C (1996) Irinotecan (CPT-11) is an active agent in untreated patients with metastatic colorectal cancer. *J Clin Oncol* **14:**709–715.
Copenhaver TW, Lin TL, and Goldberg KM (1987) Joint drug action: a review, in *American Statistical Association, Proceedings of the Biopharmaceutical Section,* pp 160–164.
Cosaceanu D, Carapancea M, Castro J, Ekedahl J, Kanter L, Lewensohn R, and Dricu A (2005) Modulation of response to radiation of human lung cancer cells following insulin-like growth factor 1 receptor inactivation. *Cancer Lett* **222:**173–181.
Coutaux AF, Mooney JJ, and Wirth DF (1994) Neuronal monoamine reuptake inhibitors enhance in vitro susceptibility to chloroquine in resistant *Plasmodium falciparum*. *Antimicrob Agents Chemother* **38:**1419–1421.
Cusack M (1983) Computers save lab animal's lives. *Scholastic Sci World* **40 (No 5):**8–11.
Dai D, Holmes AM, Nguyen T, Davies S, Theele DP, Verschraegen C, and Leslie KK (2005) A potential synergistic anticancer effect of paclitaxel and amifostine on endometrial cancer. *Cancer Res* **65:**9517–9524.
D'Aquila RT, Hughes MD, Johnson VA, Fischl MA, Sommadossi JP, Liou SH, Timpone J, Myers M, Basgoz N, Niu M, et al. (1996) Nevirapine, zidovudine, and didanosine compared with zidovudine and didanosine in patients with HIV-1 infection: a randomized, double-blind, placebo-controlled trial. National Institute of Allergy and Infectious Diseases AIDS Clinical Trials Group Protocol 241 Investigators. *Ann Intern Med* **124:**1019–1030.
David E, Sun SY, Waller EK, Chen J, Khuri FR, and Lonial S (2005) The combination of the farnesyl transferase inhibitor lonafarnib and the proteasome inhibitor bortezomib induces synergistic apoptosis in human myeloma cells that is associated with down-regulation of p-AKT. *Blood* **106:**4322–4329.
Davoudi N, Tate CA, Warburton C, Murray A, Mahboudi F, and McMaster WR (2005) Development of a recombinant *Leishmania major* strain sensitive to ganciclovir and 5-fluorocytosine for use as a live vaccine challenge in clinical trials. *Vaccine* **23:**1170–1177.
Dawson R Jr, Felheim R, and Nguyen S (1995) Mechanism of sodium nitroprusside-mediated inhibition of aromatic amino acid decarboxylase activity. *Pharmacology* **50:**74–85.
De Luca A, Grassii M, Maiello MR, Di Maio M, Mancino M, De Maio E, Gridelli C, Perrone F, and Normanno N (2004) Does the sequence of gemcitabine and vinorelbine affect their efficacy in non-small cell lung cancer in vitro? *Anticancer Res* **24:**2985–2989.
Deminie CA, Bechtold CM, Stock D, Alam M, Djang F, Balch AH, Chou TC, Prichard M, Colonno R, and Lin PF (1996) Evaluation of reverse transcriptase and protease inhibitors in two-drug combinations against human immunodeficiency virus replication. *Antimicrob Agents Chemother* **40:**1346–1351.
Desai MA, Burnett JP, Mayne NG, and Schoepp DD (1995) Cloning and expression of a human metabotropic glutamate receptor 1 alpha: enhanced coupling on co-transfection with a glutamate transporter. *Mol Pharmacol* **48:**648–657.
Dewar HA, Zar MA, and Oxley A (1989) Neuropeptide Y and platelet aggregation by adrenaline. *Life Sci* **45:**367–370.
Dewar KM, Montreuil B, Grondin L, and Reader TA (1989) Dopamine D2 receptors labeled with [^{3}H]raclopride in rat and rabbit brains: equilibrium binding, kinetics, distribution and selectivity. *J Pharmacol Exp Ther* **250:**696–706.
Dinkova-Kostova AT, Liby KT, Stephenson KK, Holtzclaw WD, Gao X, Suh N, Williams C, Risingsong R, Honda T, Gribble GW, et al. (2005) Extremely potent triterpenoid inducers of the phase 2 response: correlations of protection against oxidant and inflammatory stress. *Proc Natl Acad Sci USA* **102:**4584–4589.
Dixon M and Webb EC (1964) *Enzymes,* pp 315–331, Academic Press, New York.
Dong WQ, Schurr A, Reid KH, Shields CB, and West CA (1988) The rat hippocampal slice preparation as an in vitro model of ischemia. *Stroke* **19:**498–502.
Donson AM, Weil MD, and Foreman NK (1999) Tamoxifen radiosensitization in human glioblastoma cell lines. *J Neurosurg* **90:**533–536.
Duffy CP, Elliott CJ, O'Connor RA, Heenan MM, Coyle S, Cleary IM, Kavanagh K, Verhaegen S, O'Loughlin CM, NicAmhlaoibh R, et al. (1998) Enhancement of chemotherapeutic drug toxicity to human tumour cells in vitro by a subset of non-steroidal anti-inflammatory drugs (NSAIDs). *Eur J Cancer* **34:**1250–1259.
Durand RE (1990) Cisplatin and CCNU synergism in spheroid cell subpopulations. *Br J Cancer* **62:**947–953.
Durand RE and Goldie JH (1987) Interaction of etoposide and cisplatin in an in vitro tumor model. *Cancer Treat Rep* **71:**673–679.
Elion GB, Singer S, and Hitchings GH (1954) Antagonists of nucleic acid derivatives: Part VIII. Synergism in combinations of biochemically related antimetabolites. *J Biol Chem* **208:**477–488.
Eron JJ Jr, Johnson VA, Merrill DP, Chou TC, and Hirsch MS (1992) Synergistic inhibition of replication of HIV-1, including a zidovudine resistant isolate, by the combination of zidovudine and 2′,3′-dideoxycytidine in vitro. *Antimicrob Agents Chemother* **36:**1559–1562.
Figul M, Soling A, Dong HJ, Chou TC, and Rainov NG (2003) Combination of temozolomide with the ribonucleotide reductase inhibitors didox trimidox results in synergistic and p53-independent cytotoxicity in malignant brain tumor cells. *Cancer Chemother Pharmacol* **52:**41–46.
Finch RA, Li J, Chou TC, and Sartorelli AC (2000) Maintenance of retinoic acid receptor alpha pools by granulocyte colony-stimulating factor and lithium chloride in all-*trans* retinoic acid treated WEHI-3B leukemic cells: relevance to the synergistic induction of terminal differentiation. *Blood* **96:**2262–2268.
Finney DJ (1947) *Probit Analysis.* Cambridge University Press, London.
Finney DJ (1952) *Probit Analysis,* 2nd ed, pp 146–153, Cambridge University Press, London.
Finney DJ (1971) *Probit Analysis*, 3rd ed., pp 230–268, Cambridge University Press, Cambridge UK.
Finotti P and Palatini P (1981) Canrenone as a partial agonist at the digitalis receptor site of sodium-potassium-activated adenosine triphosphatase. *J Pharmacol Exp Ther* **217:**784–790.
Fischel JL, Ferrero JM, Formento P, Ciccolini J, Renee N, Formento JL, and Milano G (2005a) Taxotere-5′-deoxy-5-fluorouridine combination on hormone-refractory human prostate cancer cells. *Anticancer Drugs* **16:**309–316.
Fischel JL, Formento P, and Milano G (2005b) Epidermal growth factor receptor double targeting by a tyrosine kinase inhibitor (Iressa) and a monoclonal antibody (cetuximab): impact on cell growth and molecular factors. *Br J Cancer* **92:**1063–1068.
Fischel JL, Rostagno P, Formento P, Dubreuil A, Etienne MC, and Milano G (2001) Ternary combination of irinotecan, fluorouracil-folinic acid and oxaliplatin: results on human colon cancer cell lines. *Br J Cancer* **84:**579–585.
Fischl MA, Stanley K, Collier AC, Arduino JM, Stein DS, Feinberg JE, Allan JD, Goldsmith JC, Powderly WG, Raines CP, et al. (1995) Combination and monotherapy with zidovudine and zalcitabine in patients with advanced HIV disease: the NIAID AIDS Clinical Trials Group. *Ann Intern Med* **122:**24–32.
Formento P, Hannoun-Levi JM, Fischel JL, Magne N, Etienne-Grimaldi MC, and Milano G (2004) Dual HER 1–2 targeting of hormone-refractory prostate cancer by ZD1839 and trastuzumab. *Eur J Cancer* **40:**2837–2844.
Fox JJ, Watanabe KA, Chou TC, Schinazi RF, Soike KF, Fourel I, Hantz O, and Trepo C (1988) Antiviral activities of certain 2′-fluorinated arabinsyl-pyrimidine nucleosides, in *Fluorinated Carbohydrates: Chem and Biochemical Aspects* (Taylor NF ed) pp 176–190, Washington, DC.
Fraser TR (1872) The antagonism between the actions of active substances. *Br Med J* **2:**485–487.
Friedman SJ and Skehan P (1980) Membrane-active drugs potentiate the killing of tumor cells by D-glucosamine. *Proc Natl Acad Sci USA* **77:**1172–1176.
Fykse EM, Christensen H, and Fonnum F (1989) Comparison of the properties of gamma-aminobutyric acid and L-glutamate uptake into synaptic vesicles isolated from rat brain. *J Neurochem* **52:**946–951.
Galivan J, Rhee MS, Johnson TB, Chou TC, Nair MG, Bunni M, and Priest D (1989) Antifolate drug interactions. *Adv Enzyme Regul* **28:**13–21.
Gebre-Hiwot A and Frommel D (1993) The in-vitro anti-leishmanial activity of inhibitors of ergosterol biosynthesis. *J Antimicrob Chemother* **32:**837–842.
Gemmill RM, Zhou M, Costa L, Korch C, Bukowski RM, and Drabkin HA (2005) Synergistic growth inhibition by Iressa and rapamycin is modulated by VHL mutations in renal cell carcinoma. *Br J Cancer* **92:**2266–2277.
Goldin A and Mantel N (1957) The employment of combinations of drugs in the chemotherapy of neoplasia: a review. *Cancer Res* **17:**635–654.
Goldin A, Venditti JM, Mantel N, Kline I, and Gang M (1968) Evaluation of combination chemotherapy with three drugs. *Cancer Res* **28:**950–960.
Goldstein A, Aronow L, and Kalman SM (1968) *Principles of Drug Action: The Basis of Pharmacology,* pp 70–105, Harper & Row, New York.
Goldstein A and Barrett RW (1987) Ligand dissociation constants from competition binding assays: errors associated with ligand depletion. *Mol Pharmacol* **31:**603–609.
Gong Y, Raj KM, Luscombe CA, Gadawski I, Tam T, Chu J, Gibson D, Carlson R, and Sacks SL (2004) The synergistic effects of betulin with acyclovir against herpes simplex viruses. *Antiviral Res* **64:**127–130.
Gonzales RA and Moerschbaecher JM (1989) A phencyclidine recognition site is associated with *N*-methyl-D-aspartate inhibition of carbachol-stimulated phosphoinositide hydrolysis in rat cortical slices. *Mol Pharmacol* **35:**787–794.
Gonzales RA, Westbrook SL, and Bridges LT (1991) Alcohol-induced inhibition of *N*-methyl-D-aspartate-evoked release of [^{3}H]norepinephrine from brain is related to lipophilicity. *Neuropharmacology* **30:**441–446.
Gores PF, Field JF, Sutherland DER, and Chou TC (1994) Synergistic interaction of 15-deoxyspergualin and cyclosporine to prolong the survival of rat islet allografts. *Transplant Proc* **26:**745–746.
Greco WR, Bravo G, and Parsons JC (1995) The search for synergy: a critical review from a response surface perspective. *Pharmacol Rev* **47:**331–385.

Greco WR, Park HS, and Rustum YM (1990) Application of a new approach for the quantitation of drug synergism to the combination of cis-diamminedichloroplatinum and 1-β-D-arabinofuranosylcytosine. *Cancer Res* **50:**5318–5327.
Griffon-Etienne G, Merlin JL, and Marchal C (1996) In vitro evaluation of Taxol combined with radiations in human squamous cell carcinoma spheroids. *Cancer Lett* **109:**23–32.
Grindey GB, Moran RG, and Werkheiser WC (1975) Approaches to the rational combination of antimetabolites for cancer chemotherapy, in *Drug Design*, vol 5, pp 170–249, Academic Press, New York.
Grochowicz PM, Hibberd AD, Bowen KM, Clark DH, Pang G, Cowden WB, Chou TC, Grochowicz LK, and Smart YC (1997) Synergetic interaction between castanospermine and tacrolimus in a rat heart allografting model. *Transplant Proc* **29:**1259–1260.
Gu JJ, Santiago L, and Mitchell BS (2005) Synergy between imatinib and mycophenolic acid in inducing apoptosis in cell lines expressing Bcr-Abl. *Blood* **105:**3270–3277.
Hamashima T, Stepkowski SM, Chou TC, and Kahan BD (1995) Synergistic interaction of 3M KCl-extracted donor antigens (e-HAg) with cyclosporine or cyclosporine/sirolimus for prolongation of rat heart allograft survival. *Transpl Immunol* **3:**335–341.
Harris SM, Mistry P, Freathy C, Brown JL, and Charlton PA (2005a) Antitumour activity of XR5944 in vitro and in vivo in combination with 5-fluorouracil and irinotecan in colon cancer cell lines. *Br J Cancer* **92:**722–728.
Harris SM, Scott JA, Brown JL, Charlton PA, and Mistry P (2005b) Preclinical anti-tumor activity of XR5944 in combination with carboplatin or doxorubicin in non-small-cell lung carcinoma. *Anticancer Drugs* **16:**945–951.
Hartshorn KL, Sandstrom EG, Neumeyer D, Paradis TJ, Chou TC, Schooley RT, and Hirsch MS (1986) Synergistic inhibition of human T-cell lymphotropic virus type III replication in vitro by phosphonoformate and recombinant alpha-A interferon. *Antimicrob Agents Chemother* **30:**189–191.
Hartshorn KL, Vogt MW, Chou TC, Blumberg RS, Byington R, Schooley RT, and Hirsch MS (1987) Synergistic inhibition of human immunodeficiency virus in vitro by azidotymidine and recombinant interferon alpha-A. *Antimicrob Agents Chemother* **31:**168–172.
Hegedus DD and Khachatourians GG (1996) The effects of temperature on the pathogenicity of heat-sensitive mutants of the entomopathogenic fungus *Beauveria bassiana,* toward the migratory grasshopper, *Melanoplus sanguinipes. J Invertebr Pathol* **68:**160–165.
Heim A, Brehm C, Stille-Siegener M, Muller G, Hake S, Kandolf R, and Figulla HR (1995) Cultured human myocardial fibroblasts of pediatric origin: natural human interferon-alpha is more effective than recombinant interferon-alpha 2a in carrier-state coxsackievirus B3 replication. *J Mol Cell Cardiol* **27:**2199–2208.
Herman F, Hadhazy P, and Magyar K (1989) Critical evaluation of the in vivo selectivity between hypotensive and platelet antiaggregating actions of iloprost and prostacyclin in beagle dogs. *Arch Int Pharmacodyn Ther* **300:**281–291.
Heyssel R, Brill AB, Woodbury LA, Nishimura ET, Ghose T, Hoshino T, and Yamasaki M (1960) Leukemia in Hiroshima atomic bomb survivors. *Blood* **15:**313–331.
Hill AV (1910) The possible effects of the aggregation of the molecules of haemonglobin on its dissociation curves. *J Physiol (Lond)* **40:**iv–vii.
Hill AV (1913) The combinations of hemoglobin with oxygen and with carbon monoxide. *Biochem J* **7:**471–480.
Hofmann-Lehmann R, Rasmussen RA, Vlasak J, Smith BA, Baba TW, Liska V, Montefiori DC, McClure HM, Anderson DC, Bernacky BJ, et al. (2001a) Passive immunization against oral AIDS virus transmission: an approach to prevent mother-to-infant HIV-1 transmission? *J Med Primatol* **30:**190–196.
Hofmann-Lehmann R, Vlasak J, Rasmussen RA, Smith BA, Baba TW, Liska V, Ferrantelli F, Montefiori DC, McClure HM, Anderson DC, et al. (2001b) Postnatal passive immunization of neonatal macaques with a triple combination of human monoclonal antibodies against oral simian-human immunodeficiency virus challenge. *J Virol* **75:**7470–7480.
Honore S, Kamath K, Braguer D, Horwitz SB, Wilson L, Briand C, and Jordan MA (2004) Synergistic suppression of microtubule dynamics by discodermolide and paclitaxel in non-small cell lung carcinoma cells. *Cancer Res* **64:**4957–4964.
Horvath Z, Hochtl T, Bauer W, Fritzer-Szekeres M, Elford HL, Szekeres T, and Tihan T (2004) Synergistic cytotoxicity of the ribonucleotide reductase inhibitor didox (3,4-dihydroxy-benzohydroxamic acid) and the alkylating agent carmustine (BCNU) in 9L rat gliosarcoma cells and DAOY human medulloblastoma cells. *Cancer Chemother Pharmacol* **54:**139–145.
Horvath Z, Saiko P, Illmer C, Madlener S, Hoechtl T, Bauer W, Erker T, Jaeger W, Fritzer-Szekeres M, and Szekeres T (2005) Synergistic action of resveratrol, an ingredient of wine, with Ara-C and tiazofurin in HL-60 human promyelocytic leukemia cells. *Exp Hematol* **33:**329–335.
Hostetler KY, Hammond JL, Kini GD, Hostetler SE, Beadle JR, Aldern KA, Chou TC, Richman DD, and Mellors JW (2000) In vitro anti-HIV-1 activity of *sn*-2-substituted 1-*O*-octadecyl-*sn*-glycero-3-phosphonoformate analogs and synergy with zidovudine. *Antivir Chem Chemother* **11:**213–219.
Huang P, Farquhar D, and Plunkett W (1992) Selective action of 2′,3′-didehydro-2′,3′-dideoxythymidine triphosphate on human immunodeficiency virus reverse transcriptase and human DNA polymerases. *J Biol Chem* **267:**2817–2822.
Hubeek I, Litvinova E, Peters GJ, Broekhuizen R, Haarman EG, Huismans DR, Cloos J, Zwaan CM, Fleischhack G, Creutzig U, et al. (2004) The effect of G-CSF on the in vitro cytotoxicity of cytarabine and fludarabine in the FLAG combination in pediatric acute myeloid leukemia. *Int J Oncol* **25:**1823–1829.
Jackson RC (1991) Synergism and antagonistic drug interactions resulting from multiple inhibition of metabolic pathways, in *Synergism and Antagonism in Chemotherapy* (Chou TC and Rideout DC eds) pp 363–408, Academic Press, New York.
Jez JM, Schlegel BP, and Penning TM (1996) Characterization of the substrate binding site in rat liver 3α-hydroxysteroid/dihydrodiol dehydrogenase. The roles of tryptophans in ligand binding and protein fluorescence. *J Biol Chem* **271:**30190–30198.
Jin Y, Verstappen A, and Yorio T (1994) Characterization of α_2-adrenoceptor binding sites in rabbit ciliary body membranes. *Invest Ophthalmol Vis Sci* **35:**2500–2508.
Johnson VA, Barlow MA, Merrill DP, Chou TC, and Hirsch MS (1990) Three drug synergistic inhibition of HIV-1 replication in vitro by zidovudine, recombinant soluble CD4 and interferon alpha-A. *J Infect Dis* **161:**1059–1067.
Johnson VA, Merrill DP, Chou TC, and Hirsch MS (1992) Human immunodeficiency virus type 1 (HIV-1) inhibitory interactions between protease inhibitor Ro 31–8959 and zidovudine, 2′,3′-dideoxycytidine, or recombinant interferon-alpha A against zidovudine-sensitive or -resistant HIV-1 in vitro. *J Infect Dis* **166:**1143–1146.
Johnson VA, Merrill DP, Videler JA, Chou TC, Byington RE, Eron JJ, D'Aquila RT, and Hirsch MS (1991) Two-drug combinations of zidovudine, didanosine and recombinant interferon-α A inhibit replication of zidovudine-resistant HIV-1 synergistically in vitro. *J Infect Dis* **164:**646–655.
Josien H, Bom D, Curran DP, Zheng YH, and Chou TC (1997) 7-Silylcamptothecins (Silatecans): a new family of camptothecin antitumor agents. *Bio-Org Med Chem Lett* **7:**3189–3195.
Kahan BD, Gibbons-Stubbers S, Tejpal N, and Chou TC (1992) Prospects for synergistic immunosuppressive drug therapy in the coming decade. *Transplant Proc* **24:**1263–1265.
Kahan BD, Gibbons-Stubbers S, Tejpal N, Chou TC, and Stepkowski S (1991a) Synergistic effect of the rapamycin-cyclosporine combination: median effect analysis of in vitro immune performances by human T lymphocytes in PHA, CD3 and MLR proliferative also cytotoxicity assays. *Transplant Proc* **23:**1090–1091.
Kahan BD, Gibbons-Stubbers S, Tejpal N, Stepkowski SM, and Chou TC (1991b) Synergistic interactions of cyclosporine and rapamycin to inhibit immune performances of normal human peripheral blood lymphocytes in vitro. *Transplantation* **51:**232–239.
Kahan BD, Tejpal N, Gibbons-Stubbers S, Tu Y, Wang M, Stepkowski S, and Chou TC (1993) The synergistic interactions in vitro and in vivo of brequinar sodium with cyclosporine or rapamycin alone and in triple combination. *Transplantation* **55:**894–900.
Kaji H, Chou TC, Sutherland DER, Stephanian E, and Gores PR (1994) Synergistic effect of 15-deoxyspergualin and cyclosporine in prolonging survival of rat cardiac allografts. *Transplant Proc* **26:**869–870.
Kaliberov SA, Chiz S, Kaliberova LN, Krendelchtchikova V, Della Manna D, Zhou T, and Buchsbaum DJ (2006) Combination of cytosine deaminase suicide gene expression with DR5 antibody treatment increases cancer cell cytotoxicity. *Cancer Gene Ther* **13:**203–214.
Kaliberov SA, Kaliberova LN, Stockard CR, Grizzle WE, and Buchsbaum DJ (2004) Adenovirus-mediated FLT1-targeted proapoptotic gene therapy of human prostate cancer. *Mol Ther* **10:**1059–1070.
Katz Y, Weizman A, Pick CG, Pasternak GW, Liu L, Fonia O, and Gavish M (1994) Interactions between laudanosine, GABA, and opioid subtype receptors: implication for laudanosine seizure activity. *Brain Res* **646:**235–241.
Khafif A, Schantz SP, Chou TC, Edelstein D, and Sacks PG (1998) Quantitation of chemopreventive synergism between (−)-epigallocatechin-3-gallate and curcumin in normal, premalignant and malignant human oral epithelial cells. *Carcinogenesis* **19:**419–424.
Kim JY, Su TL, Chou TC, Koehler B, Scarborough A, Ouerfelli O, and Watanabe KA (1996) Cyclopent[*a*]anthraquinones as DNA intercalating agents with covalent bond formation potential: synthesis and biological activity. *J Med Chem* **39:**2812–2818.
Kitabwalla M, Ferrantelli F, Wang T, Chalmers A, Katinger H, Stiegler G, Cavacini LA, Chou TC, and Ruprecht RM (2003) Primary African HIV clade A and D isolates: effective cross-clade neutralization with a quadruple combination of human monoclonal antibodies raised against clade B. *AIDS Res Hum Retroviruses* **19:**125–131.
Knight RJ, Kurrle R, Stepkowski S, Serino F, Chou TC, and Kahan BD (1994) Synergistic immunosuppressive actions of cyclosporine with a mouse anti-rat α/β-T cell receptor monoclonal antibody. *Transplantation* **57:**1544–1548.
Koechli OR, Sevin BU, Perras JP, Chou TC, Angioli R, Steren A, Untch M, and Averette HE (1993) Characteristics of the combination paclitaxel plus doxorubicin in breast cancer cell lines analyzed with the ATP-cell viability assay. *Breast Cancer Res Treat* **28:**21–27.
Kohler B, Su TL, Chou TC, Jiang XJ, and Watanabe KA (1993) Synthesis of cyclopentanthraquinones: analogues of mitomycin C. *J Org Chem* **58:**1680–1686.
Kollmann C, Tremblay C, Giguel F, Chou TC, and Hirsch MS (2001) In vitro anti-HIV-1 synergy between non-nucleoside reverse transcriptase inhibitors nevirapine and efavirenz. *Antivir Ther* **6:**143–144.
Konecny GE and Pegram MD (2004) Gemcitabine in combination with trastuzumab and/or platinum salts in breast cancer cells with HER2 overexpression. *Oncology (Williston Park)* **18:**32–36.
Kong XB, Andreeff M, Fanucchi MP, Fox JJ, Watanabe KA, Vidal P, and Chou TC (1987) Cell differentiation effect of 2′-fluoro-1-β-D-arabinofuranosyl pyrimidines in HL-60 cells. *Leuk Res* **11:**1031–1039.
Kong XB, Fanucchi MP, and Chou TC (1988) Antagonistic interactions of hexamethylene bisacetamide in combination with 1-β-D-arabinofuranosylcytosine, Adriamycin and harringtonine on the growth and differentiation of HL-60 cells in vitro. *Leuk Res* **12:**853–859.
Kong XB, Rubin L, Chen LI, Ciszewska G, Watanabe KA, Tong WP, Sirotnak FM, and Chou TC (1992a) Topoisomerase II-mediated DNA cleavage activity and irreversibility of cleavable complex formation induced by DNA intercalator with alkylating capability. *Mol Pharmacol* **41:**237–244.
Kong XB, Vidal P, Tong WP, Chiang J, Gloff CA, and Chou TC (1992b) Preclinical pharmacology and pharmacokinetics of anti-hepatitis virus agent 2′-fluoro-5-ethyl-1-β-D-arabinofuranosyluracil (FEAU) in mice and rats. *Antimicrob Agents Chemother* **36:**1472–1477.
Kong XB, Zhu QY, Ruprecht RM, Watanabe KA, Zeidler JM, Gold JW, Polsky B, Armstrong D, and Chou TC (1991) Synergistic inhibition of human immunodeficiency virus type 1 replication in vitro by two-drug and three-drug combinations of

3′-azido-3′-deoxythymidine, phosphonoformate, and 2′,3′-dideoxythymidine. *Antimicrob Agents Chemother* **35:**2003–2011.
Kong XB, Zhu QY, Vidal PM, Watanabe KA, Polsky B, Armstrong D, Ostrander M, Lang SA Jr, Muchmore E, and Chou TC (1992c) Comparison of anti-HIV activity, cellular transport, and plasma and intracellular pharmacokinetics of 3′-fluoro-3′-deoxythymidine and 3′-azido-3′-deoxythymidine. *Antimicrob Agents Chemother* **36:**808–818.
Kopelovich L and Chou TC (1984) The proliferative response of low-density human cell cultures to tumor promoters and its relevance to carcinogenic mechanisms in vitro. *Int J Cancer* **34:**781–788.
Koshinsky HA, Hannan PJ, and Khachatourians GG (1991) HT-2 toxin, roridin A, T-2 toxin, and verrucarin A, mycotoxins inhibit carbon dioxide production by *Kluyveromyces marxianus*. *Can J Microbiol* **37:**933–938.
Koyama M, Takahashi K, Chou TC, Darzynkewicz Z, Kapuscinski J, Kelly TR, and Watanabe KA (1989) Intercalating agents with covalent bond forming capability: novel type of potential anticancer agents. *J Med Chem* **32:**1594–1599.
Kremer AB, Egan RM, and Sable HZ (1980) The active site of transketolase. Two arginine residues are essential for activity. *J Biol Chem* **255:**2405–2410.
Kufe D, Herrick D, Crumpacker C, and Schnipper L (1984) Incorporation of 1-β-D-arabinofuranosylcytosine into DNA from herpes simplex virus resistant to 9-β-D-arabinofuranosyladenine. *Cancer Res* **44:**69–73.
Kullberg BJ, Oude Lashof AM, and Netea MG (2004) Design of efficacy trials of cytokines in combination with antifungal drugs. *Clin Infect Dis* **39 (Suppl 4):** S218–S223.
Lacey BW (1958) Mechanisms of chemotherapeutic synergy, in *The Strategy of Chemotherapy* (Cowan ST and Rowatt E eds) pp 247–287, Cambridge University Press, Cambridge, UK.
Lakhdar-Ghazal N, Grondin L, Bengelloun WA, and Reader TA (1986) α-Adrenoceptors and monoamine contents in the cerebral cortex of the rodent *Jaculus orientalis*: effects of acute cold exposure. *Pharmacol Biochem Behav* **25:**903–911.
Lam YM, Pym J, and Campling BG (1991) Statistical models for assessing drug interactions. *Proc Am Stat Assoc Biopharm Sect* 214–219.
Laneuville P, Timm M, and Hudson AT (1994) bcr/abl expression in 32D cl3(G) cells inhibits apoptosis induced by protein tyrosine kinase inhibitors. *Cancer Res* **54:** 1360–1366.
Lee CB, Chou TC, Zhang XG, Wang ZG, Kuduk SD, Chappell MD, Stachel SJ, and Danishefsky SJ (2000) Total synthesis and antitumor activity of 12,13-desoxyepothilone F: an unexpected solvolysis problem at C15, mediated by remote substitution at C21. *J Org Chem* **65:**6525–6533.
Lee HY, Moon H, Chun KH, Chang YS, Hassan K, Ji L, Lotan R, Khuri FR, and Hong WK (2004) Effects of insulin-like growth factor binding protein-3 and farnesyltransferase inhibitor SCH66336 on Akt expression and apoptosis in non-small-cell lung cancer cells. *J Natl Cancer Inst* **96:**1536–1548.
Leonard CE, Chan DC, Chou TC, Kumar R, and Bunn PA (1996) Paclitaxel enhances in vitro radiosensitivity of squamous carcinoma cell lines of the head and neck. *Cancer Res* **56:**5198–5204.
Le Pelley RH and Sullivan WN (1936) Toxicity of rotenone and pyrethrins alone and in combination. *J Econ Entomol* **29:**791–797.
Levis M, Pham R, Smith BD, and Small D (2004) In vitro studies of a FLT3 inhibitor combined with chemotherapy: sequence of administration is important to achieve synergistic cytotoxic effects. *Blood* **104:**1145–1150.
Li A, Baba TW, Sodroski J, Zolla-Pazner S, Gorny MK, Robinson J, Posner MR, Katinger H, Barbas CF III, Burton DR, et al. (1997) Synergistic neutralization of a chimeric SIV/HIV-1 virus with combinations of human anti-HIV-1 envelope monoclonal antibodies or hyper immune globulins. *AIDS Res Hum Retroviruses* **13:**647–656.
Li A, Katinger H, Posner MR, Zolla-Pazner S, Gorny MK, Chou TC, Baba TW, and Ruprecht RM (1998) Synergistic neutralization of SHIV-vpu$^+$ by triple and quadruple combinations of human monoclonal antibodies and high titer anti-HIV-1 immunoglobulins. *J Virol* **72:**3235–3240.
Liang H, Salinas RA, Leal BZ, Kosakowska-Cholody T, Michejda CJ, Waters SJ, Herman TS, Woynarowski JM, and Woynarowska BA (2004) Caspase-mediated apoptosis and caspase-independent cell death induced by irofulven in prostate cancer cells. *Mol Cancer Ther* **3:**1385–1396.
Liang Y, Hannan CJ Jr, Chang BK, and Schoenlein PV (1997) Enhanced potency of daunorubicin against multidrug resistant subline KB-ChR-8-5-11 by a pulsed magnetic field. *Anticancer Res* **17:**2083–2088.
Lin JC, Zhang ZX, Chou TC, Sim I, and Pagano JS (1989) Synergistic inhibition of Epstein-Barr virus transformation of B-lymphocytes by interferon α and γ and 3′-azido-3′-deoxythymidine. *J Infect Dis* **159:**248–254.
Lineweaver H and Burk D (1934) The determination of enzyme dissociation constants. *J Am Chem Soc* **56:**658–666.
Link JT, Raghavan S, Gallant M, Danishefsky SJ, Chou TC, and Ballas LM (1996) Staurosporine and ent-staurosporine: the first total synthesis, prospect for a regioselective approach, and activity profiles. *J Am Chem Soc* **118:**2825–2842.
Loewe S (1928) Die quantitation probleme der pharmakologie. *Ergeb Physiol* **27:**47–187.
Loewe S (1953) The problem of synergism and antagonism of combined drugs. *Arzneim-Forsch* **3:**285–290.
Loewe S (1957) Antagonism and antagonist. *Pharmacol Rev* **9:**237–242.
Lombardini JB, Liebowitz SM, and Chou TC (1989) Analogues of taurine as stimulators and inhibitors of ATP-dependent calcium ion uptake in the rat retina: combination kinetics. *Mol Pharmacol* **36:**256–264.
Long BH, Willis CE, Prestayko AW, and Crooke ST (1982) Effect of anthracycline analogues on the appearance of newly synthesized total RNA and messenger RNA in the cytoplasm of erythroleukemia cells. *Mol Pharmacol* **22:**152–157.
Longo GS, Izzo J, Chang YM, Tong WP, Zielinski Z, Gorlick R, Chou TC, and Bertino JR (1998) Pretreatment of colon carcinoma cells with Tomudex enhances 5-fluorouracil cytotoxicity. *Clin Cancer Res* **4:**469–473.
Lunghi P, Tabilio A, Lo-Coco F, Pelicci PG, and Bonati A (2005) Arsenic trioxide (ATO) and MEK1 inhibition synergize to induce apoptosis in acute promyelocytic leukemia cells. *Leukemia* **19:**234–244.
Luo YL, Chou TC, and Cheng CC (1996) Design of antineoplastic agents on the basis of the "2-phenylnaphthalene type" structural pattern. 3. Synthesis and biological activity evaluation of 5H-benzo[*b*]naphtho[2,3-*d*]pyrrole-6,15-dione derivatives. *J Heterocycl Chem* **33:**113–117.
Lyu RM, Smith L, and Smith JB (1992) Ca^{2+} influx via Na^+-Ca^{2+} exchange in immortalized aortic myocytes. I. Dependence on $[Na^+]_i$ and inhibition by external Na^+. *Am J Physiol* **263:**C628–C634.
Maisin JR, De Saint-Georges L, Janowski M, Lambiet-Collier M, and Mattelin G (1987) Effect of X-rays alone or combined with diethylnitrosamine on cancer induction in mouse liver. *Int J Radiat Biol Relat Stud Phys Chem Med* **51:**1049–1057.
Manion DJ, Vibhagool A, Chou TC, Kaplan J, Caliendo A, and Hirsch MS (1996) Susceptibility of human cytomegalovirus to two-drug combinations in vitro. *Antivir Ther* **1:**237–245.
Martin JH and Symonds A (2002) Synergistic antitumour effect of a combination of toremifene and interferon-α on ZR-75–1 human breast cancer cells: dependence on interferon-alpha subtype. *Oncol Rep* **9:**379–382.
Mathis JP, Goldberg IE, Letchworth SR, Ryan-Moro JP, and Pasternak GW (1999) Identification of a high-affinity orphanin FQ/nociceptin(1-11) binding site in mouse brain. *Synapse* **34:**181–186.
Matsushita N, Hizue M, Aritake K, Hayashi K, Takada A, Mitsui K, Hayashi M, Hirotsu I, Kimura Y, Tani T, et al. (1998) Pharmacological studies on the novel antiallergic drug HQL-79: I. Antiallergic and antiasthmatic effects in various experimental models. *Jpn J Pharmacol* **78:**1–10.
Mazzulli T, Rusconi S, Merrill DP, D'Aquila RT, Moonis M, Chou TC, and Hirsch MS (1994) Alternating versus continuous drug regimens in combination chemotherapy of human immunodeficiency virus type 1 infection in vitro. *Antimicrob Agents Chemother* **38:**656–661.
Meng D, Su DS, Balog A, Bertinato P, Sorensen EJ, Danishefsky SJ, Zheng YH, Chou TC, He L, and Horwitz SB (1997) Remote effects in macrolide formation through ring-forming olefin metathesis: an application to the synthesis of fully active epothilone congeners. *J Am Chem Soc* **119:**2733–2734.
Merrill DP, Manion DJ, Chou TC, and Hirsch MS (1997) Antagonism between HIV-1 protease inhibitors, indinavir and saquinavir in vitro. *J Infect Dis* **176:**265–268.
Merrill DP, Moonis M, Chou TC, and Hirsch MS (1996) Lamivudine (3TC) or stavudine (D4T) in two- and three-drug combinations against HIV-1 replication in vitro. *J Infect Dis* **173:**355–364.
Michaelis L and Menten ML (1913) Die Kinetik der Invertinwirkung. *Biochem Z* **49:**333–369.
Mildvan D, Ruprecht R, Krown S, and Pettinelli C (1990) Methodological issues in AIDS clinical trials: application of the combination index method in the design of a clinical antiretroviral trial: ACTG 068. *J Acquir Immune Defic Syndr* **3 (Suppl 2):**S111–S113; discussion S114–S119.
Morgenstern B, Michaelis M, Baer PC, Doerr HW, and Cinatl J Jr (2005) Ribavirin and interferon-β synergistically inhibit SARS-associated coronavirus replication in animal and human cell lines. *Biochem Biophys Res Commun* **326:**905–908.
Mullerad M, Bochner BH, Adusumilli PS, Bhargava A, Hu-ni EKC, Kattan MW, Chou TC, and Fong Y (2005) Herpes simplex virus based gene therapy enhances the efficacy of mitomycin C for the treatment of human bladder transitional cell carcinoma. *J Urol* **174:**1–6.
Muller-Tidow C, Kiehl M, Sindermann JR, Probst M, Banger N, Zuhlsdorf M, Chou TC, Berdel WE, Serve H, and Koch OM (2003) Synergistic growth inhibitory effects of interferon-α and lovastatin on bcr-abl positive leukemic cells. *Int J Oncol* **23:**151–158.
Munson PJ and Rodbard D (1988) An exact correction to the "Cheng-Prusoff" correction. *J Recept Res* **8:**533–546.
Murphy KM and Snyder SH (1982) Heterogeneity of adenosine A1 receptor binding in brain tissue. *Mol Pharmacol* **22:**250–257.
Naguib M (1994) Neuromuscular effects of rocuronium bromide and mivacurium chloride administered alone and in combination. *Anesthesiology* **81:**388–395.
Nakagawa T, Ukai K, Ohyama T, Koida M, and Okamura H (1996) Effects of the synthesized growth hormone releasing peptide, KP-102, on growth hormone release in sodium glutamate monohydrate-treated low growth rats. *Life Sci* **59:**705–712.
Noonan TC, Jamieson-Leclercq T, and Desai SN (1992) Effect of BI-L-239, A-64077 and MK-886 on leukotriene B4 synthesis by chopped guinea pig lung and on antigen-induced tracheal contraction in vitro. *Prostaglandins* **44:**543–554.
Norberg L and Wahlstrom G (1986) Interactions between hexobarbital and thiopental in male rats evaluated with an anaesthesia threshold. *Acta Pharmacol Toxico* **58:**96–104.
Nordling CO (1953) A new theory on cancer-inducing mechanism. *Br J Cancer* **7:**68–72.
Nordling CO (1954) Evidence regarding the multiple mutation theory of the cancer-inducing mechanisms. *Acta Genet Stat Med* **5:**94–104.
Pan XZ, Qiu ZD, Baron PA, Gold JWM, Polsky B, Chou TC, and Armstrong D (1992) Three-drug synergistic inhibition of HIV-1 replication in vitro by 3′-fluoro-3′-deoxythymidine, recombinant soluble CD4, and recombinant interferon-α A. *AIDS Res Human Retroviruses* **8:**589–595.
Park JK, Lee SH, Kang JH, Nishio K, Saijo N, and Kuh HJ (2004) Synergistic interaction between gefitinib (Iressa, ZD1839) and paclitaxel against human gastric carcinoma cells. *Anticancer Drugs* **15:**809–818.
Pei XY, Dai Y, and Grant S (2004) The small-molecule Bcl-2 inhibitor HA14–1 interacts synergistically with flavopiridol to induce mitochondrial injury and apoptosis in human myeloma cells through a free radical-dependent and Jun NH2-terminal kinase-dependent mechanism. *Mol Cancer Ther* **3:**1513–1524.
Perelson AS, Essunger P, Cao Y, Vesanen M, Hurley A, Saksela K, Markowitz M, and Ho DD (1997) Decay characteristics of HIV-1-infected compartments during combination therapy. *Nature (Lond)* **387:**188–191.
Perez EA, Hack FM, Fletcher TS, and Chou TC (1994) Modulation of intrinsic in vitro

resistance to carboplatin by edatrexate in the A549 human non-small cell lung cancer cell line. *Oncol Res* **6:**151–156.
Perez EA, Hack FM, Webber LM, and Chou TC (1993) Schedule dependence of synergism of edatrexate and cisplatin in combination in the A549 lung-cancer cell line as assessed by the median-effect analysis. *Cancer Chemother Pharmacol* **33:**245–250.
Peters RH, Jollow DJ, and Stuart RK (1991) Role of glutathione in the in vitro synergism between 4-hydroperoxy-cyclophosphamide and cisplatin in leukemia cell lines. *Cancer Res* **51:**2536–2541.
Peto R (1974) Editorial: Guidelines on the analysis of tumour rates and death rates in experimental animals. *Br J Cancer* **29:**101–105.
Peto R, Roe FJ, Lee PN, Levy L, and Clack J (1975) Cancer and ageing in mice and men. *Br J Cancer* **32:**411–426.
Plackett RL and Hewlett PS (1948) Statistical aspects of the independent joint actions of poisons, particularly insecticides: I. The toxicity of a mixture of poisons. *Ann Appl Biol* **35:**347–358.
Poch G, Reiffenstein RJ, and Unkelbach HD (1990) Application of the isobologram technique for the analysis of combined effects with respect to additivity as well as independence. *Can J Physiol Pharmacol* **68:**682–688.
Podder H, Stepkowski SM, Napoli KL, Clark J, Verani RR, Chou TC, and Kahan BD (2001) Pharmacokinetic interactions augment toxicities of sirolimus/cyclosporine combinations. *J Am Soc Nephrol* **12:**1059–1071.
Porter DW, Yakushiji H, Nakabeppu Y, Sekiguchi M, Fivash MJ Jr, and Kasprzak KS (1997) Sensitivity of *Escherichia coli* (MutT) and human (MTH1) 8-oxo-dGTPases to in vitro inhibition by the carcinogenic metals, nickel(II), copper(II), cobalt(II) and cadmium(II). *Carcinogenesis* **18:**1785–1791.
Potmesil M, Israel M, Kirschenbaum S, Bowen J, and Silber R (1986) Effects of *N*-trifluoroacetyladriamycin-14-*O*-hemiadipate and radiation on L1210 cells. *Radiat Res* **105:**147–157.
Price M, Gistrak MA, Itzhak Y, Hahn EF, and Pasternak GW (1989) Receptor binding of [^{3}H]naloxone benzoylhydrazone: a reversible κ and slowly dissociable μ opiate. *Mol Pharmacol* **35:**67–74.
Prichard MN and Shipman C Jr (1990) A three-dimensional model to analyze drug-drug interactions. *Antiviral Res* **14:**181–205.
Prochaska HJ, Yeh Y, Baron P, and Polsky B (1993) Oltipraz, an inhibitor of human immunodeficiency virus type 1 replication. *Proc Natl Acad Sci USA* **90:**3953–3957.
Puig MM, Warner W, Tang CK, Lovitz M, and Turndorf H (1988) Synergistic interaction of morphine and halothane in the guinea pig ileum. *Anesthesiology* **68:**559–562.
Qian DZ, Wang X, Kachhap SK, Kato Y, Wei Y, Zhang L, Atadja P, and Pili R (2004) The histone deacetylase inhibitor NVP-LAQ824 inhibits angiogenesis and has a greater antitumor effect in combination with the vascular endothelial growth factor receptor tyrosine kinase inhibitor PTK787/ZK222584. *Cancer Res* **64:**6626–6634.
Rahier A, Taton M, and Benveniste P (1989) Cycloeucalenol-obtusifoliol isomerase: structural requirements for transformation or binding of substrates and inhibitors. *Eur J Biochem* **181:**615–626.
Rahmani M, Reese E, Dai Y, Bauer C, Kramer LB, Huang M, Jove R, Dent P, and Grant S (2005) Cotreatment with suberanoylanilide hydroxamic acid and 17-allylamino 17-demethoxygeldanamycin synergistically induces apoptosis in Bcr-Abl$^+$ cells sensitive and resistant to STI571 (imatinib mesylate) in association with down-regulation of Bcr-Abl, abrogation of signal transducer and activator of transcription 5 activity, and Bax conformational change. *Mol Pharmacol* **67:**1166–1176.
Rainov NG, Fels C, Droge JW, Schafer C, Kramm CM, and Chou TC (2001) Temozolomide enhances and herpes simplex virus thymidine kinase/ganciclovir therapy of malignant glioma. *Cancer Gene Ther* **8:**662–668.
Raje N, Kumar S, Hideshima T, Ishitsuka K, Chauhan D, Mitsiades C, Podar K, Le Gouill S, Richardson P, Munshi NC, et al. (2004) Combination of the mTOR inhibitor rapamycin and CC-5013 has synergistic activity in multiple myeloma. *Blood* **104:**4188–4193.
Ramel C (1986) Deployment of short-term assays for the detection of carcinogens; genetic and molecular considerations. *Mutat Res* **168:**327–342.
Rastogi K, Chang JY, Chou TC, Pan WY, Chen CH, Chen LT, and Su TL (2002) Antitumor AHMA linked to DNA minor groove binding agents: synthesis and biological evaluation. *J Med Chem* **45:**4485–4493.
Reed L and Berkson J (1929) The application of the logistic function to experimental data. *J Phys Chem* **33:**760–779.
Rezzoug H, Bezdetnaya L, A'amar O, Merlin JL, and Guillemin F (1998) Parameters affecting photodynamic activity of Foscan® or meta-tetra (hydroxyphenyl) chlorin (mTHPC) in vitro and in vivo. *Lasers Med Sci (Wash DC)* **13:**119–125.
Richman D, Rosenthal AS, Skoog M, Eckner RJ, Chou TC, Sabo JP, and Merluzzi VJ (1991) BI-RG-587 is active against AZT-resistant HIV-1 and synergies with AZT. *Antimicrob Agents Chemoth* **35:**305–308.
Rideout D and Chou TC (1991) Synergism, antagonism and potentiation in chemotherapy: an overview, in *Synergism and Antagonism in Chemotherapy* (Chou TC and Rideout DC eds) pp 3–60, Academic Press, San Diego.
Rigas JR, Kris MG, Miller VA, Pisters KMW, Keelan RT, Grant SC, Fennelly DW, Chou TC, and Sirotnak FM (1999) Phase I study of the sequential administration of edatrxate and paclitaxel in patients with advanced solid tumor. *Annal Oncol* **10:**601–603.
Rivkin A, Chou TC, and Danishefsky SJ (2005) On the remarkable antitumor properties of fludelone: how we got there. *Angew Chem Int Ed* **44:**2838–2850.
Rivkin A, Yoshimura F, Gabarda AE, Chou TC, Dong H, Tong WP, and Danishefsky SJ (2003) Complex target-oriented total synthesis in the drug discovery process: the discovery of a highly promising family of second generation epothilones. *J Am Chem Soc* **125:**2899–2901.
Romanini A, Chou TC, and Bertino JR (1989) Carboxypeptidase G_2 enhances trimetrexate cytotoxicity in CCRF-CEM cell lines sensitive and resistant to methotrexate. *Adv Enzyme Regul* **28:**323–338.
Ruprecht RM, Chou TC, Chipty F, GamaSusa M, Mullaney S, O'Brien L, and Rosas D (1990) Interferon-α and 3′-azido-3′-deoxythymidine are highly synergistic in vivo and prevent viremia after acute retrovirus exposure. *J Acquir Immune Defic Syndr* **3:**591–600.
Ryan-Moro J, Chien CC, Standifer KM, and Pasternak GW (1996) Sigma binding in a human neuroblastoma cell line. *Neurochem Res* **21:**1309–1314.
Sacks PG, Harris D, and Chou TC (1995) Modulation of growth and proliferation in squamous cell carcinoma by retinoic acid: a rationale for combination therapy with chemotherapeutic agents. *Int J Cancer* **61:**409–415.
Scarborough A, Su TL, Leteutre FF, Pommier Y, and Chou TC (1996) DNA interaction and topoisomerase II inhibition by the antitumor agent 3′-(9-acridinylamino)-5′-hydroxymethyl aniline and derivatives. *Bioorg Chem* **24:**229–241.
Scatchard G (1949) The attractions of proteins for small molecules and ions. *Ann NY Acad Sci* **51:**660–672.
Schabel FM (1975) Synergism and antagonism among antitumor agents, in *Pharmacological Basis of Cancer Chemotherapy,* pp 595–623, Williams & Wilkins, Baltimore.
Schinazi RF (1991) Combined chemotherapeutic modalities for viral infections: rationale and clinical potential, in *Synergism and Antagonism in Chemotherapy* (Chou TC and Rideout DC eds) pp 109–181, Academic Press, New York.
Schinazi RF, Chou TC, Scott RT, Yao XJ, and Nahmias AJ (1986) Delayed treatment with combinations of antiviral drugs in mice infected with herpes simplex virus and application of the median effect method of analysis. *Antimicrob Agents Chemother* **30:**491–498.
Schoepp DD, Goldsworthy J, Johnson BG, Salhoff CR, and Baker SR (1994) 3,5-Dihydroxyphenylglycine is a highly selective agonist for phosphoinositide-linked metabotropic glutamate receptors in the rat hippocampus. *J Neurochem* **63:**769–772.
Schoepp DD and Johnson BG (1989a) Comparison of excitatory amino acid-stimulated phosphoinositide hydrolysis and *N*-[^{3}H]acetylaspartylglutamate binding in rat brain: selective inhibition of phosphoinositide hydrolysis by 2-amino-3-phosphonopropionate. *J Neurochem* **53:**273–278.
Schoepp DD and Johnson BG (1989b) Inhibition of excitatory amino acid-stimulated phosphoinositide hydrolysis in the neonatal rat hippocampus by 2-amino-3-phosphonopropionate. *J Neurochem* **53:**1865–1870.
Schoepp DD and Johnson BG (1993) Metabotropic glutamate receptor modulation of cAMP accumulation in the neonatal rat hippocampus. *Neuropharmacology* **32:**1359–1365.
Schoepp DD, Johnson BG, and Monn JA (1992) Inhibition of cyclic AMP formation by a selective metabotropic glutamate receptor agonist. *J Neurochem* **58:**1184–1186.
Schoepp DD, Johnson BG, Salhoff CR, Valli MJ, Desai MA, Burnett JP, Mayne NG, and Monn JA (1995) Selective inhibition of forskolin-stimulated cyclic AMP formation in rat hippocampus by a novel mGluR agonist, 2R,4R-4-aminopyrrolidine-2,4-dicarboxylate. *Neuropharmacology* **34:**843–850.
Schoepp DD, Johnson BG, Wright RA, Salhoff CR, Mayne NG, Wu S, Cockerman SL, Burnett JP, Belegaje R, Bleakman D, et al. (1997) LY354740 is a potent and highly selective group II metabotropic glutamate receptor agonist in cells expressing human glutamate receptors. *Neuropharmacology* **36:**1–11.
Schoepp DD, Ornstein PL, Leander JD, Lodge D, Salhoff CR, Zeman S, and Zimmerman DM (1990) Pharmacological characterization of LY233053: a structurally novel tetrazole-substituted competitive *N*-methyl-D-aspartic acid antagonist with a short duration of action. *J Pharmacol Exp Ther* **255:**1301–1308.
Schoepp DD, Salhoff CR, Wright RA, Johnson BG, Burnett JP, Mayne NG, Belagaje R, Wu S, and Monn JA (1996) The novel metabotropic glutamate receptor agonist 2R,4R-APDC potentiates stimulation of phosphoinositide hydrolysis in the rat hippocampus by 3,5-dihydroxyphenylglycine: evidence for a synergistic interaction between group 1 and group 2 receptors. *Neuropharmacology* **35:**1661–1672.
Schultz C, Vaskinn S, Kildalsen H, and Sager G (1998) Cyclic AMP stimulates the cyclic GMP egression pump in human erythrocytes: effects of probenecid, verapamil, progesterone, theophylline, IBMX, forskolin, and cyclic AMP on cyclic GMP uptake and association to inside-out vesicles. *Biochemistry* **37:**1161–1166.
Seo JK, Chu SH, and Walker WA (1989) Development of intestinal host defense: an increased sensitivity in the adenylate cyclase response to cholera toxin in suckling rats. *Pediatr Res* **25:**225–227.
Seo Y, Yan T, Schupp JE, Yamane K, Radivoyevitch T, and Kinsella TJ (2006) The interaction between two radiosensitizers: 5-iododeoxyuridine and caffeine. *Cancer Res* **66:**490–498.
Shair MD, Yoon T, Chou TC, and Danishefsky SJ (1994) Enediyne quinone emines: truncated biologically active dynemicin congeners. *Angew Chem Ed Engl* **33:**2477–2479.
Shair MD, Yoon TY, Mosny KK, Chou TC, and Danishefsky SJ (1996) The total synthesis of dynemicin A leading to development of a fully contained bioreductivity activated enediyne prodrug. *J Am Chem Soc* **118:**9509–9525.
Shan B, Medina JC, Santha E, Frankmoelle WP, Chou TC, Learned RM, Nanbut MR, Stott D, Wu P, Jaen JC, et al. (1999) Selective, covalent modification of β-tubulin residue Cys-239 by T138067, an antitumor agent with in vivo efficacy against multidrug-resistant tumors. *Proc Natl Acad Sci USA* **96:**5686–5691.
Shanks RH, Rizzieri DA, Flowers JL, Colvin OM, and Adams DJ (2005) Preclinical evaluation of gemcitabine combination regimens for application in acute myeloid leukemia. *Clin Cancer Res* **11:**4225–4233.
Sharma AD and Klein GJ (1988) Comparative quantitative electrophysiologic effects of adenosine triphosphate on the sinus node and atrioventricular node. *Am J Cardiol* **61:**330–335.
Sharom FJ, Lu P, Liu R, and Yu X (1998) Linear and cyclic peptides as substrates and modulators of P-glycoprotein: peptide binding and effects on drug transport and accumulation. *Biochem J* **333 (Pt 3):**621–630.
Singh B, Reddy PG, Goberdhan A, Walsh C, Dao S, Ngai I, Chou TC, O'Charoenrat P, Levine AJ, Rao PH, et al. (2002) p53 regulates cell survival by inhibiting PIK3CA in squamous cell carcinomas. *Gene Dev* **16:**984–993.
Skipper HE (1974) Combination therapy: some concepts and results. *Cancer Chemother Rep 2* **4:**137–145.

Smith JB, Dwyer SD, and Smith L (1989) Lowering extracellular pH evokes inositol polyphosphate formation and calcium mobilization. *J Biol Chem* **264:**8723–8728.
Soike KF, Chou TC, Fox JJ, Watanabe KA, and Gloff CA (1990) Inhibition of simian varicella virus infection of monkeys by 1-(2-deoxy-2-fluoro-1-β-D-arabinosyl)-5-ethyl-uracil (FEAU)and synergistic effects of combinations with human recombinant interferon-β. *Antiviral Res* **13:**165–174.
Soike KF, Epstein DA, Gloff CA, Cantrell C, Chou TC, and Gerone PJ (1987) Effect of 9-(1,3-dihydroxy-2- propoxymethyl)-guanine and human recombinant β interferon alone and in combination on simian varicella infection in monkeys. *J Infect Dis* **156:**607–614.
Somers WJ, Felsen D, Chou TC, Marion DN, Chernesky CE, and Vaughan ED Jr (1989) An in vivo evaluation of α adrenergic receptors in canine prostate. *J Urol* **141:**1230–1233.
Soriano AF, Helfrich B, Chan DC, Heasley LE, Bunn PA, and Chou TC (1999) Synergistic effects of new chemopreventive agents and conventional cytotoxic agents against human lung cancer cell line. *Cancer Res* **59:**6178–6184.
Stachel SJ, Chappell MD, Lee CB, Danishefsky SJ, Chou TC, and Horwitz SB (2000) On the total synthesis and preliminary biological evaluations of 15(*R*) and 15(*S*) Aza-dEpoB: a Mitsunobu inversion at C15 in pre-epothilone fragments. *Org Lett* **2:**1637–1639.
Steckel J, Roberts J, Philips FS, and Chou TC (1983) Kinetic properties and inhibition of *Acinetobacter* glutaminase-asparaginase. *Biochem Pharmacol* **32:**971–977.
Steel GG and Peckham MJ (1979) Exploitable mechanisms in combined radiotherapy-chemotherapy: the concept of additivity. *Int J Radiat Oncol Biol Phys* **5:**85–91.
Stepkowski SM, Napoli KL, Wang MR, Qu X, Chou TC, and Kahan BD (1996) Effects of the pharmacokinetic interaction between orally administered sirolimus and cyclosporine on the synergistic prolongation of heart allograft survival in rats. *Transplantation* **62:**986–994.
Stepkowski SM, Tian L, Napoli KL, Ghobrial R, Wang ME, Chou TC, and Kahan BD (1997) Synergistic mechanisms by which sirolimus and cyclosporin inhibit rat heart and kidney allograft rejection. *Clin Exp Immunol* **108:**63–68.
Stepkowski SM, Tu Y, Chou TC, and Kahan BD (1994) Synergistic interactions of cyclosporine, rapamycin, and brequinar on heart allograft survival in mice, in *Cyclosporine: The Ten-Year Experience* (Kahan BD ed) pp 2025–2027, Appleton & Lange, Norwalk, CT.
Su DS, Balog A, Meng D, Bertiano P, Danishefsky SJ, Zheng YH, Chou TC, He L, and Horwitz SB (1997a) Structure-activity relationships of the epothilones and the first in vivo comparison with paclitaxel. *Angew Chem Int Ed Engl* **36:**2093–2096.
Su DS, Meng D, Bertinato P, Balog A, Sorensen EJ, Danishefsky SJ, Zheng YH, Chou TC, He L, and Horwitz SB (1997a) Total synthesis of (−) epothilone B: an extension of the Suzuki coupling method and insights into structure-activity relationship of the epothilones. *Angew Chem Int Ed Engl* **36:**757–759.
Su TL, Bacherikov V, Chou TC, Dong HJ, Chen CH, Lin YW, and Tsai TJ (2005) Potent antitumor 9-anilinoacridines bearing an alkylating N-mustard residue on the anilino ring: synthesis and biological activity. *Bioorg Med Chem* **13:**3993–4006.
Su TL, Chen EH, Huang LF, Basu K, and Chou TC (1999) Synthesis and structure-activity relationship of potential anticancer agents alkylcarbamates of 3-(9-acridinylamino)-5-hydroxymethylaniline. *J Med Chem* **42:**4741–4748.
Su TL and Chou TC (1994) Experimental antitumor activity of acridine alkaloids, acronycine and glyfoline. *Chin Pharm J* **46:**371–391.
Su TL, Chou TC, Kim JY, Huang JT, Ciszewska G, Ren WY, Otter GM, Sirotnak FM, and Watanabe KA (1995) 9-Substituted acridine derivatives with long half-life and potent antitumor activity: synthesis and structure-activity relationships. *J Med Chem* **38:**3226–3235.
Su TL, Chou TC, and Watanabe KA (1992a) Overview DNA topoisomerase targeted anticancer agents: new trends and developments. *Curr Opin Ther Patents* **2:**1121–1139.
Su TL, Kohler B, Chou TC, Chun MW, and Watanabe KA (1992b) Synthesis of the acridone alkaloids, glyfoline and congeners: structure-activity relationship studies of cytotoxic acridones. *J Med Chem* **35:**2703–2710.
Su TL, Yang YK, Huang JT, Chou TC, Ren WY, and Watanabe KA (1993) Synthesis of 4-[(1,3-diaminopyrrolo[3′4′:4,5]pyrido[2,3-*d*]pyrimidin-8-yl]-L-glutamic acid as potential antifolate. *J Heterocycl Chem* **30:**1437–1443.
Suhnel J (1990) Evaluation of synergism or antagonism for the combined action of antiviral agents. *Antiviral Res* **13:**23–40.
Takahashi N, Li WW, Banerjee D, Guan Y, Wada-Takahashi Y, Brennan MF, Chou TC, Scotto KW, and Bertino JR (2002) Sequence dependent synergistic cytotoxicity of ecteinascidin-743 and paclitaxel in human breast cancer cell lines *in vitro* and *in vivo*. *Cancer Res* **62:**6909–6915.
Takemura Y, Ohnuma T, Chou TC, Okano T, and Holland JF (1985) Biologic and pharmacologic effects of harringtonine on human leukemia-lymphoma cells. *Cancer Chemother Pharmacol* **14:**206–210.
Tallarida RJ (1992) Statistical analysis of drug combinations for synergism. *Pain* **49:**93–97.
Tanaka R, Ariyama H, Qin B, Shibata Y, Takii Y, Kusaba H, Baba E, Mitsugi K, Harada M, and Nakano S (2005a) Synergistic interaction between oxaliplatin and SN-38 in human gastric cancer cell lines in vitro. *Oncol Rep* **14:**683–688.
Tanaka R, Ariyama H, Qin B, Takii Y, Baba E, Mitsugi K, Harada M, and Nakano S (2005b) In vitro schedule-dependent interaction between paclitaxel and oxaliplatin in human cancer cell lines. *Cancer Chemother Pharmacol* **55:**595–601.
Thompson WR (1947) Use of moving averages and interpolation to estimate median-effective dose: I. Fundamental formulas, estimation of error, and relation to other methods. *Bacteriol Rev* **11:**115–145.
Tilley SA, Honnen WJ, Racho ME, Chou TC, and Pinter A (1992) Synergistic naturalization of HIV-1 by HuMAbs against the V3 loop and the CD4 binding site of gp120. *AIDS Res Hum Retroviruses* **8:**461–467.
Traversa U, Rosati AM, Florio C, and Vertua R (1994) Effects of divalent cations on adenosine agonist binding to A1 receptors and non-A1/non-A2 sites in rat cerebral cortex. *Pharmacol Toxicol* **75:**28–35.
Tremblay C, Merrill DP, Chou TC, and Hirsch MS (1999) Interactions among combinations of two and three protease inhibitors against drug-susceptible and drug–resistance HIV-1 isolates. *J Acquir Immune Defic Syndr* **22:**430–438.
Tremblay CL, Giguel F, Kollmann C, Guan Y, Chou TC, Baroudy BM, and Hirsch MS (2002) Anti-human immunodeficiency virus interactions of SCH-C (SCH 351125), a CCR5 antagonist with other antiretroviral agents in vitro. *Antimicrob Agents Chemother* **46:**1336–1339.
Tremblay CL, Kollmann C, Giguel F, Chou TC, and Hirsch MS (2000) Strong *in vitro* synergy between the fusion inhibitor T-20 and the CXCR4 blocker AMD-3100. *J Acquir Immune Defic Syndr* **25:**99–102.
Triozzi PL, Avery KB, Abou-Issa HM, and Chou TC (1989) Combined effect of interferon and steroid hormones on 2′,5′-oligoadenylate synthetase activity in chronic lymphocytic leukemia cells. *Leuk Res* **13:**437–443.
Trzaskos JM, Ko SS, Magolda RL, Favata MF, Fischer RT, Stam SH, Johnson PR, and Gaylor JL (1995) Substrate-based inhibitors of lanosterol 14α-methyl demethylase: I. Assessment of inhibitor structure-activity relationship and cholesterol biosynthesis inhibition properties. *Biochemistry* **34:**9670–9676.
Tseng PH, Lin HP, Zhu J, Chen KF, Hade EM, Young DC, Byrd JC, Grever M, Johnson K, Druker BJ, et al. (2005) Synergistic interactions between imatinib mesylate and the novel phosphoinositide-dependent kinase-1 inhibitor OSU-03012 in overcoming imatinib mesylate resistance. *Blood* **105:**4021–4027.
Tu Y, Stepkowski SM, Chou TC, and Kahan BD (1995) The synergistic effects of cyclosporine, sirolimus, and brequinar on heart allograft survival in mice. *Transplantation* **59:**177–183.
Upton AC (1961) The dose-response relation in radiation-induced cancer. *Cancer Res* **21:**717–729.
U.S. Department of Agriculture, Animal Welfare Act and Animal Welfare Regulations, May 13, 2002.
U.S. Public Health Service Policy on Humane Care and Use of Laboratory Animals. Office of Laboratory Animal Welfare, National Institutes of Health, Bethesda, MD, 2002.
Van Schaeybroeck S, Karaiskou-McCaul A, Kelly D, Longley D, Galligan L, Van Cutsem E, and Johnston P (2005) Epidermal growth factor receptor activity determines response of colorectal cancer cells to gefitinib alone and in combination with chemotherapy. *Clin Cancer Res* **11:**7480–7489.
Vaskinn S, Sundkvist E, Jaeger R, and Sager G (1999) The effect of Mg^{2+}, nucleotides and ATPase inhibitors on the uptake of [3H]-cGMP to inside-out vesicles from human erythrocytes. *Mol Membr Biol* **16:**181–188.
Vathsala A, Chou TC, and Kahan BD (1990) Analysis of the interactions of immunosuppressive drugs with cyclosporine in inhibiting DNA proliferation. *Transplantation* **49:**463–472.
Vathsala A, Goto S, Yoshimura N, Stepkowski S, Chou TC, and Kahan BD (1991) Immunosuppressive antagonism of low doses of FK506 and cyclosporine. *Transplantation* **52:**121–128.
Veldstra H (1956) Synergism and potentiation with special reference to the combination of structural analogues. *Pharmacol Rev* **8:**339–387.
Venditti JM and Goldin A (1964) Drug synergism in anti-neoplastic chemotherapy, in *Advances in Chemotherapy* (Goldin A and Hawking F eds) vol 1, pp 397–498, Academic Press, New York.
Vijayaraghavan S, Jing B, Vrablik T, Chou TC, and Regen SL (2003) Enhanced hydrolytic stability and water solubility of an aromatic nitrogen mustard by conjugation with molecular umbrellas. *Bioconjug Chem* **14:**667–671.
Vogiatzis AK and Loumbourdis NS (1998) Cadmium accumulation in liver and kidneys and hepatic metallothionein and glutathione levels in *Rana ridibunda,* after exposure to CdCl2. *Arch Environ Contam Toxicol* **34:**64–68.
Vogt MW, Durno AG, Chou TC, Coleman LA, Paradis TJ, Schooley TT, Kaplan JC, and Hirsch MS (1988) Synergistic interaction of 2′,3′-dideoxycytidine (ddCyd) and recombinant interferon-α A (rIFNaA) on HIV-1 replication. *J Infect Dis* **158:**378–385.
Vogt MW, Hartshorn KL, Furman PA, Chou TC, Fyfe JA, Coleman LA, Crumpacker C, Schooley RT, and Hirsch MS (1987) Ribavirin antagonizes the effect of azidothymidine on HIV replication. *Science (Wash DC)* **235:**1376–1379.
Vucenik I, Passaniti A, Vitolo MI, Tantivejkul K, Eggleton P, and Shamsuddin AM (2004) Anti-angiogenic activity of inositol hexaphosphate (IP6). *Carcinogenesis* **25:**2115–2123.
Wang M, Qu X, Stepkowski SM, Chou TC, and Kahan BD (1996) Beneficial effect of graft perfusion with anti-T cell receptor monoclonal antibodies on survival of small bowel allografts in rat recipients treated with brequinar alone or in combination with cyclosporine and sirolimus. *Transplantation* **61:**458–464.
Webb JL (1963) Effect of more than one inhibitor, in *Enzyme and Metabolic Inhibitors*, vol 1, pp 66–79, 488–512, Academic Press, New York.
Whitmore MM, DeVeer MJ, Edling A, Oates RK, Simons B, Lindner D, and Williams BR (2004) Synergistic activation of innate immunity by double-stranded RNA and CpG DNA promotes enhanced antitumor activity. *Cancer Res* **64:**5850–5860.
Wiener H and van Os CH (1989) Rabbit distal colon epithelium: II. Characterization of (Na^+,K^+,Cl^-)-cotransport and [^{3}H]-bumetanide binding. *J Membr Biol* **110:**163–174.
Woodward JJ and Blair R (1991) Redox modulation of *N*-methyl-D-aspartate-stimulated neurotransmitter release from rat brain slices. *J Neurochem* **57:**2059–2064.
Woodward JJ and Cueto S (1993) Effects of the putative polyamine antagonists diethylenetriamine and 1,10-diaminodecane on *N*-methyl-D-aspartic acid-stimulated [^{3}H]norepinephrine release from rat hippocampal slices. *J Pharmacol Exp Ther* **266:**563–569.
Woodward JJ and Gonzales RA (1990) Ethanol inhibition of *N*-methyl-D-aspartate-stimulated endogenous dopamine release from rat striatal slices: reversal by glycine. *J Neurochem* **54:**712–715.
Woodward JJ and Harms J (1992) The putative polyamine antagonists ifenprodil and SL 82.0715 enhance dopamine efflux from rat striatal slices independent of NMDA receptor activation. *Eur J Pharmacol* **210:**265–270.
Xu W, Smith-Franklin BA, Li PL, Wood C, He J, Du Q, Bhat GJ, Kankasa C, Katinger H, Cavacini LA, et al. (2001) Potent neutralization of primary HIV clade

C isolates with a synergistic combination of human monoclonal antibodies raised against clade B. *J Hum Virol* **4:**55–61.
Yanagida K, Baba C, and Baba M (2004) Inhibition of bovine viral diarrhea virus (BVDV) by mizoribine: synergistic effect of combination with interferon-alpha. *Antiviral Res* **64:**195–201.
Yang ZH, Crouch JY, Chou TC, and Hsiung GD (1990) Combined antiviral effects of paired nucleosides against guinea pig cytomegalovirus replication in vitro. *J Antiviral Res* **14:**249–266.
Yee KW, Schittenhelm M, O'Farrell AM, Town AR, McGreevey L, Bainbridge T, Cherrington JM, and Heinrich MC (2004) Synergistic effect of SU11248 with cytarabine or daunorubicin on FLT3 ITD-positive leukemic cells. *Blood* **104:**4202–4209.
Yen WC, Prudente RY, and Lamph WW (2004) Synergistic effect of a retinoid X receptor-selective ligand bexarotene (LGD1069, Targretin) and paclitaxel (Taxol) in mammary carcinoma. *Breast Cancer Res Treat* **88:**141–148.
Yonetani T and Theorell H (1964) Studies on liver alcohol hydrogenase complexes. 3. Multiple inhibition kinetics in the presence of two competitive inhibitors. *Arch Biochem Biophys* **106:**243–251.
You X, Schinazi RF, Arrowood MJ, Lejkowski M, Juodawlkis AS, and Mead JR (1998) In-vitro activities of paromomycin and lasalocid evaluated in combination against *Cryptosporidium parvum*. *J Antimicrob Chemother* **41:**293–296.
Young DH, Michelotti EL, Swindell CS, and Krauss NE (1992) Antifungal properties of Taxol and various analogues. *Experientia (Basel)* **48:**882–885.
Zahniser NR and Molinoff PB (1983) Thermodynamic differences between agonist and antagonist interactions with binding sites for [^{3}H]spiroperidol in rat striatum. *Mol Pharmacol* **23:**303–309.
Zemelman BV, Chu SH, and Walker WA (1989) Host response to *Escherichia coli* heat-labile enterotoxin via two microvillus membrane receptors in the rat intestine. *Infect Immun* **57:**2947–2952.
Zhang G, Lu H, Lu Y, Jiang S, and Chen YH (2005) Neutralization of HIV-1 primary isolate by ELDKWA-specific murine monoclonal antibodies. *Immunobiology* **210:**639–645.
Zhang LQ, Ramratnam B, Tenner-Racz K, He Y, Vesanen M, Lewin S, Talal A, Racz P, Perelson AS, Korber BT, et al. (1999) Quantifying residual HIV-1 replication in patients receiving combination antiretroviral therapy. *N Engl J Med* **340:**1605–1613.
Zhou Y, Li S, Hu YP, Wang J, Hauser J, Conway AN, Vinci MA, Humphrey L, Zborowska E, Willson JK, et al (2006) Blockade of EGFR and ErbB2 by the novel dual EGFR and ErbB2 tyrosine kinase inhibitor GW572016 sensitizes human colon carcinoma GEO cells to apoptosis. *Cancer Res* **66:**404–411.
Zhu QY, Scarborough A, Polsky B, and Chou TC (1996) Drug combinations and effect parameters of zidovudine, stavudine, and nevirapine in standardized drug-sensitive and resistant HIV-type 1 strains. *AIDS Res Hum Retroviruses* **12:**507–517.
Zucker K, Rosen A, Tsaroucha A, de Faria L, Roth D, Ciancio G, Esquenazi V, Burke G, Tzakis A, and Miller J (1997) Unexpected augmentation of mycophenolic acid pharmacokinetics in renal transplant patients receiving tacrolimus and mycophenolate mofetil in combination therapy, and analogous in vitro findings. *Transpl Immunol* **5:**225–232.
Zuckerman A, Bolan E, de Paulis T, Schmidt D, Spector S, and Pasternak GW (1999) Pharmacological characterization of morphine-6-sulfate and codeine-6-sulfate. *Brain Res* **842:**1–5.

Correction to "Theoretical Basis, Experimental Design, and Computerized Simulation of Synergism and Antagonism in Drug-Combination Studies"

Two errors were introduced during the composition stages of the article above [Chou TC (2006) *Pharmacol Rev* **58:**621–681] that are hereby corrected below.

First, in the denominator of eq. 20 on page 633, "$(D)_m)_j$" should be "$(D_m)_j$."

Second, in Table 13 on page 662, data that dropped out under the column heading "For a Given Dose (in D_m)" should be restored from top to bottom as follows: "**0.001**, **0.01**, **0.1**, **0.5**, **1**, and **2**."

Finally, in addition to these two errors, in the last row under the heading "Calculated Cumulative Dose," "4739.6" should be replaced by "**3157.6**."

The online version of this article has been corrected in departure from the print version.

Both the printers and author regret these errors and apologize for any confusion they may have caused.